Reactions of Non-Heme Iron(II) Centers with Dioxygen in Biology and Chemistry

Andrew L. Feig and Stephen J. Lippard*

Department of Chemistry, Massachusetts Institute of Technology, Cambridge, Massachusetts 02139

Received October 11, 1993 (Revised Manuscript Received February 9, 1994)

Contents

I. Introduction

Reactions of dioxygen with ferrous ion and its complexes occur widely in nature. In biology, the best known and probably most studied systems are proteins that contain one or more iron–porphyrin units, examples being hemoglobin and cytochrome P-450. Another large and diverse category of proteins contains non-heme iron, especially the ubiquitous iron–sulfur clusters. Summaries of the chemistry of iron–porphyrin and iron–sulfur proteins are available elsewhere.[1-6] In the present review, we describe the chemistry of non-heme iron(II) centers with dioxygen. (Hereafter we exclude iron–sulfur complexes from this category.) Like their heme counterparts, proteins containing these units transport dioxygen and oxygenate a variety of substrates. Iron(II)–dioxygen reactions also mediate the controlled generation of protein and nucleic acid radicals as well as the assembly of the mineral core in the iron storage protein ferritin.

As information about biological non-heme iron systems has emerged, chemists have prepared models to mimic their structures and functions. These models have in turn enhanced our understanding of the physical properties and reactivities of the biological iron centers. Such knowledge has practical applications in chemical industry as well as the health sciences. One example of this applicability is methane monooxygenase (MMO), which has the unusual ability to oxidize hydrocarbons and halocarbons, among other substrates. Because of their broad range of substrates, methanotrophic bacteria have been used in bioremediation of the environment, for example, to remove chlorinated hydrocarbons from drinking water and oil from contaminated beaches.[7-10] Functional mimics of this chemistry could provide an economical source of methanol for use as an alternative fuel or as new catalysts for use in water purification and the cleanup of toxic waste. Important insights into developing such catalysts could arise from learning how dioxygen and methane are activated in the biological system. Apart from such practical applications, however, the selective oxidation of methane to methanol is fundamentally difficult to achieve under mild conditions. The desire to unravel how nature has solved this challenging problem in methane monooxygenase systems is in itself sufficient incentive for scientific investigation.

Most of the previous reviews of non-heme iron focused primarily on structural and physical properties, with less emphasis on dioxygen reactivity.[11-18] In the present article we approach the topic from a mechanistic point of view, paying special attention to the reactions of iron(II) centers with dioxygen. Structural properties are discussed and tabulated, but mainly to illustrate how they affect the reactivity of the iron center under consideration. Although often synthetically useful,[19-24] reactions of iron complexes with reduced forms of dioxygen (superoxide and peroxide) are treated only if generated in a reaction of ferrous precursors with dioxygen. A similar comment applies to the use of oxo-transfer reagents to mimic postulated high oxidation

0009-2665/94/0794-0759$14.00/0

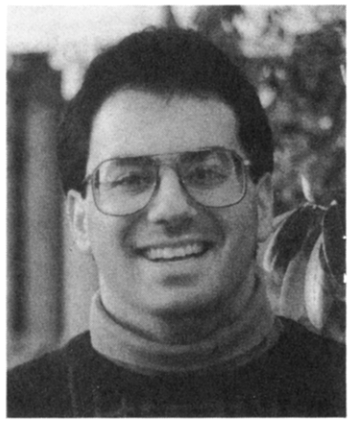

Andrew Feig (b. 1968) began research while a high school student, at which time he worked under Robert Seeger at the UCLA School of Medicine studying the N-*myc* oncogene product. This research was the foundation of a Westinghouse Science Talent Search Scholarship (1986). He received a B.S. in chemistry from Yale University in 1990. During his undergraduate years, he worked for two summers in the laboratory of David Sigman at UCLA studying copper(II) phenanthroline-mediated DNA cleavage and did an undergraduate thesis in the laboratory of Robert Crabtree on the synthesis of new ligands for the modeling of nickel hydrogenase. He is currently working on his Ph.D. in inorganic chemistry at MIT in the laboratory of Stephen Lippard where his research focuses on the reactions of dioxygen with iron(II) compounds. When not in the laboratory or out hiking in the mountains, he often relaxes in the kitchen where cooking and baking are two of his favorite pastimes.

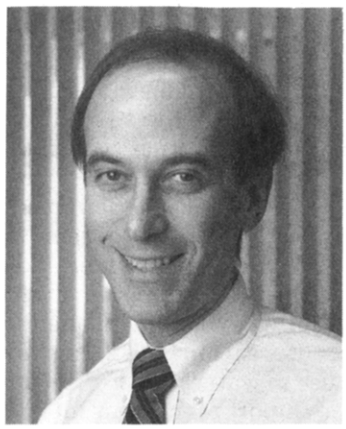

Stephen J. Lippard is the Arthur Amos Noyes Professor of Chemistry at MIT. His research interests center around the role of metal ions in biology, with particular focus on non-heme dimetallic centers and platinum anticancer drugs. He is an Associate Editor of the *Journal of the American Chemical Society* and has recently co-authored a book on bioinorganic chemistry with Jeremy Berg. He is a member of the National Academy of Sciences, the Institute of Medicine, and the American Academy of Arts and Sciences and has won several awards, including both the Monsanto and Mallinckrodt inorganic awards of the American Chemical Society. For relaxation he enjoys running along the Charles River, playing harpsichord, and being with his family and extended family, the latter of whom include present and past members of his research group.

state intermediates in the reaction of iron(II) species with dioxygen. No effort is made to provide comprehensive coverage of small molecule catalysts. Instead, we present a few key systems that react by different mechanisms to illustrate the types of reactivity observed. The relevance of this chemistry to the biological systems will be noted.

Our discussion begins with a summary of the redox properties of dioxygen and iron including autoxidation reactions of aquated ferrous iron and complexes with chelating ligands. Next we examine biological systems, classifying them on the basis of their iron core structures. Three categories are delineated, mononuclear centers in 4-methoxybenzoate *O*-demethylase, extradiol catechol dioxygenases, isopenicillin N synthase, pteridine-dependent enzymes, and α-keto acid-dependent enzymes; dinuclear centers in hemerythrin, methane monooxygenase and ribonucleotide reductase; and polynuclear centers in ferritin. The antitumor antibiotic bleomycin is covered next and serves to bridge our discussion of proteins and model compounds. We treat model systems in the final section, beginning with the most stable dioxygen adducts formed in the reaction of ferrous compounds with dioxygen then moving to autoxidations and catalytic reactions that proceed through transient dioxygen intermediates. Wherever possible, we attempt to relate chemical reactivity to molecular structure.

Several enzymes that utilize the chemistry of non-heme iron, and for which redox chemistry has sometimes been invoked, have been explicitly excluded. Soybean lipoxygenase is not discussed because recent evidence indicates that the functional form of the enzyme is the ferric state.[25] The chemistry of intradiol catechol dioxygenases is also not treated because the predominant evidence favors substrate rather than dioxygen activation.[26-29] Iron-dependent superoxide dismutase has been omitted because it acts on a reduced form of dioxygen.[30] The recently discovered dinuclear iron protein Δ-9 desaturase is not discussed because at present there is insufficient knowledge of its mechanistic chemistry.[31] Finally, we do not cover non-enzymatic lipid peroxidation involving ferrous ions. The iron chemistry does not differ substantially from that involved in the oxidation of aqueous ferrous ions except that the radical generated is intercepted by an organic substrate.[32,33]

II. Redox Properties of Dioxygen and Iron

A. Kinetic, Thermodynamic, and Structural Properties

Life on earth depends upon the kinetic stability of the O_2 molecule with respect to its reactions with organic compounds, which are quite exothermic. The origin of this stability is the spin-triplet ground state of dioxygen.[34-36] Since organic and biological molecules usually have paired electrons and singlet ground states, their reactions with dioxygen are spin forbidden. This kinetic barrier to reactivity can be surmounted by exciting the O_2 molecule to one of its singlet states, by a free-radical pathway, or by complexation with a paramagnetic metal ion. The first process is endergonic, requiring 22.53 or 37.51 kcal/mol for excitation to the lowest ($^1\Delta_g$) or second lowest ($^1\Sigma_g^+$) lying singlet states, respectively.[35] It is usually accomplished photochemically.[37] Radical mechanisms circumvent the spin restrictions by producing two doublet molecules, but the processes by which radicals are generated are usually quite endothermic and inaccessible at ambient temperatures.[36] Metal ions can also overcome the spin barrier and provide a low-energy pathway for oxidation reactions. Thus metal ion cofactors are often used in biology for reactions involving dioxygen. When the

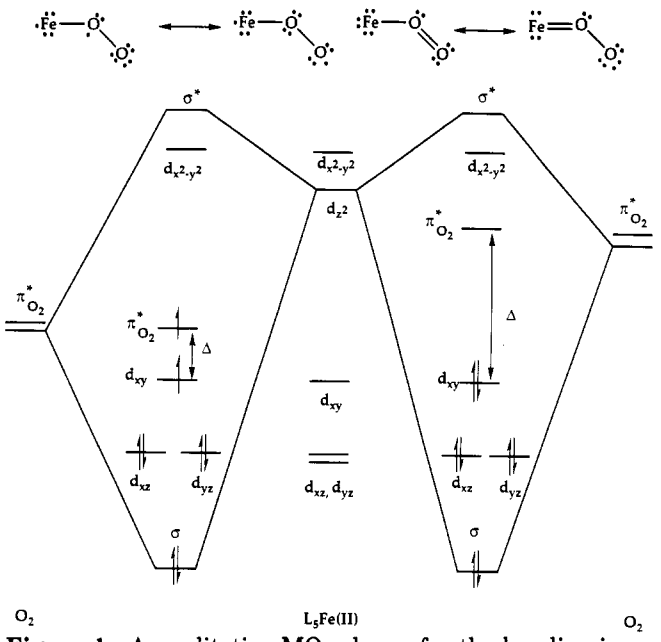

Figure 1. A qualitative MO scheme for the bonding in a hypothetical mononuclear iron–dioxygen complex, showing both σ and π interactions between iron and coordinated O_2. When $\Delta >$ pairing energy, this scheme is analogous to the $Fe^{II}(O_2)$–$Fe^{IV}(O_2^{2-})$ valence-bond resonance hybrids. (Adapted with permission from ref 35.)

dioxygen molecule binds to a metal ion, its 2p electrons interact with the d orbitals of the metal as shown, for example, for a hypothetical $Fe^{II}L_5$ species in Figure 1. Depending on the energy separation Δ, the adduct can have either a singlet or a triplet ground state. Regardless of the ground spin state of the adduct, its low-lying excited states can usually facilitate a spin-allowed reaction with singlet molecules. Although the beneficial use of such metal–dioxygen complexes in biology will dominate the ensuing discussion, the toxicity of the O_2 molecule can also be traced to the formation of highly reactive oxygen species that are similarly produced in reactions with metal ions.[38,39]

A second salient feature of metal ions with respect to their ability to mediate biological oxidations is the availability of multiple redox states. In the case of iron, the biologically relevant oxidation states are most often +2 and +3. That iron is required by an enzyme does not necessarily imply a redox role in dioxygen activation, however.[26] For example, some oxygenases, such as catechol 1,2-dioxygenase, use the Lewis acidity of iron(III) to induce substrate activation of dioxygen. In these cases, iron redox chemistry does not appear to be directly involved. The best way to establish a redox function is to observe oxidation state changes during enzyme turnover. Less direct evidence is the requirement of the reduced, ferrous state for activity. In addition to the common oxidation states, ferryl (Fe^{IV}=O) and perferryl (Fe^{V}=O) units have been invoked in several iron–dioxygen systems discussed below. Such species might arise from two-electron oxidation of iron(II) in a manner analogous to well-precedented chemistry of iron(II) porphyrins.[40,41] In these systems, high oxidation state iron is stabilized by electron delocalization from the porphyrin ring, which

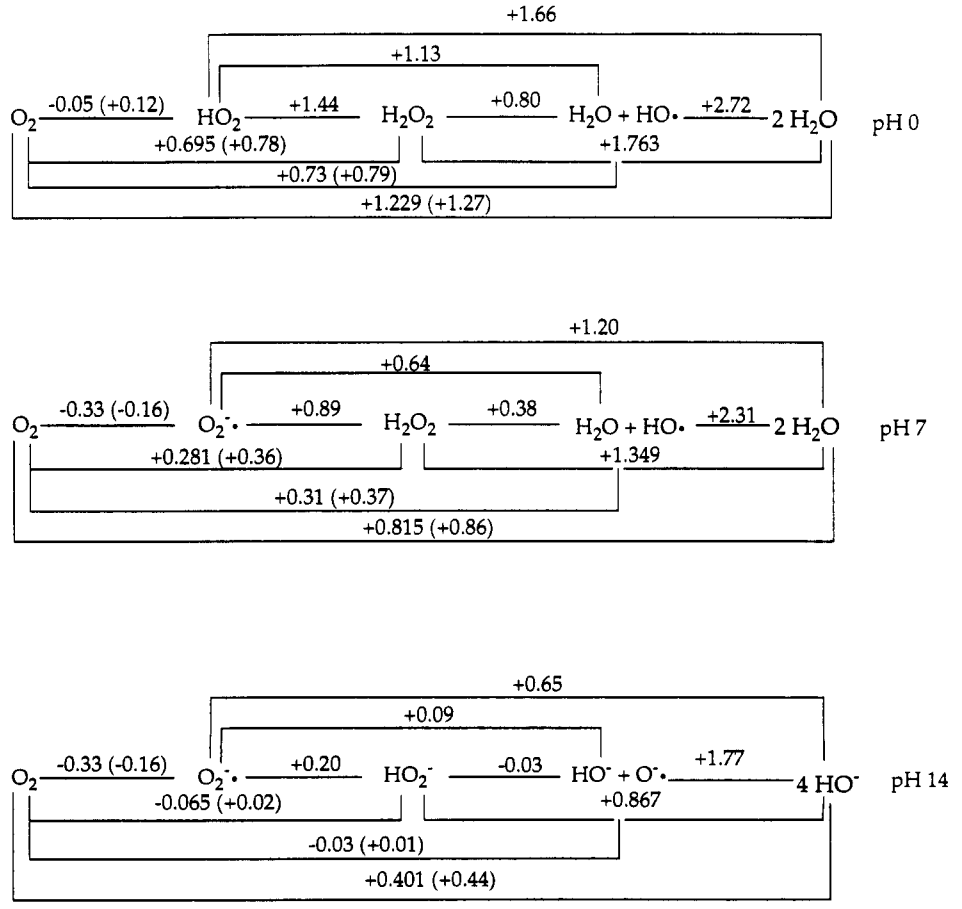

Figure 2. Standard reduction potentials (in volts) for dioxygen species in water. Formal potentials are given for O_2 at 1 atm or (in parentheses) at unit activity. (Reprinted from ref 362. Copyright 1988 Plenum.)

forms a cation radical.[23,40-44] For non-heme iron, the ability of ligands to act in a similar manner is less obvious. In some of the model complexes, metal-bound pyridyl radicals could be invoked as a means of reducing the formal oxidation state of the iron center from +4 to +3. A second iron center can also delocalize and stabilize the charge of the perferryl unit, as will be shown.

One important property of the dioxygen molecule is its propensity to accept electrons in pairs. Single electron transfer reactions, available at an energetic price, are less frequently encountered. This thermodynamic preference is manifest by electrochemical potentials of the dioxygen molecule in aqueous solution (Figure 2). An examination of the diagrams in this figure shows that reduction of dioxygen to superoxide in a one-electron step occurs at a potential ~0.5 V more negative than the two-electron reduction at the same pH. Even more negative electronic barriers are required for the one-electron reduction of hydrogen peroxide relative to its two-electron reduction. This property strongly influences the chemistry of iron(II) with dioxygen. Since the common redox step for Fe(II) is oxidation to Fe(III), there is a natural mismatch between the electron-transfer preferences of the metal ion and dioxygen. One solution is to combine two ferrous ions into a single unit. Such species, formerly designated as diiron oxo units because of the occurrence of (μ-oxo)diiron(III) cores in several non-heme iron proteins,[11,15] are more appropriately referred to as diiron carboxylates on the basis of recent structural revelations.[45,46] Reaction of such a diiron carboxylate center in its reduced form with dioxygen can generate a diiron(III) peroxide species. Alternatively, four-electron reduction of the O_2 molecule can yield two Fe(IV) ions and two H_2O molecules. In mononuclear systems it is less certain how two-electron redox reactions are accommodated. Since an external reductant such as ascorbate, NADH, or [2Fe-2S] is usually required for both mono- and dinuclear iron systems, it is possible that the mononuclear iron center cycles through two or more one-electron steps during each round of catalysis. Another possibility is that the ferrous ion is oxidized to an iron(IV) peroxide which then accepts electrons from an exogenous reductant. A third option is that, since many of the proteins are multimers, long-distance electron-transfer pathways might supply electrons from remote iron centers to the mononuclear catalytic site. Finally, a protein side chain such as that of tyrosine or cysteine could provide the required electron.

Apart from these kinetic and thermodynamic properties, the chemistry of iron and dioxygen is characterized by the favored modes of coordination of the O_2 molecule to mono- and dinuclear centers. Figure 3 presents several known and postulated binding modes. Three of these geometries have been structurally characterized, the bent end-on coordination (h) found in hemoglobin,[4] the *syn*-terminal mode (e) of hemerythrin,[47] and the μ^4-mode (j) found in $[Fe_6(O_2)(O)_2(OBz)_{12}(H_2O)_2]$ (1), the only crystallographically characterized ferric peroxide model complex.[48] Which ones are likely to be found in metalloproteins? By comparison to copper–dioxygen systems, which have been more thoroughly investigated, binding modes a–e might be expected for dinuclear centers,[49] whereas g and h are known for dioxygen complexes of other transition

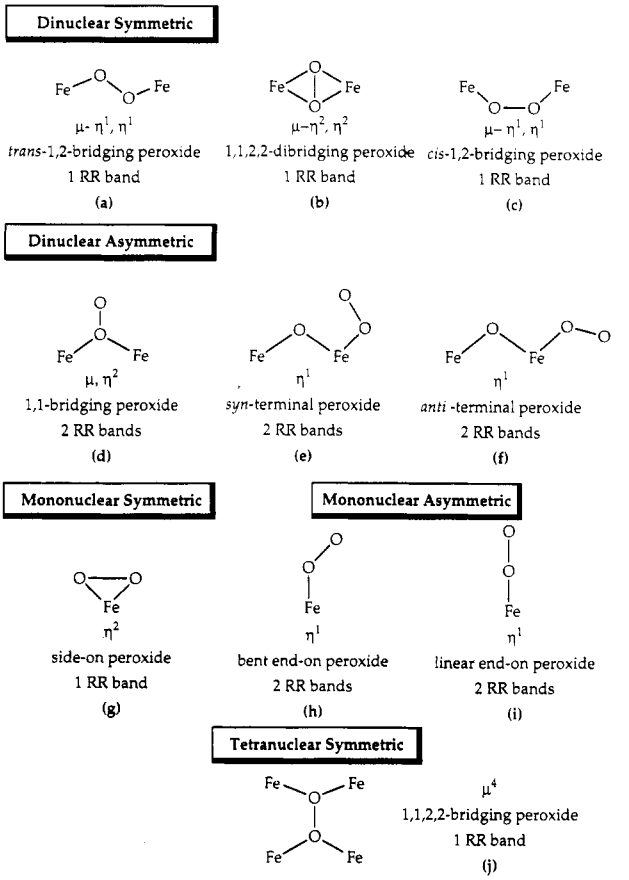

Figure 3. Potential dioxygen binding modes for mono- and dinuclear iron compounds. The number of resonance Raman (RR) bands refers to the O–O or Fe–O stretching frequencies when using ^{16}O–^{18}O.

metals.[34,35] The 1,2-bridging peroxide model has been proposed for several iron systems to be discussed below.[50-52] Some of these coordination geometries can be experimentally distinguished by vibrational spectroscopy, especially with the aid of isotopically labeled dioxygen (^{16}O–^{18}O).[53,54]

Theoretical calculations favor end-on binding of dioxygen to an iron atom.[55] Experimental evidence on ferrous and ferric dioxygen adducts formed by matrix isolation techniques indicate predominance of the side-on geometry (g), for which ν(O–O) = 956 cm^{-1}.[56,57] These studies employ "naked" metal ions and are extremely crude models for biological or even small molecule analogs of non-heme iron. The steric and electronic effects of other ligands in the coordination sphere on the binding modes and reactivity of dioxygen are likely to be quite significant. This property is exemplified by the different chemical reactivities of hemerythrin, methane monooxygenase, and ribonucleotide reductase, all of which contain similar diiron carboxylate cores.

B. Autoxidation Reactions of Iron(II)

As an introduction to the reaction chemistry of dioxygen with iron(II), we first discuss the autoxidation of aqueous ferrous ion in the absence and presence of chelating ligands. These processes have been investigated for many years, and although they appear deceptively simple, the reactions are in fact extremely complex and difficult to define mechanistically. We begin with this discussion because it raises key issues

that will appear later in our treatment of the chemistry of the biological and model systems. Formally, autoxidation has been defined as a spontaneous and self-catalyzed oxidation reaction.[58] In this review, we use the term specifically to denote reactions with dioxygen that result in its complete reduction to water without diverting oxidizing equivalents toward an external substrate. In the case of autoxidation involving Fe(II), the reaction is given in eq 1.

$$4Fe^{II} + O_2 + 4H^+ \rightarrow 4Fe^{III} + 2H_2O \quad (1)$$

When autoxidation occurs in biological systems or small molecule mimics, it is usually an undesired side reaction proceeding in parallel with the main oxidation process and resulting in the loss of catalytic activity. In biological systems, autoxidation often leads to inactive, or met, forms of a protein. In vivo there are usually specific reductases present to reduce the iron atoms to their functional oxidation states and restore activity. Formation of the met form of a purified protein in vitro, however, usually terminates the reaction. In a similar manner, catalytic systems that consume O_2 can also undergo autoxidation leading to loss of activity.

Several issues are important to raise at the beginning of our discussion of the reactions of non-heme iron(II) systems with dioxygen. One is whether O_2 and O_2^- coordinate directly to iron during the reaction. The issue of inner- versus outer-sphere mechanisms attains special importance during our treatment of reactions involving coordinatively saturated species such as $[Fe^{II}(EDTA)]^{2-}$. Other points of general interest are the extent to which pH influences the course of the reaction and whether radicals derived from dioxygen are present as intermediates in the chemistry. These last two properties are controlled in non-heme iron proteins by the choice of ligands and the composition of the protein pocket surrounding the active site.

1. Reactions of Aquated Iron(II)

Iron(II) reacts with dioxygen in water by multiple pathways. Early workers assumed that the reaction occurs by a mechanism in which ferrous ion is first oxidized to the ferric state with concomitant reduction of dioxygen to superoxide ion (O_2^-) (eq 2).[59] The

$$Fe^{II} + O_2 \rightleftarrows Fe^{III} + O_2^- \quad (2)$$

$$O_2^- + H^+ \rightleftarrows HO_2 \quad (3)$$

$$Fe^{II} + HO_2 \rightarrow Fe^{III} + HO_2^- \quad (4)$$

$$HO_2^- + H^+ \rightleftarrows H_2O_2 \quad (5)$$

superoxide produced in this step was then postulated to react immediately with another equivalent of ferrous ion yielding, upon protonation, hydrogen peroxide and a second equivalent of ferric ion (eqs 3–5). Hydrogen peroxide reacts rapidly with iron(II) via the Haber–Weiss scheme (Fenton's reaction), ultimately yielding water and more ferric ion (eqs 6–8).[60] The stoichiometry of the net reaction is given in eq 1. The rate constant for the oxidation of $[Fe(H_2O)_6]^{2+}$ by dioxygen in the first step is several orders of magnitude less than the back-reaction (eq 2).[61] From this observation and a

Fenton chemistry

$$Fe^{II} + H_2O_2 \rightarrow Fe^{III} + OH^- + OH\cdot \quad (6)$$

$$Fe^{II} + OH\cdot \rightarrow Fe^{III} + OH^- \quad (7)$$

$$OH^- + H^+ \rightleftarrows H_2O \quad (8)$$

theoretical analysis it was concluded that dioxygen must coordinate to the metal ion in order to be activated.[62] Interestingly, such a conclusion is similar to that reached in later work on inner- and outer-sphere electron-transfer pathways[63] and requires modification of the mechanism postulated in eqs 2–8.

Support for an inner-sphere electron-transfer pathway was provided by the effects of counterions and chelating agents on the rate law for the autoxidation reaction.[62] Depending upon the pH and the choice and concentration of counterions, the reaction can be either first or second order with respect to the concentration of iron(II) (eqs 9 and 10).[62,64-67] At constant pH, the

$$\frac{d[Fe^{III}]}{dt} = k'[Fe^{II}][O_2] \quad (9)$$

$$\frac{d[Fe^{III}]}{dt} = k''[Fe^{II}]^2[O_2] \quad (10)$$

$$\frac{d[Fe^{III}]}{dt} = k'[Fe^{II}(L^-)][O_2] + k''[Fe^{II}]^2[O_2] \quad (L^- = \text{bound anion}) \quad (11)$$

rate of oxidation decreases in the series pyrophosphate[66] > phosphate[65] > chloride[68,69] > sulfate[69,70] > perchlorate.[64] Two parallel reactions occur, the relative importance of which depends on the binding constant of the anion for the aquated ferrous iron. The complete rate law (eq 11) could be accounted for by the mechanism depicted in eqs 12–20. Anion binding favors

$$[Fe^{II}(H_2O)_6]^{2+} \rightleftarrows [Fe^{II}(H_2O)_5(OH)]^+ + H^+ \quad (12)$$

$$[Fe^{II}(H_2O)_6]^{2+} + L^- \rightleftarrows [Fe^{II}(H_2O)_5(L^-)]^+ + H_2O \quad (13)$$

$$[Fe^{II}(H_2O)_6]^{2+} + O_2 \rightleftarrows [Fe^{II}(H_2O)_5(O_2)]^{2+} + H_2O \quad (14)$$

$$[Fe^{II}(H_2O)_5(O_2)]^{2+} \rightleftarrows [Fe^{III}(H_2O)_5(O_2^-)]^{2+} \quad (15)$$

$$[Fe^{III}(H_2O)_5(O_2^-)]^{2+} + [Fe^{II}(H_2O)_6]^{2+} \rightarrow [(H_2O)_5Fe^{III}(O_2^{2-})Fe^{III}(H_2O)_5]^{4+} + H_2O \quad (16)$$

$$[(H_2O)_5Fe^{III}(O_2^{2-})Fe^{III}(H_2O)_5]^{4+} + 2H^+ + 2H_2O \rightarrow 2[Fe^{III}(H_2O)_6]^{3+} + H_2O_2 \quad (17)$$

$$[Fe^{III}(H_2O)_5(O_2^-)]^+ + H^+ + H_2O \rightleftarrows [Fe^{III}(H_2O)_6]^{3+} + HO_2 \quad (18)$$

$$[Fe^{II}(H_2O)_6]^{2+} + HO_2 \xrightarrow{\text{fast}} [Fe^{III}(H_2O)_5(HO_2^-)]^{2+} + H_2O \quad (19)$$

$$[Fe^{III}(H_2O)_5(HO_2^-)]^{2+} + H^+ + H_2O \rightarrow [Fe^{III}(H_2O)_6]^{3+} + H_2O_2 \quad (20)$$

the pathway that is first order in iron(II), depicted in eq 9, whereas the second-order pathway (eq 10) dominates for species containing no bound anion.[62,65,66,71] The equilibrating species shown in eqs 12 and 13 should be considered to be present in each of the subsequent reactions even though they are not explicitly indicated. Hydrogen peroxide formed by eqs 17 and 20 will react rapidly with more Fe(II) as indicated in eqs 6–8. These equations (9, 10, 12–20) differ from those previously proposed (eqs 2–8), owing to dioxygen coordination to iron(II). As indicated above, the result is electron transfer by an inner rather than an outer-sphere mechanism. The anion-dependent rate acceleration arises from stabilization of ferric species, including those postulated in the transition state.[66]

The pH dependence is more complex than expected on the basis of a shift in the redox potentials and can be rationalized in a manner similar to the effects of anion binding. At higher pH values, one of the coordinated water molecules is deprotonated, again stabilizing iron(III). Because of the insolubility of ferric species with increasing pH, studies have been limited to pH values ≤ 2. Moreover, the reactions were usually followed for only a fraction of a half-life, with the analyses being based on initial rates. This limitation results from the relatively sluggish reaction velocities. For example, $k \approx 3.1 \times 10^{-5}$ to 1.4×10^{-6} M^{-1} atm^{-1} s^{-1} for $Fe(SO_4)$ in water at 140–180 °C, $[Fe]_0 = 1.0 - 30.0$ mM, 1 atm O_2,[66] corresponding to $t_{1/2} \approx 6600$–9000 h.

The high dielectric constant of water makes it an extremely good solvent for stabilizing the charge separation required by solvated ion pairs. By shifting from water to solvents with lower dielectric constants, the effects of anion binding to iron are enhanced. For example, the ability of chloride ion and solvent to affect the autoxidation of $FeCl_2$ in alcohols has been studied.[72,73] A large solvent-dependent rate enhancement and overall third order kinetics were observed (eq 10), consistent with formation of a diferric peroxide intermediate and increased anion binding.[73]

2. Reactions of Chelated Iron(II) Complexes

Several workers have examined the effects of chelating ligands on the autoxidation of Fe(II).[61,74–78] In the presence of chelating agents such as EDTA, a two-term rate law was obtained (eq 21).[74] These results were

$$\frac{d[Fe^{III}]}{dt} = k_p[Fe^{II}(HZ)]^-[O_2] + k_n[Fe^{II}(Z)]^{2-}[O_2] \quad (21)$$

$$[Fe^{II}(Z)]^{2-} + H^+ \rightleftarrows [Fe^{II}(HZ)]^- \quad (22)$$

interpreted as evidence for an equilibrium involving the parent chelate and its monoprotonated form (eq 22), the latter providing an open coordination site on iron. Both forms react with dioxygen, but at different rates. The fact that the $k_p > k_n$ in every case suggested that a vacant coordination site on iron, provided by the dissociation of a single arm of the chelating ligand, accelerated the reaction rate by removing steric hindrance to the attacking O_2 molecule.[74] From an electronic point of view, this trend is counter-intuitive since protonation reduces the negative charge of the ligand and should stabilize the iron(II) form. It should also be noted that ferric ion can become 7-coordinate, as in the crystallographically characterized $[Fe^{III}(EDTA)(OH_2)]^-$ complex.[79] Thus, a site might be available for O_2 coordination regardless of the ligand protonation state. An alternative possibility is that the protonated arm of the ligand facilitates hydrogen ion transfer to bound superoxide, releasing HO_2.[74] Formation of free HO_2 was not definitively demonstrated, however. Analysis of the pH dependence of the reaction showed the maximal rate to occur at pH 3, with high and low pH limits determined by the values at which ligand dissociation occurred.[75]

The kinetics of this process were more recently examined in greater detail.[61] It was concluded that the mechanism involved only outer-sphere pathways (eqs 2–7). The pH dependence of the reaction would then arise from protonation of free superoxide ion and attendant changes in its redox potential. In this scheme, reactions with hydrogen peroxide are rapid, so only eqs 2 and 4 affect the observed rate law and rate constant. Radical trapping studies of this autoxidation reaction revealed multiple species including superoxide ion, hydroxyl radical, and buffer-based radicals.[78,80] The exact origin of their formation was not demonstrated experimentally, although radical chain mechanisms initiated by $OH^\bullet$ or O_2^- were proposed.[78] Unfortunately, the ability to trap radicals is consistent with either inner- or outer-sphere mechanisms. Other studies contradict these findings and support inner-sphere oxidation pathways.[75,77] Furthermore, a dioxygen adduct of $Fe^{III}(EDTA)$ was prepared by addition of superoxide to the ferrous chelate complex at high pH[19] or of hydrogen peroxide to the ferric chelate.[81] The isolation of such an adduct provides strong evidence for binding, at least at high pH, but does not provide any insight into what might be happening under other conditions.

To summarize, the primary finding from these studies is that chelation significantly increases the rate of autoxidation. Autoxidation reactions have been studied for more than 40 years and are deceptively simple when written in the form of eq 1. The detailed mechanism is still being debated, and in view of the conflicting evidence, it is difficult to determine whether an inner-sphere or outer-sphere pathway predominates. Most likely, both pathways are available, and by varying reaction conditions, one may observe either mechanism. These considerations raise an important point regarding the interpretation of kinetic data. Although comparisons are frequently made among studies from different laboratories, unless the experimental conditions are identical it may be impossible to reconcile discrepancies.

III. Reactions of Biological Iron(II) Centers with Dioxygen

Protein systems that use the reaction of dioxygen with Fe(II) are functionally quite diverse. They can be divided into general classes, mononuclear, dinuclear, and polynuclear according to the number of iron atoms in the active site. The ferroxidase center in ferritin, which loads iron into the mineral core of the protein, is classified here as polynuclear. On a functional level, however, it falls somewhere between the other two classes. As discussed below, its redox chemistry follows multiple pathways, one of which results in the formation of mononuclear and dinuclear intermediates. A non-

Table 1. Spectroscopic Properties of Putidamonooxin and Protocatechuate Dioxygenase

	parameter	PMO + NO, no substrate	PMO + (4-NH_2)OBz + NO[a]	PMO + (4-OMe)OBz + NO[b]	oxidized PMO	3,4-PCD	reduced 4,5-PCD	reduced 4,5-PCD + substrate	reduced 4,5-PCD + substrate + NO	oxidized 4,5-PCD
Mössbauer	D, cm^{-1}			12	−1.8	−2			12	
	E/D			0.01	0.05	0.03			0.02	
	ΔE_Q, mm s^{-1}			−1.4	0.55	−0.5	2.22	2.33 2.80	−1.67	
	η			0.2	0.15				0.07	
	$A_0/g_N\beta_N$, T[c]			−23.5	−21.05				−32	
	Γ, mm s^{-1}			0.30	0.30					
	δ, mm s^{-1}			0.68	0.50	0.44	1.28	1.27 1.22	0.66	
	T, K				1.5–4.2	4.2–20	4.2	4.2	4.2	
EPR	g_1[d]	4.162	4.170							
	g_1[e]	4.093	4.08	4.101						
	g_2[e]	3.975	3.99	3.960						
	g_2[d]	3.892	3.882							
	g_3,[d] g_3[e]	2.0	2.0	2.0						
	g						silent	4.35	4.21 3.77 1.99	6.4 5.5 4.3 2.0
ref		94	94	94	94	365	101	101	101	101

[a] Uncoupling substrate. [b] Tight coupling substrate. [c] The parameter $A_0/g_N\beta_N$ is in units of internal field per spin 1, where $A_0 = A_x = A_y = A_z$, g_N is the nuclear g factor, and β_N is the nuclear magneton. [d] Indicates spectral species with large tetragonal distortion. [e] Indicates spectral species with small tetragonal distortion.

protein system, iron–bleomycin, is presented at the end of this section because it is a natural product used in medicine as an antitumor agent. In our discussion of each system we focus on the reaction of iron(II) with dioxygen. Sufficient background will be presented to place the dioxygen reaction in context; for greater detail, however, the reviews cited should be consulted. As stated above, several non-heme iron enzymes have been excluded from discussion. Reviews on these systems, which include iron-dependent superoxide dismutase,[30,82] lipoxygenases,[83] and intradiol catechol dioxygenases,[26,27] are available elsewhere.

A. Mononuclear Enzymes

1. 4-Methoxybenzoate O-Demethylase (Putidamonooxin)

In addition to methanotrophs which require methane, there are numerous other bacteria that consume aromatic hydrocarbons as their sole carbon and energy source.[84] Like MMO, the enzymes used by these organisms are of interest for their potential application in the bioremediation of chemical waste. One such enzyme, obtained from *Pseudomonas putida*, is 4-methoxybenzoate *O*-demethylase (putidamonooxin, PMO), which contains both a [2Fe-2S] cluster and a mononuclear non-heme iron site.[85-90] This enzyme catalyzes the conversion of 4-methoxybenzoic acid into 4-hydroxybenzoic acid and formaldehyde (eq 23). Many other substrates can bind to the enzyme,[91] however, some of which get hydroxylated and others of which do not. Substrates falling in the former category are termed "coupled", whereas "uncoupled" substrates are competitive inhibitors that bind to the active site and allow enzyme turnover, but are not oxidized in the process. In the latter case, reductant is consumed and dioxygen is converted stoichiometrically to hydrogen peroxide.[88] When 3- or 4-hydroxybenzoate is used, the hydroxylation reaction affords the corresponding catechol (eq 24).[92] This chemistry is similar to the F208Y R2 mutant, described in detail below, which oxidizes a tyrosyl residue to dopamine on exposure of its ferrous form to dioxygen. In PMO, dioxygen reacts with the mononuclear ferrous center, and a ferric peroxide has been postulated as the active species.[93] NADH donates electrons by way of the iron–sulfur cluster during turnover. It should be noted that, in certain cases, the observed product of the catalytic reaction is the result of further rearrangement after the hydroxylation step.[92]

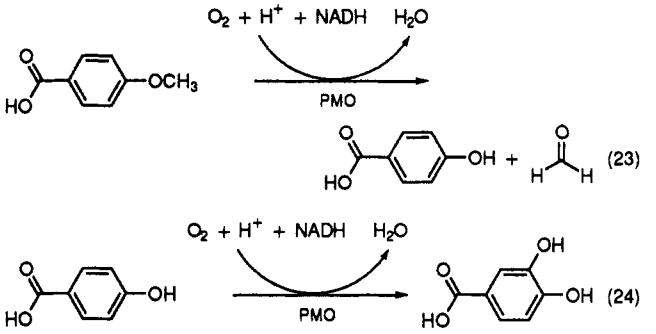

The structure of the non-heme iron center of PMO is less well defined than those of many other iron enzymes. Data obtained from EPR[93] and Mössbauer[94] spectroscopic studies, summarized in Table 1, are similar to those for the iron center in 3,4-protocatechuate dioxygenase discussed below,[94] but further work is required to establish the identity of the two enzyme-active sites. The only certainty regarding the iron coordination sphere in PMO is the availability of exogenous ligand binding sites, which was demonstrated by the effect of ^{14}NO binding on the EPR spectrum. NO mimicked the dioxygen binding step but did not turn over the enzyme.[93] Addition of coupled substrates to the NO–enzyme complex significantly altered the EPR spectrum, but uncoupled substrates caused no change. This result indicates that coupled substrates

either bind directly to the metal center or induce structural rearrangements in the active site. The ferrous ion is bound quite loosely to the enzyme. In the absence of substrate, the equilibrium is such that $^2/_3$ of the iron is free in solution.[93] The binding of both substrate and NO to the metalloenzyme stabilizes the iron center, preventing dissociation of ferrous ion.

Equation 25 sets forth a scheme for the dioxygen chemistry of PMO,[93] in which the iron–sulfur clusters feed electrons to the non-heme iron center one at a time. Species B–D are postulated to be EPR silent, and E and F never form in sufficient quantities to detect under turnover conditions.[93] With NO, D′ (the NO

$$\underset{A}{Fe^{III}} \xrightarrow{+e^-} \underset{B}{Fe^{II}} \xrightarrow{+O_2} \underset{C}{Fe^{II}-O_2} \rightarrow \underset{D}{Fe^{III}-O_2^-} \xrightarrow{+e^-} \underset{E}{Fe^{II}-O_2^-} \rightarrow \underset{F}{Fe^{III}-O_2^{2-}} \quad (25)$$

analog of D) has been observed. Although D′ should have a partially reduced [2Fe-2S] cluster, its EPR signal was unaffected by addition of NO.

On the basis of results obtained with 4-vinylbenzoate, a ferric peroxide intermediate was postulated as the active hydroxylating species.[95] By using $^{18}O_2$, it was found that both oxygen atoms in the product, 4-(1,2-dihydroxyethyl)benzoate, were derived from the dioxygen molecule. The ability of the enzyme to function as a dioxygenase rules out the possible involvement of a ferryl species, the formation of which would require one of the oxygen atoms to be lost to solvent.

Any complete mechanism for this enzyme must also account for the high proportion of NIH-shifted product observed during turnover.[96] This property is usually interpreted as evidence for opening of an epoxide intermediate at either of its two C–O bonds. It is unclear at present whether ferric peroxides are capable of catalyzing such reactions without first decomposing heterolytically into a perferryl species. The intermediate in such a non-ferryl mechanism might be a dioxetane, a four-membered cyclic peroxide, which could lead to significant NIH shifts by a ring-opening mechanism analogous to that of an oxirane.

2. Extradiol Catechol Dioxygenases

Catechol dioxygenases are important enzymes involved in the catabolism of aromatic compounds. They catalyze the cleavage of aromatic rings to form linear unsaturated diacids or acid–aldehydes (Figure 4). The extradiol catechol dioxygenases, such as protocatechuate 4,5-dioxygenase, catechol 2,3-dioxygenase, and many others, are not nearly as well studied as their intradiol counterparts, catechol 1,2-dioxygenase and protocatechuate 3,4-dioxygenase.[26,27,36,97] The intradiol enzymes use a novel substrate activation mechanism in which catechol binds to a ferric site that does not undergo redox chemistry during turnover.[26,27,36,97-100] In these enzymes, dioxygen reacts directly with the substrate-bound ferric form of the enzyme rather than with the ferrous form. The extradiol catechol dioxygenases, on the other hand, require the ferrous form of the enzyme.[26,27] This finding was an initial indication that an iron–dioxygen intermediate was involved in the

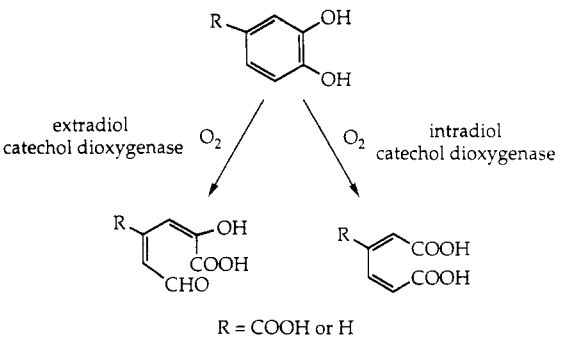

Figure 4. Reactions of extradiol and intradiol catechol dioxygenases.

enzyme mechanism. For simplicity, we focus our discussion on the chemistry of protocatechuate 4,5-dioxygenase (4,5-PCD) from *Pseudomonas testosteroni*, the best studied of the extradiol enzymes.

4,5-PCD contains a single ferrous site per $\alpha_2\beta_2$ tetramer (MW = 52.3 kDa),[101] the nature of which has been examined spectroscopically (Table 1). Mössbauer studies on the *Pseudomonas testosteroni* enzyme revealed a high-spin octahedral ferrous ground state (δ = 1.28 mm s^{-1}, ΔE_Q = 2.22 mm s^{-1} at 4.2 K).[101] Mössbauer parameters for 4,5-PCD from other organisms are slightly different but still characteristic of a high-spin ferrous center.[102] One of the most interesting findings is that the Mössbauer parameters shift upon addition of substrate, providing evidence, although not proof, for inner-sphere coordination. Longer range interactions due to side-chain reorganization upon substrate binding can also lead to spectral changes for the iron center. In the presence of catechol, the data revealed two quadrupole doublets assigned to substrate bound and free forms of the enzyme.[101] In both the presence and absence of substrate, NO binding also affected the iron Mössbauer spectrum.[101]

A series of EPR experiments has been carried out on this enzyme. The ferrous form was EPR silent, but after oxidation to Fe(III) species several signals appeared (g = 6.4, 5.5, 4.3) and were assigned to a heterogeneous mixture of products.[101] Once again, substrate and NO binding affected the spectra, further supporting the existence of a ternary (E–S–O_2) complex in which each component is bound to the iron center.[103] The use of isotopically labeled water ($^{17}OH_2$) indicated that at least two, and possibly a third, iron coordination sites contained bound water in the absence of substrate and dioxygen.[104] Detailed studies of the electronic structure of the iron center in catechol 2,3-dioxygenase using MCD were interpreted by a slightly different model having a 5-coordinate, square pyramidal active-site geometry.[105]

A postulated mechanism for the reaction is shown in Figure 5.[103] Following enzyme–substrate complex formation, dioxygen binds to the ferrous form of the enzyme without oxidizing it to a ferric superoxide intermediate. This conclusion was based on the observation that autoxidation of the enzyme is slow. Whereas most ferrous enzymes must be kept strictly anaerobic to prevent such oxidative inactivation, 4,5-PCD must be oxidized with hydrogen peroxide or some other suitable oxidant to inactivate it completely.[101] This property indicates that, in the absence of substrate, the ferric–superoxide species is not thermodynamically favored in this system. A dioxygen adduct, although

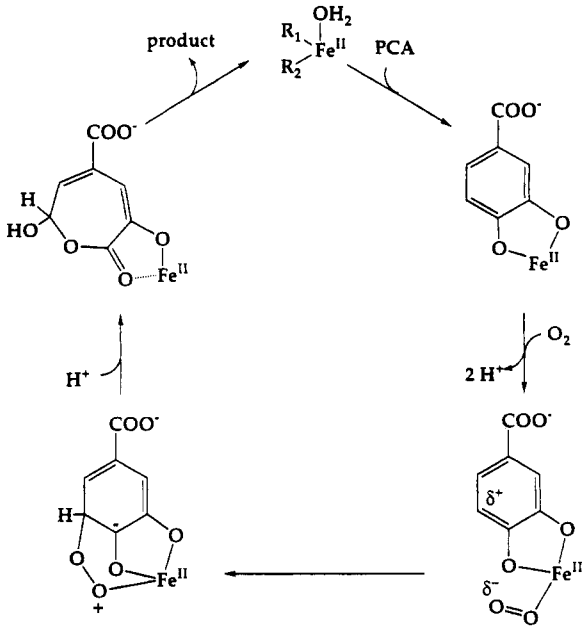

Figure 5. Proposed mechanism for the oxidation of protocatechuate by protocatechuate 4,5-dioxygenase. (Adapted with permission from ref 103.)

not detected in the absence of substrate, is inferred from the NO complex mentioned above. In addition, in the presence of substrate, the binding constants for NO and other exogenous ligands are significantly larger, an effect similar to the one discussed above for PMO.[104,105] The exact cause of such substrate effects is not known, but substrate binding may change the redox potential of the iron center, making it more susceptible to oxidation by dioxygen.[106,107] In the presence of substrate, the bound dioxygen molecule is postulated to attack the coordinated catecholate leading ultimately to ring opening, as indicated in Figure 5.[103] This reaction amounts to a nucleophilic attack on a benzene ring. If C-5 were to acquire semiquinone character during oxidation of iron(II) to iron(III), however, a radical attack of the coordinated dioxygen might be possible. More work is required to establish the mechanism.

3. Pteridine-Dependent Reactions

This class contains three known iron enzymes that utilize dioxygen, phenylalanine hydroxylase (PAH), tyrosine hydroxylase (TH), and tryptophan hydroxylase (TRH). The reactions catalyzed, shown in Figure 6, are all used in mammalian amino acid metabolism. The product of the TH-catalyzed reaction, the catecholamine L-DOPA, is especially important because it is the precursor of the neurotransmitters epinephrine and norepinephrine. Most work in this area has been carried out on PAH, primarily because of its ease of isolation. We therefore focus our discussion on this enzyme, since others in the class are likely to behave similarly.[108] The pteridine used naturally by these systems is tetrahydrobiopterin (H_4BP), which gets oxidized to quinonoid dihydrobiopterin (H_2BP) during turnover.[108] Many analogs of this reductant are active in the catalytic system and their use has been instrumental in determining the enzyme mechanism.[109] Complete reviews on all the pterine-dependent enzymes are available elsewhere.[109,110]

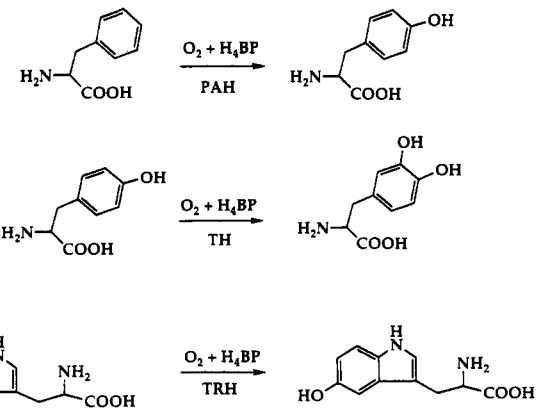

Figure 6. Reactions of the pteridine-dependent non-heme iron enzymes. PAH = phenylalanine hydroxylase; TH = tyrosine hydroxylase; TRH = tryptophan 5-hydroxylase; H_4-BP = tetrahydrobiopterin.

The nature and structure of the iron site in PAH have been somewhat neglected. Our ability to make reasonable interpretations regarding structure–function relationships in this system is therefore hampered. A discussion of the chemical properties of the system will allow comparisons to be made with other reactions of ferrous iron with dioxygen, however. When more structural information is available, a reanalysis will be necessary.

By analogy to flavin systems, it was originally proposed that dioxygen reacts directly with the organic cofactor to generate 4a-hydroperoxy-tetrahydrobiopterin (4a-OOH), which decays to form the active oxidant. Substantial evidence has been acquired in support of this hypothesis.[109,111,112] According to this mechanism, iron(II) would react with the peroxidated cofactor, rather than with dioxygen itself, forming an iron(II) peroxypterine (Fe-OO-4a) adduct. Heterolytic decomposition of this intermediate is proposed to yield 4a-OH and a ferryl species that is the active oxidant. This theory appeared to be supported by the existence of what was believed to be a PAH that contained no metal ion isolated from *Chromobacterium violaceum*,[113] since the heterolytic cleavage of hydroperoxides is known to occur under certain metal-free conditions. In such a case, OH• would be the active species. It was subsequently shown, however, that a Cu(I) cofactor had been overlooked.[114] Thus, all known enzymes of this class require reduced metal cofactors for activity.[114a]

This fact raises the possibility that a reaction between reduced metal and dioxygen precedes formation of the 4a-OOH intermediate. The strongest evidence for such a role for iron in PAH is the diminished oxidation rate of the cofactor in its absence. Were the synthesis of the 4a-OOH intermediate independent of protein-bound Fe(II), the unstable peroxide should still form rapidly, although its decomposition would be altered by the lack of functional protein. On the basis of chemistry observed in other enzymes and model systems and the clear requirement for reduced iron, it may be that a ferric–superoxide/ferrous–dioxygen adduct forms initially which then peroxidizes H_4BP. The reaction would yield the same Fe^{II}-OO-4a cofactor adduct discussed above and possibly result in the same heterolytic decomposition pathway. The current experimental data unfortunately cannot differentiate these two pathways. Recent NMR studies on the active

site of TH have measured the distance between the phenylalanine C3/C4 positions and the metal center at 6.8 ± 1.2 Å.[115] This constraint positions the amino acid in approximately the right place for a perferryl oxo or ferric peroxide to act upon it during enzyme turnover.

If the activation steps are based on iron chemistry, release of superoxide or hydrogen peroxide might be a potential side reaction. There is conflicting evidence regarding H_2O_2 formation during the coupled and uncoupled reactions.[111,116,117] Superoxide dismutase is more effective than catalase in preventing damage to the enzyme,[117] and small amounts of released superoxide have been detected during turnover.[111] Both of these results are consistent with a ferric–superoxide intermediate. These findings support an active role for the iron center in a reaction with O_2, but could also be explained by nonspecific ferrous ion activity.

4. α-Keto Acid-Dependent Reactions

The α-keto acid-dependent enzymes, of which there are at least eight variants, comprise one of the largest classes of non-heme iron proteins.[96] These enzymes are characterized by their requirement for Fe(II), ascorbate, dioxygen, and an α-keto acid, usually α-ketoglutarate (2-KG). In one example, (*p*-hydroxyphenyl)pyruvate hydroxylase, the keto acid moiety is an integral part of the substrate.[96] The general reaction catalyzed by these enzymes hydroxylates substrate and decarboxylates 2-KG, with one oxygen atom from O_2 being transferred to substrate and the other to the carboxylate group of the newly formed succinate (eq 26).[118,119] The best studied system to date is prolyl

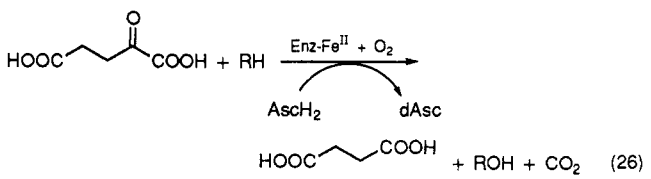

(26)

4-hydroxylase which oxidizes proline residues of pre-collagen, but again, since all the enzymes in this class are expected to function similarly, discussion can be generalized to the other systems. Two reviews are available.[120,121]

The mononuclear iron center in these enzymes has a rather accessible coordination sphere. In studies with cofactor analogs, it was found that both 2-KG and ascorbate bind directly to iron, and it was assumed that there must also be an available coordination site for dioxygen.[120,121] Binding of 2-KG to the apoenzyme prevented subsequent incorporation of iron, so it was postulated that 2-KG occludes the metal binding site.[123] In prolyl hydroxylase, iron binding to the enzyme was proposed to require three ligands, at least one of which may be cysteinyl thiolate.[124–126] The identity of the other ligands is unknown and much work remains to be done. The only biophysical data available for the iron center come from EPR studies. In the absence of substrate or 2-KG, a signal appears at $g = 4.3$, typical of high-spin ferric ion.[127] Upon addition of 2-KG, the amplitude of this signal increases, possibly indicating stronger coordination of ferric ion to the enzyme in its presence. Upon further addition of $AscH_2$, the $g = 4.3$ signal decays with concomitant growth of a signal at $g = 2$. The role of ascorbate therefore appears to be to reduce the ferric form of the enzyme.

Despite the lack of detailed information about the coordination environment of the iron center in prolyl hydroxylase, a mechanism consistent with all the experimental evidence has been proposed (Figure 7).[120] The mechanism consists of five main steps: (1) dioxygen binding to form ferric superoxide; (2) attack of superoxide on bound 2-KG; (3) decomposition of 2-KG into CO_2 and a succinate-bound ferryl; (4) attack by ferryl on the C-4 of proline; and (5) product release. Under normal turnover conditions, the iron returns to its original ferrous state at the end of the catalytic cycle. Several lines of evidence support this mechanism. First, substoichiometric amounts of ascorbate are consumed during turnover, whereas, in the absence of substrate, 1 mol of ascorbate is consumed per mole of CO_2 produced.[128–130] If the enzyme is reconstituted with ferrous ions, the initial rate of oxidation is constant whether or not ascorbate is present, but falls off within the first minute.[131] This behavior indicates two parallel pathways, a productive one leading to hydroxylated substrate and regenerated ferrous ion, and a nonproductive one that leaves the enzyme stranded in the ferric state unless ascorbate is present to reactivate it. Such a stepwise mechanism is consistent with kinetic and EPR data showing a multiphase reaction, including an initial activation step and CO_2 release at different rates than the appearance of dehydroascorbate.[127,130] Furthermore, the mechanism explains the very small observed intermolecular deuterium kinetic isotope effect. The rate-determining step involves enzyme binding and release of the cofactors and substrates, none of which is involved in the C–H bond-breaking step.[120] The active ferryl species turns over whether or not substrate is in place, leading to the substoichiometric reduction of $AscH_2$.[132] Additional work to reveal the structural features of this and other 2-KG enzymes is necessary to understand fully the attributes of this system that are responsible for its robust nature and widespread use in biology. Furthermore, the enzymes are good targets for potential trapping of non-heme ferryl species through adjustments in the cofactor–enzyme interactions. Several cofactor analogs have already been studied in detail from a kinetic perspective,[122,129,133] but do not appear to have been used in attempts to obtain spectroscopic evidence for this elusive high-valent iron species. Model studies using ferrous benzoyl formate complexes have been able to duplicate the 2-keto acid decarboxylation reaction with concomitant oxidation of phenols to biphenols.[134,135] The nature of the active intermediate has not yet been determined, however.

The portion of the mechanism that remains murky pertains to the reaction of the ferryl species with substrate. For prolyl hydroxylase, it is difficult to approach this question because the substrate is a protein, typically $(Pro\text{-}Pro\text{-}Gly)_x$, in the in vitro assays.[136] Possibly this phase of the mechanism might be clarified through investigation of alternative enzymes such as thymine 7-hydroxylase.[137] This enzyme hydroxylates the exocyclic methyl group of thymine, but recent work has shown that it can epoxidize olefins, oxidize thiol ethers to sulfones and sulfoxides, and demethylate the 1-methyl group of 1-methylthymine.[138]

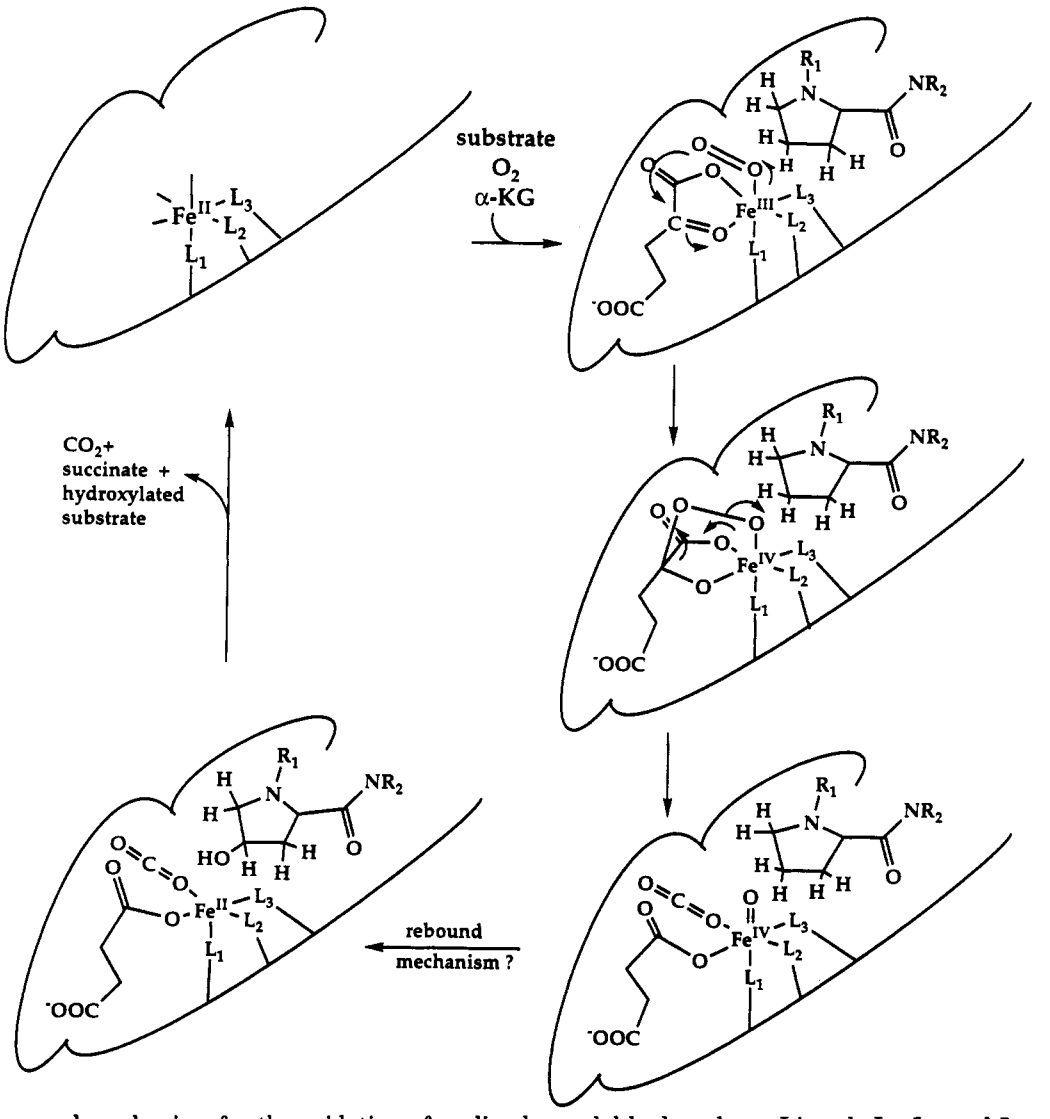

Figure 7. Proposed mechanism for the oxidation of proline by prolyl hydroxylase. Ligands L_1, L_2, and L_3 are amino acid residues. R_1 and R_2 are the peptide attachments of the proline substrate. (Adapted with permission from ref 120.)

It therefore mimics all the activities associated with the putative ferryl species of the heme system cytochrome P-450.[40] Currently, only an outline of this activity has been elucidated, but the mechanistic results are sure to add greatly to our understanding of species involved in the reactions of non-heme iron proteins with dioxygen.

5. *Isopenicillin N Synthase*

The final mononuclear enzyme to be discussed is isopenicillin N synthase (IPNS), a polypeptide with a molecular weight of 37–40 kDa depending on the species from which it is isolated.[139–141] This iron(II)-containing enzyme differs substantially from those previously discussed in that, although dioxygen is consumed in the reaction, the substrate, δ-[5-amino-5-(hydroxycarbonyl)pentanoyl]-L-cysteinyl-D-valine (ACV), is not oxygenated. Instead, a process called desaturative cyclization occurs in which the loss of hydrogen atoms results in ring closure.[139–141] The overall reaction shown in eq 27 results in the stereospecific formation of both the β-lactam and thiazoline rings. The two ring-forming steps occur with retention of configuration, and the complete process consumes 1 equiv of dioxygen.[142,143]

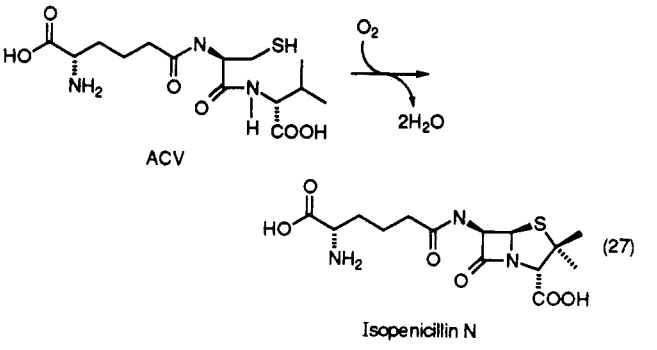

(27)

Since two covalent bonds are formed, the transformation results in no net change in iron oxidation state although transient, high-valent species are proposed as discussed below.

Whereas many of the mononuclear iron(II) enzymes discussed above have poorly understood metal centers, extensive spectroscopic data on IPNS provide as clear a picture of the active site as possible without a crystal structure. Mössbauer,[144,145] EPR,[144–146] NMR,[146,147] EXAFS,[148,149] and optical spectroscopy,[144–146] summarized in Table 2, have been used to construct a model (Figure 8) in which the low-spin octahedral iron(II)

Table 2. Spectroscopic Properties of Isopenicillin N Synthase[a]

	parameter	IPNS, no substrate	IPNS + NO, no substrate	IPNS + NO + ACV	IPNS + ACV
Mössbauer	D, cm^{-1}		14	14	
	E/D		0.015	0.035	
	ΔE_Q, mm s^{-1}	2.70	−1.0	−1.2	3.40
	η		0.1	1.0	
	δ, mm s^{-1}	1.30	0.75	0.65	1.10
	T, K	4.2	4.2	4.2	4.2
EPR	g	n.o.	4.09	4.22	n.o.
			3.95	3.81	
			2.0	1.99	
	E/D		0.015	0.035	
	S		$^3/_2$	$^3/_2$	
optical	λ, nm	none > 280	340	508 (1600)	none > 280
	(ϵ, M^{-1} cm^{-1})		430	720	
			600		

[a] Data from refs 144 and 145. n.o. = not observed.

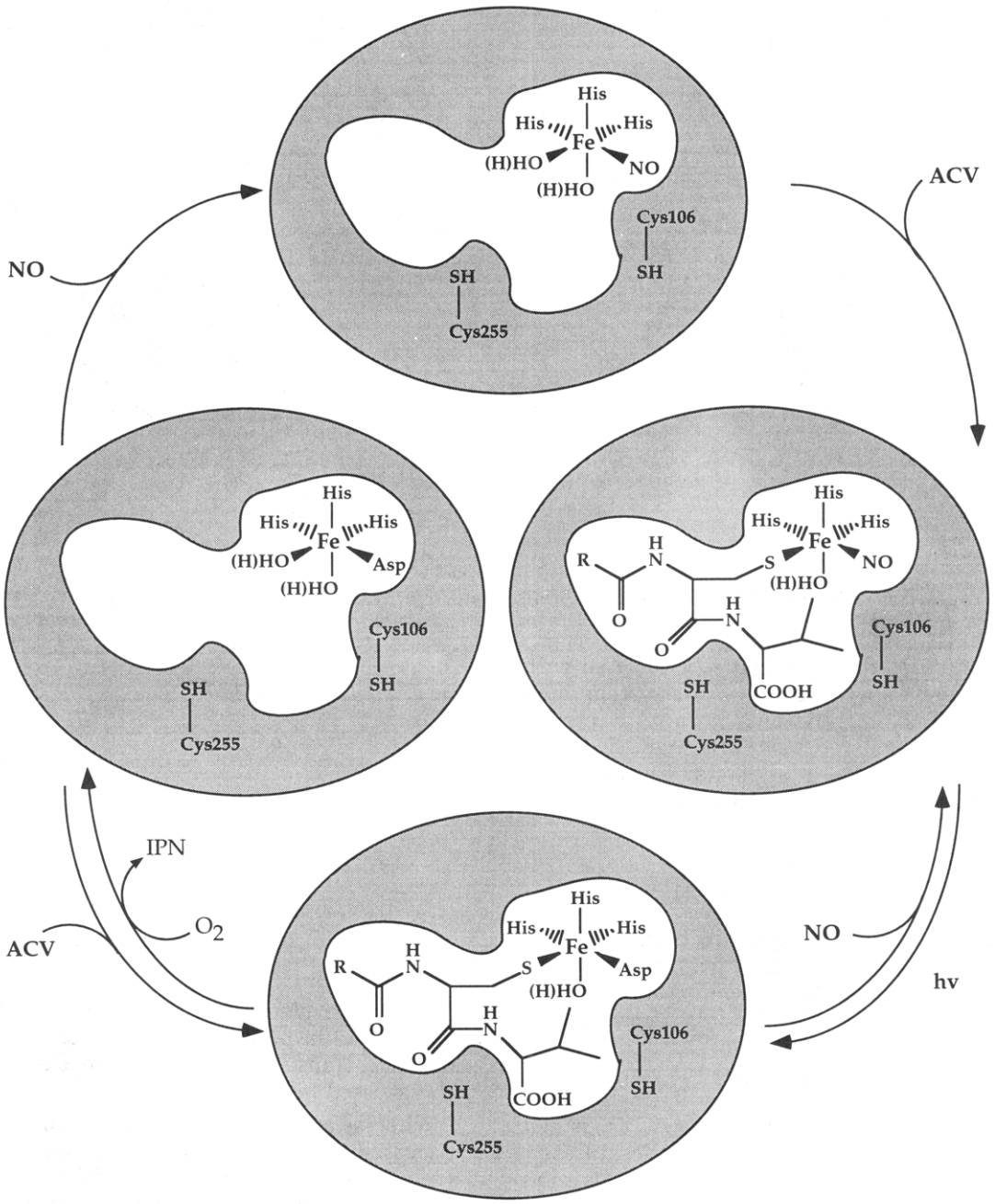

Figure 8. Proposed structure of the isopenicillin N synthase (IPNS) active site in its native, substrate bound, and nitrosyl forms. The relative positions of the ligands around the iron center are arbitrary. (Adapted with permission from ref 145.)

center is coordinated to one aspartate and three histidine residues in the resting state. There are two conserved cysteine residues that affect the reactivity of the enzyme, but are not essential to catalysis, as shown

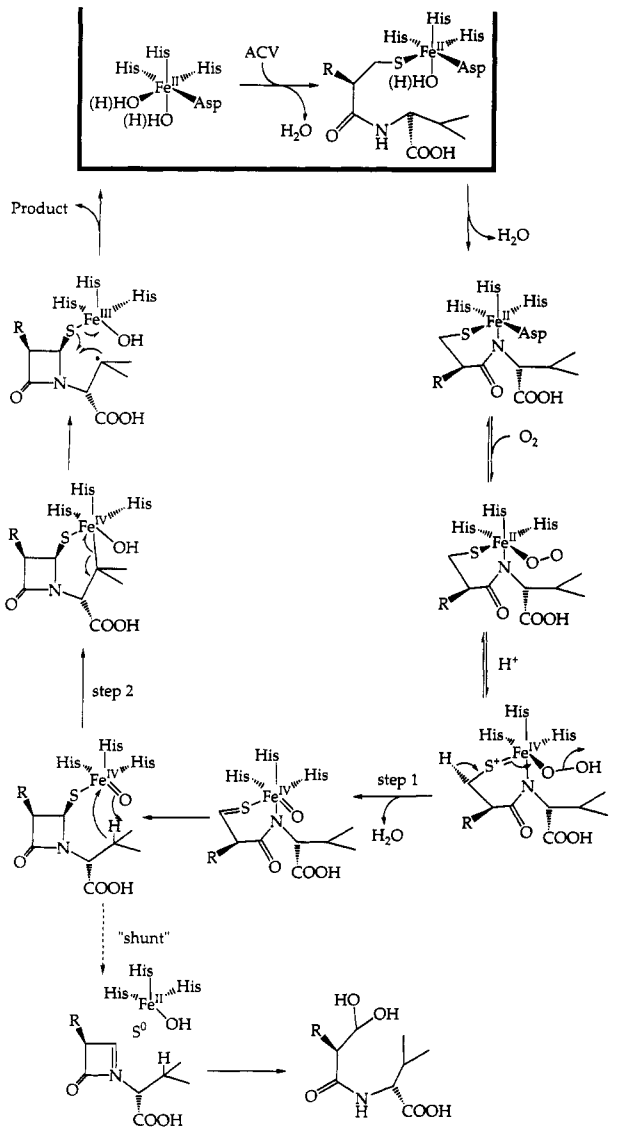

Figure 9. Mechanism proposed for the desaturative cyclization of ACV by isopenicillin N synthase. Steps 1 and 2 refer to processes affected by isotopic labeling of the depicted hydrogen atom. The shunt pathway is written as a branch between steps 1 and 2, but is generally not observed for the ACV substrate. The existence of this pathway is postulated on the basis of studies using substrate analogs and deuterated ACV. (Adapted with permission from ref 159.)

by mutagenesis experiments.[150,151] Upon addition of substrate, spectroscopic changes occur at the iron center consistent with direct coordination.[144-149] It has been postulated that, under anaerobic conditions, the peptide substrate coordinates through the cysteinyl sulfur. Binding of NO has been used to probe the structures of the O_2 and substrate adducts formed immediately prior to turnover, with somewhat conflicting results.[145,147] NO is postulated to displace either a histidine[147] or an aspartate residue.[145] In either case, coordinated water or hydroxide occupies the remaining coordination site(s).

The foregoing spectroscopic studies have not provided much evidence regarding the nature of the enzyme mechanism, however, and in work with the natural substrate, no intermediates, such as a monocyclic peptide, have been observed.[140] On the other hand, substrate analogs and isotopic labeling experiments have revealed several features of the reaction mechanism.[140,152-159] A current model, which is comprised of multiple steps, is presented in Figure 9. Two hydrogen atom positions exhibit large kinetic isotope effects when deuterated substrate is used. Cleavage of these two C–H bonds, designated as steps 1 and 2 in Figure 9, is therefore important in initiating the respective ring closure reactions. As indicated, four-electron oxidation of the substrate–iron complex occurs prior to the closure of either heterocycle. Two of the oxidizing equivalents are used to oxidize the cysteinyl sulfur of the substrate while the other two electrons convert Fe(II) to ferryl, Fe(IV). An internal rearrangement then occurs to generate a monocyclic intermediate bound to the ferryl through the sulfur atom. Evidence for this intermediate can be derived from so-called "shunt" substrates that fail to undergo closure of the thiazolidine ring. These tripeptide substrates fall into several classes including some deuterated at the valine C-3 position or others containing homocysteine instead of cysteine.[140,159] The ferryl complex is then proposed to insert into the carbon–hydrogen bond at the valine C-3 position to form the organo–iron species shown in Figure 9. This intermediate then cleaves the Fe–C bond homolytically to eliminate, after rearrangement, product and water, while returning the enzyme to its initial iron(II) oxidation state.

The participation of a ferryl in this phase of the reaction has been supported by several experiments using amino acid analogs in place of valine. One of these derivatives, designed to show the role of a ferryl through the interception of the radical intermediate, contained a cyclopropyl group attached to the substrate.[152,160] Upon incubation with IPNS and dioxygen, a 3:1 ratio of ring-opened to unrearranged products was observed, indicative of a radical intermediate. An intermediate containing a weak iron–carbon bond capable of radical dissociation could explain these results and has been proposed.[152,161] Certain other derivatives, notably those containing allylglycine residues in place of valine, were oxygenated by IPNS in reactions remarkably similar to those of cytochromes P-450.[140] In these cases, the incorporated oxygen atom derived primarily from dioxygen.

B. Proteins with Diiron Centers

1. Hemerythrin

Hemerythrin (Hr) is the oxygen-carrier protein in marine invertebrates including sipunculids, annelids, priapulids and brachiopods. It functions in a manner directly comparable to the mammalian proteins myoglobin and hemoglobin.[12,14,54,162,163] In most species, the protein is an octamer although monomeric and other oligomeric forms are known. Each subunit, ranging in molecular weight from 13.5–13.9 kDa, contains two ligand-bridged iron atoms.[14] There are two major classes of hemerythrins, those exhibiting cooperative binding of O_2 and those that do not. Unless otherwise specified, all studies mentioned here refer to non-cooperative hemerythrins.

The crystal structures of oxyhemerythrin[164] and higher resolution structures of oxy, deoxy, met, and azidomet forms of the protein have been solved.[47,165-168] This extensive structural work revealed that the basic three-dimensional motif of the protein is evolutionarily

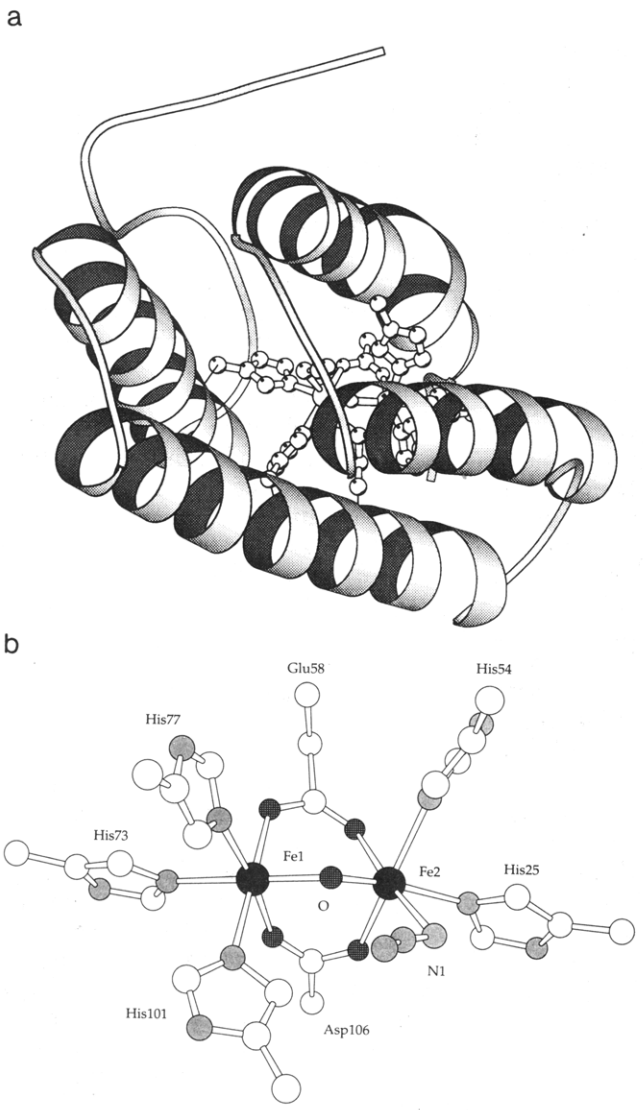

Figure 10. (a) MOLSCRIPT[363] drawing of azidometHr showing the active site and protein fold and (b) schematic diagram of the diiron center in azidometHr.

conserved[169] and confirmed many predictions made based on a variety of biophysical studies. Together with the available spectroscopic,[170–176] kinetic,[177–181] and thermodynamic[177,178] data on the reaction of the dinuclear iron center in Hr with dioxygen, the structural details make this protein one of the best understood of all non-heme iron systems.[12,14,162,163,182]

The structure of Hr is shown in Figure 10. The dinuclear iron center, which residues within a 4-helix bundle, has several distinguishing features. In the reduced, deoxy form, the core is asymmetric, having one 5-coordinate and one 6-coordinate iron atom. Two protein carboxylates and one solvent-derived hydroxide bridge link the two iron atoms. In the met and oxy forms, the bridge is deprotonated. Terminal ligation sites are filled by nitrogen atoms donated from the imidazole side chains of five histidine residues and, in the met and oxy forms, by an additional, exogenous ligand. Key distances and angles are presented in Table 3. One of the more important findings of the structural work was proof that, upon reaction of dioxygen with the diiron(II) core, hydroperoxide coordinates in a bent, end-on fashion to one of the ferric ions. Binding of dioxygen to deoxyHr is a two-electron transfer reaction,

Table 3. Average Bond Distances (Å) and Angles (Deg) in the Different Forms of Hr[a]

	deoxy	oxyHr	metHr	azidometHr
Fe1–Glu58	2.33	2.20	2.26	2.17
Fe1–His73	2.23	2.22	2.22	2.24
Fe1–His77	2.21	2.18	2.15	2.20
Fe1–His101	2.24	2.21	2.15	2.22
Fe1–Asp106	2.17	2.13	2.08	2.15
Fe1–O	2.15	1.88	1.92	1.80
Fe2–His25	2.15	2.14	2.07	2.21
Fe2–His54	2.28	2.25	2.23	2.24
Fe2–Glu58	2.140	2.20	2.04	2.25
Fe2–Asp106	2.14	2.15	2.08	2.09
Fe2–O	1.88	1.79	1.66	1.79
Fe1–Fe2	3.32	3.27	3.25	
Fe1–O–Fe2	111	125	127	135
O–peroxy O_2		2.80		
Fe2–peroxy O1		2.15		
Fe2–N1				2.34

[a] Data taken from refs 47 and 166. See Figure 10 for labeling scheme.

predicted as early as 1955 on the basis of extraction studies with iron chelators.[183] More conclusive evidence was later provided by spectroscopic work (Table 4). Mössbauer spectra of deoxyHr display a single quadrupole doublet at 4.2 K with isomer shift (δ = 1.14 mm s^{-1}) and quadrupole splitting parameters (ΔE_Q = 2.76 mm s^{-1}) indicative of high-spin Fe(II).[184] The spectrum of oxyHr, on the other hand, has two distinct doublets with similar isomer shifts (δ = 0.51, 0.52 mm s^{-1}) but different quadrupole splitting parameters (ΔE_Q = 0.91, 1.93 mm s^{-1}), consistent with an asymmetric, antiferromagnetically coupled diferric site.[14,184] Resonance Raman spectroscopy revealed the presence of a ν_{O-O} stretching band at 844 cm^{-1}, characteristic of bound peroxide ion.[174] Assignment of this band was further verified by isotopic labeling experiments.[170,171]

The bent peroxide moiety in oxyHr can have two extreme orientations relative to the iron core, *syn* or *anti*, binding modes e and f, respectively, in Figure 3. The crystal structure of oxyHr revealed exclusively the *syn* orientation, which allows for hydrogen bonding between the hydroperoxide ligand and the oxo bridge. The O···O distance between these two units is 2.8 Å,[47] well within the range of hydrogen-bonding interactions. Proof for the existence of a hydrogen bond to the coordinated hydroperoxide was provided by resonance Raman studies of oxyHr. Spectra of samples prepared in H_2O versus D_2O were compared. The ν_s (Fe–O–Fe) bend in oxyHr shifts by 4 cm^{-1} toward higher energy in D_2O.[172] With the sole exception of hydroxymetHr, a derivative that can also use a proton to form a hydrogen bond with the oxo bridge, no other form of the protein exhibited such a deuterium isotope effect. The reaction of deoxyHr to form oxyHr can therefore be written as indicated in eq 28, in which a proton from the hydroxo bridge is shuttled to the newly formed peroxide upon binding and reduction of dioxygen.

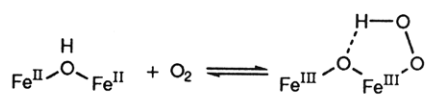

(28)

The protonation state of the bound peroxide in oxyHr has some interesting consequences. Protonation removes electron density from the oxygen p orbitals, which

Table 4. Spectroscopic Properties of the Different Forms of Hr

		deoxyHr	oxyHr	metHr	azidometHr	ref
Raman	ν_s(Fe–O–Fe), cm^{-1}		486	510	507	366
	ν_{as}(Fe–O–Fe), cm^{-1}		753	750	768	366
	ν(O–O), cm^{-1}		844		2050[a]	170
	ν(Fe–L), cm^{-1}		503		375	12
optical	$^6A_1 \rightarrow {}^4T_2(^4G)$		750 (210)		680 (190)	12
	λ, nm (ϵ, M^{-1} cm^{-1})					
	$^6A_1 \rightarrow {}^4T_1(^4G)$		990 (10)		1010 (10)	12
	λ, nm (ϵ, M^{-1} cm^{-1})					
	charge transfer		500 (2200)		445 (3700)	12
	(ϵ, M^{-1} cm^{-1})					
magnetics	J, cm^{-1} [b]	−15	−90	−130		12
CD	CD max, nm ($\Delta\epsilon$, M^{-1} cm^{-1})		520 (−2.5)		500 (−4.3)	12
	excitation max, nm		525		490	12
Mössbauer	Fe1 δ, mm s^{-1}	1.14	0.51	0.46	0.51	14
	Fe1 ΔE_Q, mm s^{-1}	2.76	0.91	1.57	1.96	14
	Fe2 δ, mm s^{-1}		0.52		0.51	14
	Fe2 ΔE_Q, mm s^{-1}		1.93		1.47	14
EPR		silent	silent			12

[a] ν(N–N), from ref 171. [b] These values are reported using the convention $\mathcal{H} = -2JS_1 \cdot S_2$.

otherwise might form π-bonds to the metal d orbitals. Such weakening of the π-interaction might facilitate dissociation of dioxygen and return to the ferrous, deoxy form of the protein.[173] Non-cooperative hemerythrins do not exhibit any pH-dependent kinetic or thermodynamic changes in their dioxygen-binding properties. This striking insensitivity to pH has been ascribed to the internal proton transfer mechanism of eq 28.[185]

Kinetic studies of the dioxygen-binding reaction have been carried out for several forms of Hr.[177-181] Kinetic constants measured by temperature-jump relaxation, stopped-flow, and laser-photolysis techniques are in relatively good agreement with one another. A summary of the results is given in Table 5, together with corresponding values for the oxygenation reactions of hemoglobin and myoglobin for comparison purposes. The rate of Hr oxygenation is limited by the diffusion of O_2 to the diiron(II) binding site.[179] As expected for an oxygen transport or storage protein, oxyHr has good stability ($K_d \approx 10^{-6}$), and oxidation to the inactive met form is highly disfavored. Some of the early studies on the kinetics of oxygenation reported biphasic behavior that was ascribed to multiple binding geometries or sample heterogeneity;[177] for these cases, initial reaction velocities were measured. Biphasic kinetics were also observed in laser photolysis investigations of Hr and attributed to solution viscosity effects.[186] In at least one experiment significant changes in the kinetic parameters occurred under different salt conditions.[178] The enthalpy and entropy of the oxygenation reaction have been measured for some hemerythrins (*Themiste zostericola*, *Siphonosoma nudus*, and *Golfingia gouldii*) and are in reasonably good agreement.[177-179]

Kinetic isotope effect (KIE) experiments carried out on the oxygenation reaction revealed an interesting difference from results for hemoglobin and myoglobin.[185] In Hr, only the dissociation rate constant (k_{off}) was affected by changing to D_2O as solvent (k_H/k_D = 1.2); k_{on} was unaffected. In the heme systems, both the binding and the dissociation rates had KIE values of $\approx$1.2.[185] These small isotope effects are consistent with hydrogen-bonding interactions stabilizing the oxygenated forms of the proteins, but equally well could reflect internal proton transfer reactions within the active site. The lack of a KIE for the O_2 binding reaction in Hr indicates that the proton-transfer step is more important for dioxygen release than uptake by the protein.

One puzzling aspect of Hr oxygenation chemistry is the nature of the cooperativity displayed for certain species. This behavior is pH dependent. Lowering the pH results in a sharp loss of cooperativity between pH 7.6 and 7.0,[180] implying that cooperativity depends upon a specific protonation event. The cooperative versus non-cooperative oxygenation reaction rate is strikingly different for *T. zostericola* (Table 5). The rate of binding is 10 times faster for the non-cooperative form of the protein. This difference in activity has been ascribed to a two-state model for allostery,[180] suggesting that the rate of interconversion between the two affinity forms is much slower than the rate of dioxygen binding. More recently, it was shown that, although the subunits were initially thought to be identical, in the cooperative species they are in fact not so.[187] The source of the cooperativity is therefore presumed to be an interaction at the subunit interface. Studies of the allostery by resonance Raman spectroscopy revealed a shift in the O–O stretching frequency as a function of pH in cooperative systems.[175] No such shift was observed for non-cooperative hemerythrins nor was a pH dependent effect observed for the Fe–O stretching vibration. In each case, cooperativity was observed only at higher pH values under dioxygen saturating conditions.[175] From this evidence, it was proposed that the cooperativity reflects a structural change that takes place after O_2 binding, in contrast to the nature of the cooperativity found in hemoglobin where the binding affinity of the deoxyHb is affected by a structural change.[188]

The specific model for cooperativity postulated to explain these results is shown in Figure 11. In this model, a hydrogen bond from the bound hydroperoxide to an unidentified protein residue is responsible for the shift to a high affinity form of Hr. This hydrogen bonding arrangement is preferred to one involving the hydroperoxide ligand and the oxo bridge because a change in the latter interaction would be expected to alter the Fe–O stretching vibration, which was not observed. Furthermore, no cooperative effects occurred in other oxidized forms of the protein such as azidometHr. The model is consistent with this behavior since it depends upon the specific geometric relation-

Table 5. Kinetic and Thermodynamic Data on the Reaction of Dioxygen with Hemerythrin

species	$k_{on} \times 10^{-6}$, $M^{-1}\ s^{-1}$	k_{off}, s^{-1}	$K_d \times 10^6$, M	$\Delta H^{\ddagger}_{on}$, kcal/mol	$\Delta S^{\ddagger}_{on}$, eu	$\Delta H^{\ddagger}_{off}$, kcal/mol	$\Delta S^{\ddagger}_{off}$, eu	ΔH, kcal/mol	ΔS, eu	Hill coefficient	conditions	ref
Lingula unguis (octamer, cooperative)	0.44	15	34								0.08 M phosphate, pH 6.8 at 17 °C, stopped-flow	181
	0.63	61	97							1.86[a] (1.11)	0.08 M phosphate, 0.1 M NaCl, pH 6.8 and/or pH 7.6 at 15 °C T-jump	180
Siphonosoma cumanense (trimer, non-cooperative)	11.3	9.1	1.24								0.08 M phosphate, 0.1 M NaCl, pH 6.8 at 15 °C T-jump	180
Themiste zostericola (monomer, non-cooperative)	78	315	4.0	4	−11	16.8	9	−23	−20		Tris, pH 8.2, I = 0.1 M at 25 °C T-jump	179
Themiste zostericola (octamer, non-cooperative)	7.5	82	10.9							1.1	Tris, pH 8.2, I = 0.1 M, at 25 °C T-jump	179
Golfingia gouldii (octamer, non-cooperative)	7.4[b]	51	6.9	8.2	1	20.6	19	−12.4	−18	1.1	Tris, pH 8.2, I = 0.015 M, at 25 °C T-jump	178
	12	43.1	3.6								0.1 M Na_2SO_4, pH 8.55, at 25 °C in H_2O T-jump, stopped-flow	185
	12	35	2.9								0.1 M Na_2SO_4, pH 8.55, at 25 °C in D_2O T-jump, stopped-flow	185
Siphonosoma nudus (octamer, non-cooperative)	26	120	4.6			12.7[c]		−10.5		1.15	0.1 M phosphate, pH 7.0, at 25 °C T-jump	177
	29[d]			−4.4 ± 0.5[c]							Tris, pH 8.2 or phosphate pH 7.0 laser photolysis	186
deoxymyoblobin (sperm whale muscle)	19	11	0.58	6–7[e]		19–21[e]					0.1 M phosphate, 0.1 M KNO_3, pH 7.0 at 20 °C T-jump	368
deoxyhemoglobin human erythrocyte, fourth oxygen	33	50	1.5								0.1 M phosphate, pH 7.0 at 21.5 °C stopped-flow	369

[a] The first values is for pH 7.6, the value in parenthese is for pH 6.8. [b] A strong ClO_4^- effect was observed in this study. [c] This value is an activation energy, not an activation enthalpy. [d] A strong viscosity effect was observed during this study. [e] Data point from ref 367.

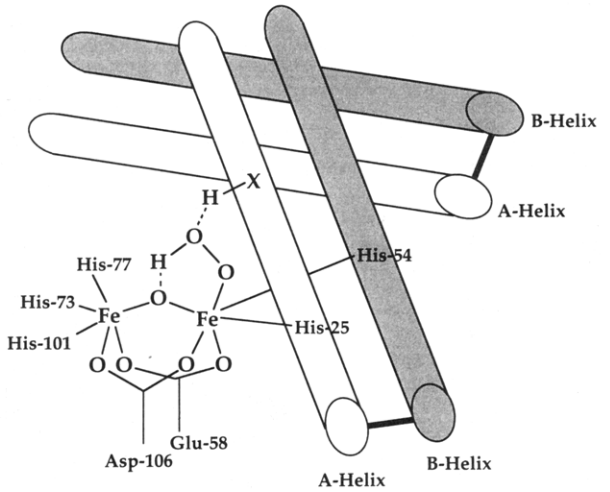

Figure 11. Schematic model for the dinuclear iron center in a cooperative oxyHr. The A- and B-helices of the α-subunit are assumed to be in contact with the A- and B-helices of the β-subunit. The unknown residue X is postulated to form a hydrogen bond to the bound hydroperoxide as discussed in the text. (Adapted with permission from ref 175.)

ships between the hydrogen-bond donor and acceptor pairs of the hydroperoxide ligand and protein residue.

The foregoing proposals to explain the nature of the cooperativity are compatible with one another. Hydrogen-bond formation between the protein side chain and the bound hydroperoxide should be fast, but propagation of the structural changes down the α-helix might not be as rapid. The nature of the changes in the coordination environment of a diiron(II) site transmitted to another subunit is uncertain and likely to be subtle. The motion of the helix following the formation of the proposed second hydrogen bond to the coordinated hydroperoxide might result in a more favorable alignment of the equivalent hydrogen bond at a distant site, but there is no experimental evidence to support such a proposal. Further work on the nature of the cooperativity is required to define the reorganization involved and could be approached by site-directed mutagenesis experiments.

As a final consideration, we now address the specificity of the reaction of deoxyHr with dioxygen. A problem common to most dioxygen-utilizing ferrous proteins is oxidation to the inactive, ferric (met) form. In the case of Hr, such oxidation can result from dissociation of hydrogen peroxide from oxyHr. The dissociation rate of HO_2^- has been estimated to be approximately 1.0×10^{-5} s^{-1}.[12] This slow dissociation rate is postulated to be a result of the extremely hydrophobic nature of the hemerythrin dioxygen-binding pocket. Reactions of hemerythrins with alternative oxidants are quite slow in the absence of anionic ligands but significantly enhanced by their presence.[189] The semimet, $Fe^{II}Fe^{III}$, form has also been investigated, but is unstable with respect to disproportionation without an external reductant or oxidant. This instability reflects the preference of the diiron core in Hr to undergo two-electron redox steps,[162] a feature that is both interesting and important. The propensity of dioxygen to be reduced in two-electron steps was mentioned above, and we now see that this preference is shared by the dinuclear iron center in Hr. In this system, the electron-transfer properties of the dinuclear metal site and the exogenous ligand are beautifully tuned to accommodate one another. As discussed below, not all dinuclear iron sites in proteins and models present metastable mixed-valent forms.

The foregoing discussion illustrates several important features about the reaction of O_2 with a diiron(II) center. DeoxyHr reduces dioxygen to the peroxide level and the resulting hydroperoxide is stabilized by the protein sheath. As will be shown, most of the other systems use all four oxidizing equivalents of the O_2 molecule. The stability of the ferric hydroperoxide complex in Hr results in part from hydrogen bonding to the oxo bridge, inaccessibility to reactive diiron(II) units in adjacent subunits, and possibly the nitrogen-rich histidine ligand environment of the core. These features render Hr unique among non-heme iron systems and are shared to some extent by the coordination spheres of the reversible dioxygen-binding heme proteins Hb and Mb. As will be discussed, one small molecule system, the hydroxo-bridged diiron(II) complex $[Fe_2(Me_3TACN)_2(OH)(OAc)_2]^+$, mimics several of the structural and spectroscopic properties of the deoxyHr core quite accurately. It lacks an open coordination site on iron(II) ion for dioxygen binding, however. Kinetic studies on its oxidation (discussed below) indicate that, following a carboxylate shift reaction to free an O_2-binding site, the compound reacts with dioxygen but fails to do so in a reversible manner because the oxygenated intermediate attacks a second equivalent of the diferrous complex to form, ultimately, $2[Fe_2(Me_3TACN)_2(O)(OAc)_2]^{2+}$.[190-192] These results show that simply recreating the coordination environment of iron in the Hr core is not necessarily sufficient to model the activity of the protein. Secondary interactions such as hydrogen-bonding relationships might be necessary to stabilize properly a peroxide species, rendering it less reactive toward reductive decomposition.

2. Methane Monooxygenase

This enzyme system is currently one of the most intensively studied non-heme iron proteins. Recent investigations of the three-dimensional structure of the hydroxylase component and its catalytic mechanism have yielded significant insights into the workings of this enzyme. MMO is a mixed-function oxidase; one atom of O_2 is transferred to substrate and the other forms water. As indicated in eq 29, the system converts

$$CH_4 + O_2 + H^+ + NADH \rightarrow CH_3OH + H_2O + NAD^+ \quad (29)$$

methane to methanol in a process that is coupled to the oxidation of NADH. Several forms of MMO exist including soluble and membrane-bound varieties.[193,194] Only the soluble form contains iron, the other having copper as its redox active metal ion. Most studies have focused on MMO isolated either from *Methylococcus capsulatus* (Bath) or *Methylosinus trichosporium* (OB3b), which differ in the temperature at which they operate (45 °C versus ambient, respectively), their morphology, and metabolic pathways following methane hydroxylation. The active-site structures and hydroxylation mechanisms of MMOs from the two different organisms share many common features, but

Table 6. Spectroscopic Properties for the Different Forms of MMO Hydroxylase

		M. trichosporium (OB3b)				*M. capsulatus* (Bath)			
		H_{red}	H_{mv}	H_{ox}	ref	H_{red}	H_{mv}	H_{ox}	ref
optical	λ_{max}, nm			282	201			280	208
magnetics	J,[a] cm^{-1}	0.35	−30	−7 ± 3	371–373		−32		208
Mössbauer	Fe1 δ, mm s^{-1} (T, K)	1.3 (4.2)	0.48 (150)	0.51 (4.2)	371	1.30 (80)		0.50 (80)	208
	Fe1 ΔE_Q, mm s^{-1}	3.10	−1.3	1.16	371	3.014		1.05	
	Fe2 δ, mm s^{-1}	1.3	1.19	0.50	371				
	Fe2 ΔE_Q, mm s^{-1}	2.4–3.0	2.4	0.87	371				
ENDOR	A, MHz		13–23[b]		213		14–30[b]		212
EPR	g_x		1.94		211		1.92		208
	g_y		1.86		211		1.86		208
	g_z		1.75		211		1.71		208
	g_{av}	16	1.85	4.3	211		1.83		207
redox potentials	$E°$, mV vs NHE	21		76	220	−135		48	202
	$E°$, mV vs NHE + additives	−115[c]		−52[c]	220	<100[d]			202

[a] These values are reported using the convention $\mathcal{H} = -2JS_1 \cdot S_2$. [b] This signal arises from the hydroxide bridge; other resonances not listed (see text). [c] Potential in the presence of B. [d] Two electron addition in the presence of B, reductase, and substrate.

there are some interesting differences manifest in the mechanistic studies to be discussed below. One of the current goals in this field is to define the unifying features of the reaction and to understand or reconcile conflicting results.[195–199]

The MMO enzyme system contains three proteins, a hydroxylase, housing two dinuclear non-heme iron centers, a reductase containing one FAD and one [2Fe-2S] cluster, and protein B, a coupling unit that facilitates electron transfer from the reductase to the hydroxylase and modulates the properties of the latter.[200–203] In this review we focus primarily on the dinuclear iron core in the hydroxylase and its reactions with dioxygen. For more general discussions, other recent works can be consulted.[9,12–15,199–208]

The hydroxylase protein has an $\alpha_2\beta_2\gamma_2$ composition with a molecular weight of 251 kDa.[201,209] The crystal structure of the oxidized *M. capsulatus* (Bath) enzyme has recently been solved to 2.2 Å,[46] confirming, and considerably elaborating on, the structure that had been proposed based on spectroscopic and other evidence (Table 6). As shown in Figure 12, the diiron(III) centers reside in the α subunits, which are related by a noncrystallographic 2-fold symmetry axis, at a distance of 45 Å from one another. The distance between iron atoms in each dinuclear core is 3.4 Å, in good agreement with EXAFS studies of the oxidized hydroxylase.[208] The two iron atoms are bridged by a glutamate side chain, E144, a hydroxide ion, and an acetate ion from the crystallization buffer. The terminal ligands are comprised of two histidine nitrogens (H147 and H246), three carboxylate oxygen donors (E114, E243, and E209), and a water molecule which is hydrogen bonded to E114 and E243.

The presence of a hydroxo, rather than an oxo, bridge in the ferric enzyme was initially suggested from optical, EXAFS and magnetic studies. These experiments revealed the absence of the visible absorption band, short Fe–Fe distance, and large antiferromagnetic exchange coupling, features characteristic of diiron(III) centers containing oxo and carboxylate bridges.[207,208,210,211] The identity of the monoatomic bridge was recently established by ENDOR studies of the mixed-valent form of the hydroxylase which revealed spectra displaying anisotropic coupling of the unpaired electron to an exchangable proton assigned to hydroxide ion.[212,213] The proton ENDOR results also indicated the coordination of at least one water molecule to the dinuclear iron center, a feature also revealed by the X-ray structure of the *M. capsulatus* (Bath) hydroxylase.

The dinuclear iron center is positioned in the center of a 4-helix bundle in the α-subunit. The $[Fe_2(OH)]^{5+}$ moiety is bound by two Glu-X-X-His sequences, an i, $i + 3$ motif found in many metalloenzymes.[214,215] The exogeneous acetate bound to the diiron center may indicate the site at which dioxygen, substrate, or methoxide product interacts with the core, and further studies are in progress to address these questions. The carboxylate side chain of E243, hydrogen bound to the coordinated water, is properly situated to undergo carboxylate shift chemistry upon redox cycling of the system in a manner analogous to that observed in RR (see below).[216,217] The hydrophobic pocket adjacent to the active site of the hydroxylase is larger than the one found in R2 (see below) and contains a cysteine at the position corresponding to the location of Y122 in R2. Entry of substrate to this pocket may occur through the α-subunit where there are several contiguous hydrophobic cavities. The canyon that straddles the non-crystallographic 2-fold axis on one face of the enzyme is a possible site for binding component B. Docking of B along canyon walls comprised of two of the helices involved in iron coordination would allow the modulation of activity as discussed below.

Investigations of the redox properties of the diiron center in MMO hydroxylase reveal three accessible oxidation states, $Fe^{III}Fe^{III}$, $Fe^{III}Fe^{II}$, and $Fe^{II}Fe^{II}$.[218] As isolated, the enzyme is in the fully oxidized state, whereas the reduced form is the one that reacts with dioxygen. The mixed-valent hydroxylase is inactive, but has important physical properties, such as the ENDOR spectrum mentioned above, that have been used to characterize the protein. For the *M. capsulatus* (Bath) hydroxylase, the iron redox couples occur at +48 and −135 mV versus NHE[202] and are shifted toward slightly more negative potentials upon addition of substrate. Addition of a 1:1 mixture of protein B and reductase had a striking influence on the redox properties of the diiron core, however. In the presence of the

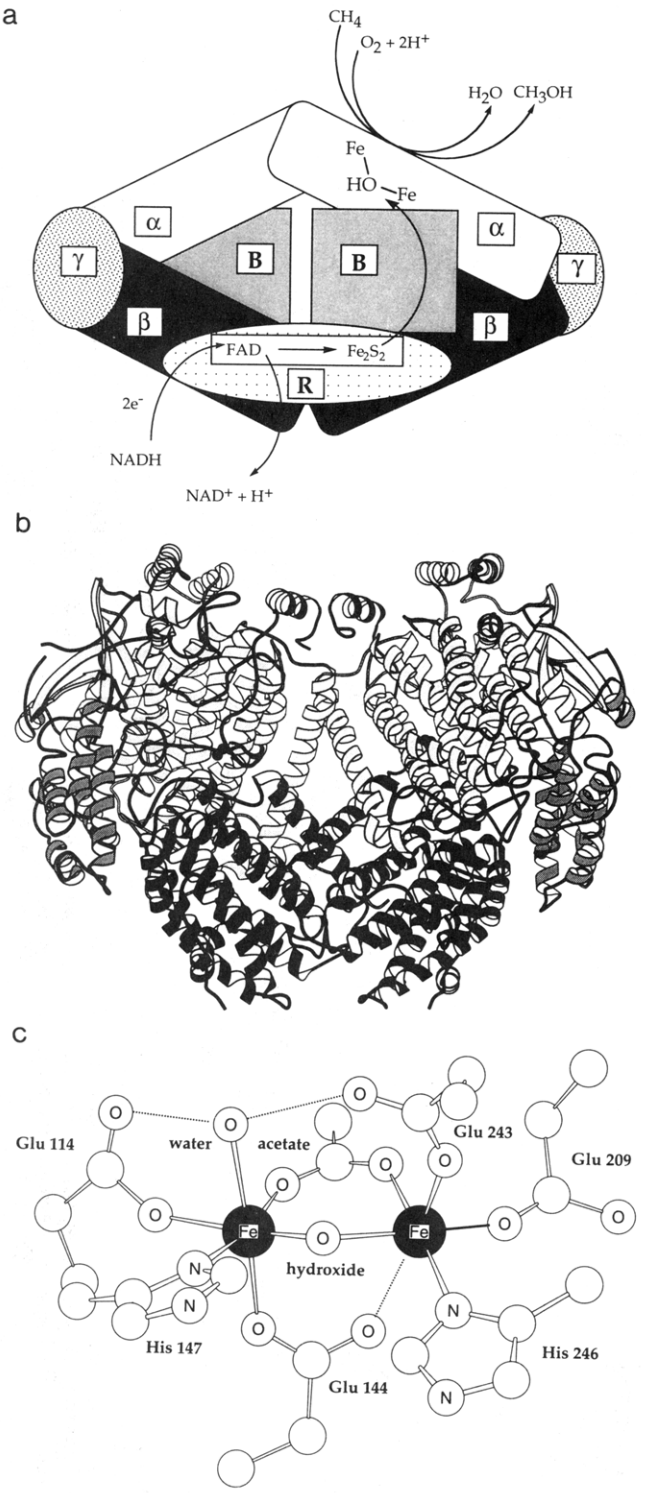

Figure 12. (a) Schematic drawing showing the quaternary structure of the active MMO hydroxylase–reductase–protein B complex from *M. capsulatus* (Bath); (b) MOLSCRIPT[363] ribbon drawing showing the protein fold of the MMO hydroxylase protein and the diiron center from *M. capsulatus* (Bath); and (c) schematic representation of the diiron center.

fully constituted protein system without substrate, the iron could not be reduced by dithionite in the presence of mediators even at −200 mV. In the presence of substrate, however, reduction occurred, and the potentials of the two redox steps were altered such that it was easier to add the second electron than the first. The system thus bypassed the inactive mixed-valent form of the hydroxylase; substrate binding triggered the reduction of iron and primed the enzyme for oxidation chemistry. Since alkanes are unlikely to bind directly to the dinuclear iron center, the effect must be indirect. For example, substrate binding might displace a bound water molecule or lead to a carboxylate shift.[219] Related studies have recently been reported for the *M. trichosporium* OB3b system, for which iron redox couples of +76 and +21 mV were obtained.[220] The addition of protein B shifted the reduction potentials of the dinuclear iron center by −132 mV. In the presence of B and reductase, there was no difficulty in reducing the protein with dithionite and mediators and the shift from a one-electron to a two-electron process was less clearly apparent, in contrast to the results for the *M. capsulatus* (Bath) protein. The differences between the two studies must be addressed by further work. The redox properties of MMO just discussed are quite different from those described above for Hr. The most notable difference is the relative stability of the mixed-valent species of the hydroxylase. Once generated, this $Fe^{II}Fe^{III}$ species can be purified and studied even though it is catalytically inactive.

Several general features of the MMO hydroxylation mechanism are understood. Dioxygen reacts with the reduced form of the enzyme, probably leading to the formation of a diiron(III) peroxide intermediate (Figure 13). One of the oxygen atoms then gets incorporated into substrate by a sequence of events currently being probed by several different experiments. The roles that substrate radicals and/or a ferryl intermediate might play are of primary interest. When no reductase is present, the reduced hydroxylase alone will function in a single turnover experiment yielding stoichiometric amounts of product and the diiron(III) form of the enzyme. The reductase is thus essential only for recycling the enzyme. It has become clear, however, that important effects are occurring which render the hydroxylase more efficient in the presence of the other two proteins.[202,203] Protein B, in particular, greatly accelerates the rate of hydroxylation. Elucidating the details of these interactions will require more work. One of the current approaches to this problem is to study the enzyme kinetics during single turnover experiments. This work has begun to yield information regarding discrete steps of the hydroxylation process. Previous studies using multiple turnover conditions revealed that electron transfer from the reductant to the diiron(III) hydroxylase is faster than the rate of hydroxylation.[204,205] The reduction step is therefore not rate limiting, leaving substrate binding, substrate release, or some step in the oxygenation as potential rate-limiting processes of the complete catalytic system.

Elaboration of the MMO hydroxylase mechanism is usually written in a manner that mimics the rebound mechanism postulated for cytochrome P-450 (Figure 13, path C)[40,195,221–223] because of similarities in the overall stoichiometry and substrates for the two systems. Both hydroxylate a wide variety of hydrocarbons and incorporate oxygen atoms from the dioxygen molecule with minimal solvent exchange. For the *M. trichosporium* hydroxylase, there is some evidence to justify the comparison with the generally accepted, if unproven, cytochrome P-450 mechanism. Radical clock studies using 1,1-dimethylcyclopropane gave ring-opened products consistent with the formation of both radical and carbocation intermediates.[195] Although the

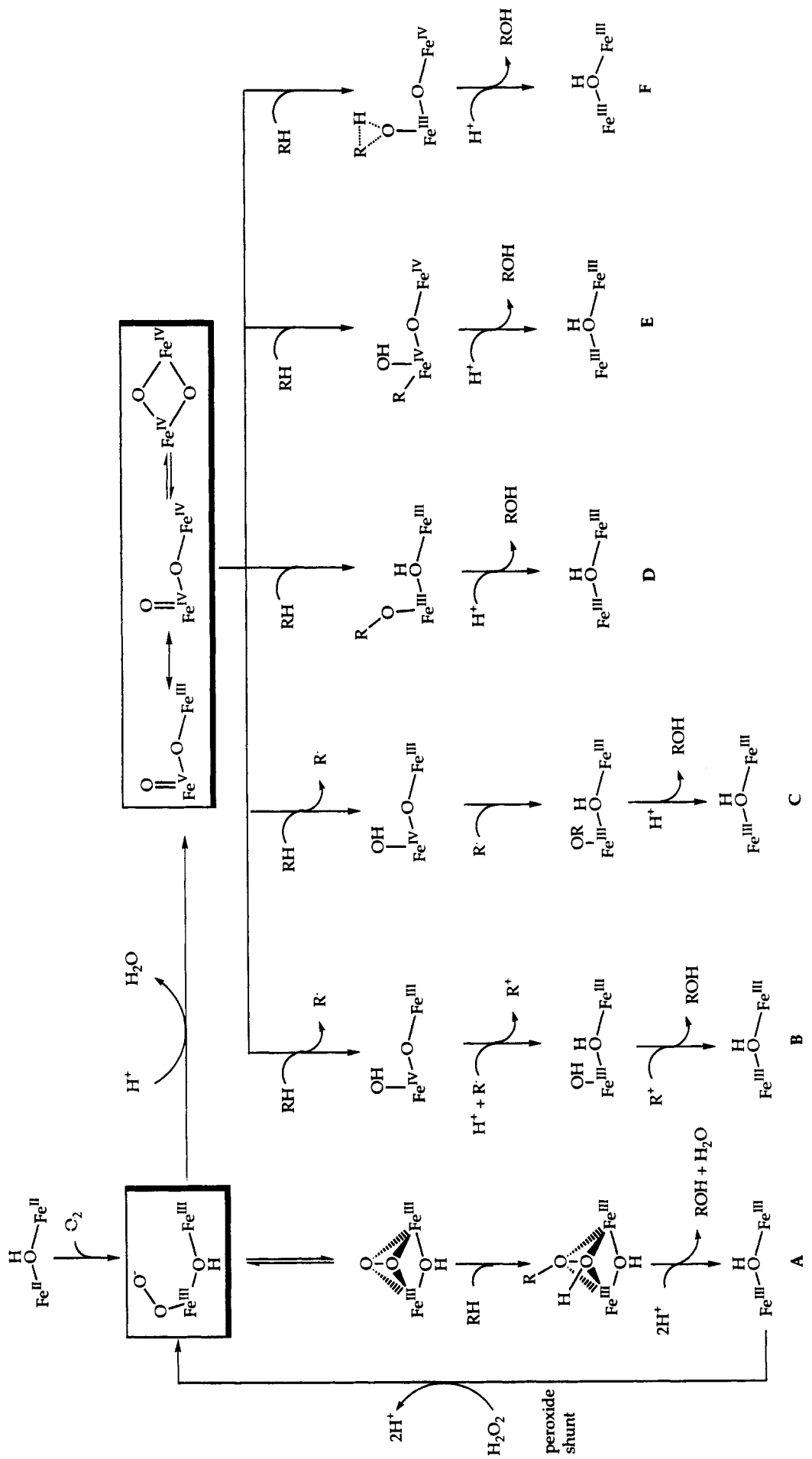

Figure 13. Mechanistic proposals for the hydroxylation of hydrocarbon substrates by MMO. Only the iron center and hydroxide bridge are shown. The other ligands have been removed for greater clarity. Pathway B follows the proposal put forth for *M. trichosporium* in ref 195. The radical, R·, refers to a substrate radical, but could potentially be either hydroxyl radical or a protein based species. Pathway C is the rebound mechanism directly analogous to that proposed for cytochrome P-450. Pathways A, D, E, and F are possibilities suggested for *M. capsulatus* based on ref 198. During enzyme turnover, the final oxidized state is returned to the active ferrous form by NADH reduction mediated by the reductase and coupling proteins.

Table 7. Percentage Distribution of ^3H Label in the Methylene Group of the (2*R*)-2-Acetoxy-2-phenylethanoate Derivative of the Samples Generated by MMO[a]

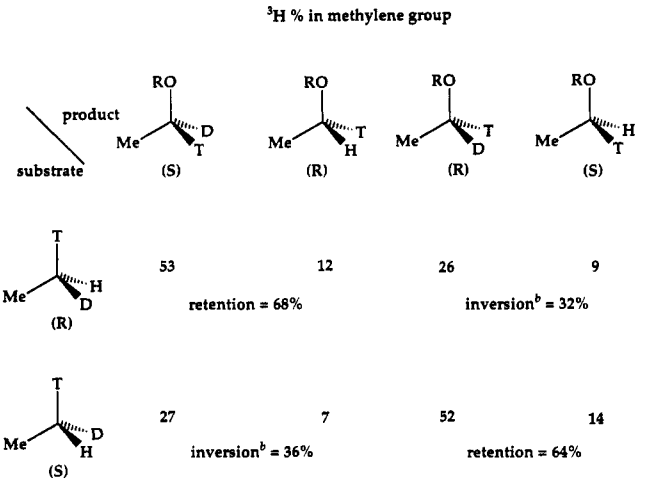

[a] Inversion/retention data have been corrected for the enantiomeric purity of the substrates. Data taken from ref 196. [b] Indicates configurational inversion is due to flipping of the intermediate radical.

yield of the ring-opened species was small, this result could be attributed to the use of a relatively sluggish radical clock. It was therefore proposed that the mechanism of MMO hydroxylation was similar to, but more complicated than, a simple rebound process. The mechanistic proposal from this study is shown as pathway B of Figure 13. Following generation of a high-valent ferryl intermediate, a hydrogen atom is abstracted to yield a substrate radical which is then oxidized by one electron and oxygenated. The rate constant measured for this rebound reaction is 2×10^{10} s^{-1}.[195]

Further support for a substrate radical intermediate was provided from studies using chiral ethane.[196] In this work, the stereochemistry of the hydroxylation of (*R*)- and (*S*)-[1-^{2}H,1-^{3}H]ethane by the *M. trichosporium* enzyme was examined. Retention of configuration predominated, but 35% inversion also occurred and an intramolecular deuterium kinetic isotope effect (KIE) of 4.2 was measured (Table 7).[196] The result supports a role for a substrate radical constrained within the enzyme-active site, but does not provide additional evidence for or against the possible presence of a carbocation. In addition, the observed KIE indicates a role for C–H bond cleavage in the rate-determining step of the hydroxylation reaction. This value falls outside the KIE range of 7–14 reported for P-450 systems.[40] By using a value of 0.5 kcal/mol for rotation around the C–C bond in the ethyl radical, one can calculate a radical rebound rate on the basis of the percentage of inversion, which yields a value of 6×10^{12} s^{-1}.[224] This rate is significantly faster than that measured from the aforementioned radical clock study.

In another study, *trans*-1,2-disubstituted and 1,2,2-trisubstituted cyclopropanes, some of the fastest known radical clock substrates, were used to measure radical rebound rates for both the *M. trichosporium* and the *M. capsulatus* (Bath) enzymes.[198] No evidence was obtained for radicals or carbocations with *M. capsulatus* MMO, although some previous studies using EPR spin traps had reported radical species.[225] The extremely fast ring opening rates [$(4–5) \times 10^{11}$ s^{-1}] for the substituted cyclopropyl radical clocks makes them ideal for studying putative short-lived intermediates in the oxidation pathway. The ratio of the rearranged to the unrearranged product alcohol is used to calculate the recombination rate for a potential substrate radical and, in this case, gave a maximum lifetime for the intermediate of 2.5×10^{-14} s.[198] The rebound must therefore take place in less than the duration of a single vibration, an unrealistically fast reaction rate for a cytochrome P-450 type mechanism. It is possible that binding of the radical clock substrate to the enzyme somehow slows down the rate of the ring opening, but this caveat was deemed unlikely on the basis of a semiquantitative analysis using Marcus theory and the fact that neither *trans*-2-phenyl- nor 2,2-diphenylmethylcyclopropane gave ring-opened products.[198] Through the use of specifically deuterated substrates in this study, intermolecular and intramolecular KIE values were also measured for the *M. capsulatus* (Bath) system. The KIE_{inter} value was 1.0 and KIE_{intra} was 5.1. The latter value can be compared to the intramolecular KIE of 4.2 ± 0.2 obtained for MMO from *M. trichosporium*[196] and the 7–14 range of cytochrome P-450.[40]

Use of the diphenylmethylcyclopropane radical clock substrate probe with the *M. trichosporium* OB3b hydroxylase enzyme showed a small amount of rearranged product indicative of a radical intermediate. The calculated rebound rate constant was $(6–10) \times 10^{12}$ s^{-1}, a value consistent with the chiral ethane experiments discussed above.[196] The consistency between the *M. trichosporium* radical clock and chiral ethane data lends credence to the interpretation of the experimental findings for the *M. capsulatus* MMO.

Unlike ribonucleotide reductase (see below), no stable enzyme-bound radical has been observed for the MMO hydroxylase. Recent freeze–quench, chemical–quench, and low-temperature stopped-flow optical spectroscopic studies of the *M. trichosporium* hydroxylase have detected several intermediates.[197,197a] One was assigned as a symmetric Fe^{IV}–Fe^{IV} compound on the basis of its isomer shift (δ = 0.17 mm s^{-1}) and single quadrupole doublet (ΔE_Q = 0.53 mm s^{-1}) at 4.2 K.[197] Magnetic Mössbauer experiments revealed this transient to be diamagnetic.[197] A subsequently formed intermediate, obtained in the presence of nitrobenzene, was assigned as the enzyme–product complex.[197a] Although arguments to exclude a diiron(III) assignment for the first intermediate were presented, an η^2,η^2-peroxide-bridged diiron(III) structure, similar to that of oxyhemocyanin,[226] is an alternative that should be considered. If the diferryl assignment can be verified, then pathway C in Figure 13 would be a good candidate for the mechanism.

Another similarity between the *M. trichosporium* MMO hydroxylase reaction and the P-450 mechanism is the ability of peroxide ion to activate the chemistry through a shunt pathway (Figure 13). This property provides strong support for the postulated diiron(III) peroxide intermediate in the reaction of the reduced enzyme with dioxygen. For the *M. trichosporium* enzyme, this peroxide shunt afforded hydroxylation products, but only at very high hydrogen peroxide concentrations.[222] Peroxide was consumed at a rate

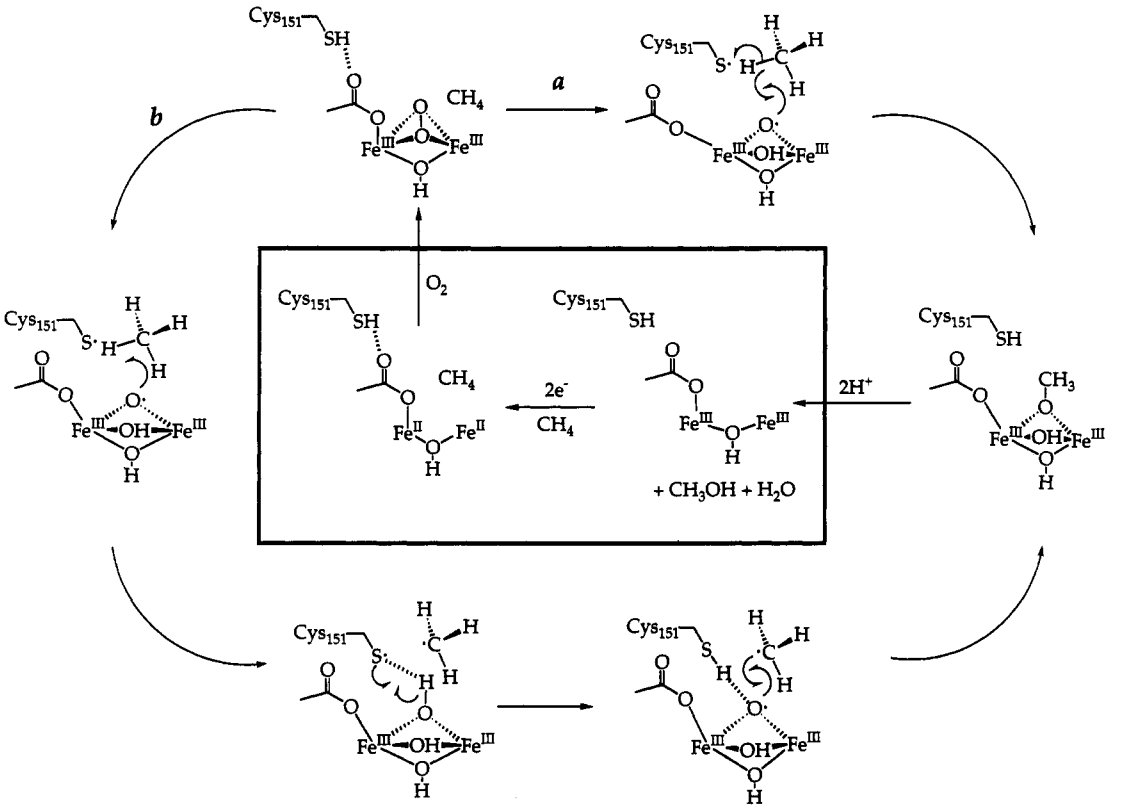

Figure 14. Two speculative diradical mechanisms for the activation of methane by the MMO hydroxylase that involve reductive activation of dioxygen by the active-site cysteine residue. Pathway ***a*** involves concerted cleavage of the C–H bond. Pathway ***b*** is a form of the standard rebound mechanism, modified to facilitate formation of the C–O bond according to ref 230. Although the oxyl moiety is depicted as bridging the two iron atoms, alternative structures in which it occupies a terminal position are not excluded.

that varied with the ratio of H_2O_2 to substrate, indicating the presence of an uncoupled reaction that did not lead to product formation. Furthermore, in the presence of protein B, the product ratio differed for oxidation of propane; the dioxygen reaction showed 3-fold greater selectivity for hydroxylation at the primary carbon relative to the hydrogen peroxide-induced reaction.[203] These results raise the question of whether the hydroxylation mechanism with the diiron(III) enzyme and H_2O_2 is identical to that operating when O_2 is added to the reduced enzyme. Appropriate controls were run to assure that the reaction occurred within the protein-active site, but were insufficient to prove that the enzyme reentered the normal catalytic mechanism. To verify such a convergence of mechanisms, parallel KIE or stereochemical selectivity experiments would be required. It should also be noted that other oxo-transfer agents such as iodosylbenzene, sodium periodate, sodium chlorite, and *tert*-butyl hydroperoxide, all of which are active in the P-450 shunt mechanism, are ineffective in initiating hydroxylation chemistry in MMO.[227] This result raises doubts about the possible participation of a ferryl intermediate in the reaction mechanism. Attempts to hydroxylate substrates via a peroxide shunt mechanism by addition of H_2O_2 to the oxidized *M. capsulatus* enzyme gave only low product yields.[227,228]

Several alternative pathways consistent with the radical trap and KIE data for the *M. capsulatus* hydroxylase have been set forth (Figure 13, pathways A, D, E, and F). Pathways D–F are examples of hydroxylation mechanism that might employ a ferryl intermediate, but do not require the intermediacy of a substrate radical. Pathway A is an alternative in which the ferryl intermediate is also omitted. The ability of an η^2,η^2-diferric peroxide to hydroxylate alkanes has not been definitively proven. Precedence exists for similar reactivity (hydroxylation of arenes) in dicopper(I) dioxygen chemistry, however.[229]

Another scheme that might be considered for the hydroxylation chemistry is set forth in Figure 14. In particular, these mechanisms suggest the possible participation of a radical involving Cys-151. This amino acid occupies the equivalent region of space as the tyrosyl radical of RR, as indicated by sequence homology and recent X-ray crystallographic results.[45,46] Pathway ***a*** considers a diradical mechanism similar to one discussed below for ribonucleotide reductase. One radical is Cys-151 and the other is postulated to be an iron-bound oxyl, a seven-electron oxygen atom, distinct from the six-electron oxene of the ferryl species. The two units, Fe^{III}–O• and Fe^{IV}=O, are likely to have quite different reactivities. Mechanism ***a*** depicted in Figure 14 would account for the lack of rearranged products in the radical clock study for *M. capsulatus* MMO because the C–H bond is broken in a concerted manner yielding a coordinated alcohol and the cysteine thiol. The small amount of rearrangement observed in the *M. trichosporium* system could result from misalignment of the substrate within the active site such that C–H bond cleavage proceeds in two fast sequential steps with a transient substrate radical intermediate. Since only a small fraction of the product is formed from a substrate radical intermediate, the remainder resulting from the concerted attack, less rearranged alcohol is produced than would be expected from a purely radical

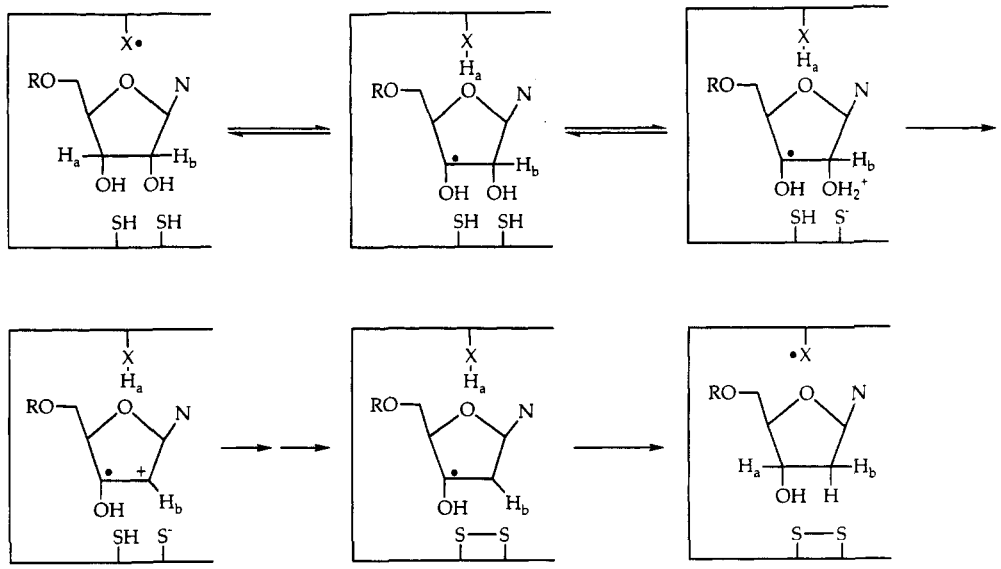

X = Protein residue

Figure 15. Postulated mechanism for ribonucleotide reductases involving radical cation intermediates. (Adapted with permission from ref 233.)

process. This characteristic would artificially inflate the rate constants for the rebound step measured in a radical clock study. Pathway ***b*** in Figure 14 is similar to the classic rebound mechanism except that the sulfur radical facilitates recombination of the bound oxyl and alkyl radicals. Similar steps have recently been postulated for dopamine β-monooxygenase,[230] but with a tyrosyl rather than a cysteinyl radical. There is currently no experimental evidence to support or refute these mechanisms.

To summarize, there is currently no mechanism that explains all the data from the two MMO systems. The results may depend on substrate, protein B, and temperature. The *M. capsulatus* (Bath) enzyme operates at 45 °C, whereas the *M. trichosporium* enzyme has good activity at 30 °C. Because the systems can hydroxylate a variety of substrates, the active site must be large, as indicated by the X-ray study, and relatively flexible. Cytochromes P-450 behave very differently in this regard. There are many variants of cytochrome P-450, most tuned for a single substrate.[40] The broad specificity of the MMO hydroxylase might lead to variable alignment of the substrate and active oxidant. Without a highly confining substrate binding pocket in the active site, variable experimental results might be observed. As further evidence accrues, it is reasonable to expect that a single unifying mechanism will be found. In proposing new mechanisms, care should be taken to address what are currently contradictory findings for the systems. Contacts between the protein components of the quaternary system are likely to be important, and elucidating the role of the coupling protein should enhance understanding of how these protein–protein interactions modulate the hydroxylation chemistry at the dinuclear iron active site.

3. Ribonucleotide Reductase

In methane monooxygenase, the diiron center actively participates in substrate oxidation. The role of the metal cofactor in ribonucleotide reductase (RR) from *Escherichia coli* is quite different, however, despite structural and chemical similarities in the active sites of the two enzymes. As the name implies, RR reduces ribo- to deoxyribonucleotides in the first committed step in DNA biosynthesis.[216,231-235] The chemical transformation and a model for its mechanism are depicted in Figure 15. Note that no metal cofactor is involved in the dehydroxylation reaction, which is catalyzed by a protein radical designated **X** located on subunit R1 of the enzyme. The dinuclear iron cofactor is involved in the activation step by which this radical is generated in the *E. coli* enzyme and is located on a different protein subunit known as R2. This subunit houses a stable tyrosyl radical that is generated by reaction of dioxygen with the diferrous core, the process of interest in the present context.

The X-ray crystal structure of the R2 protein has been determined in both the reduced and oxidized (met) forms.[217,236,237] The protein structure and coordination geometry of the dinuclear iron center are shown in Figure 16. The latter resembles the Hr and MMO cores, but with several distinguishing features. Although both Hr and R2 contain an oxo–carboxylato-bridged dinuclear iron center, Hr has a total of five histidine ligands, whereas there are only two histidines coordinated to the dinuclear iron center in R2. The rest of the coordination sphere is composed of oxygen donors. In this respect, the active site is identical to that of the MMO hydroxylase. In its reduced form, R2 lacks the hydroxide bridge that links the ferrous ions in deoxyHr (Figure 16b). Oxidation to met- or oxyHr is accompanied by only very small RMS displacements of the iron atoms and ligand side chains.[47] In the R2 protein, however, oxidation leads to a distinct carboxylate shift for Glu-238. One oxygen atom dissociates such that the carboxylate becomes a terminal rather than a bridging ligand (Figure 16b). Like those in Hr and MMO, the R2 diiron center is surrounded by hydrophobic residues, with the exception of the functionally important tyrosine residue located 5.3 Å from Fe1. The differences in the iron coordination environments of Hr and R2 centers are undoubtedly of

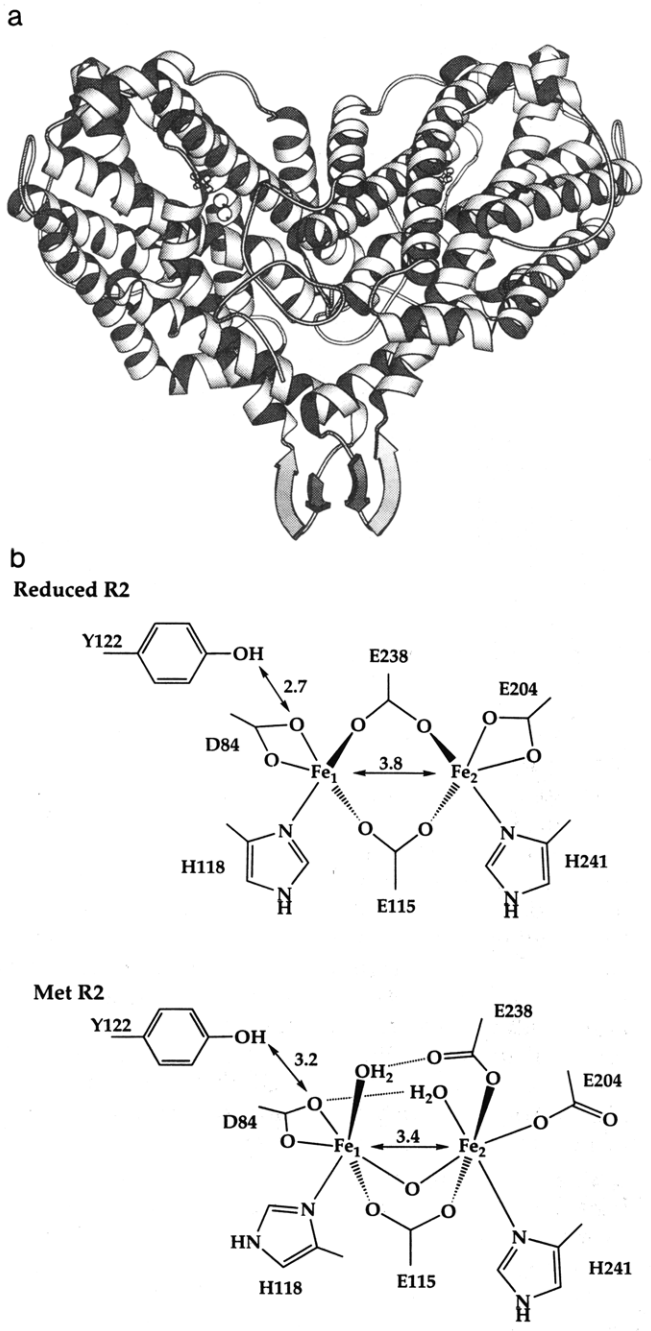

Figure 16. (a) MOLSCRIPT[363] diagram of the ribonucleotide reductase R2 protein showing the protein fold and (b) active-site structure of oxidized and S211A mutant reduced R2 protein from *E. coli*. Distances are given in angstroms. (Adapted with permission from ref 216.)

functional significance,[45] as discussed further below.

The presumed function of the non-heme iron center in R2 is to generate the tyrosyl radical through a redox cycle such as that depicted in Figure 17. This figure also shows interconversions among the apo, reduced, met, and active forms of the enzyme. Spectroscopic characteristics of the dinuclear iron center in each of these states are presented in Table 8. During normal enzyme turnover, the iron remains in the diferric state while the tyrosyl radical appears to be responsible, either directly or indirectly, for the catalytic activity.[233-235] Generation of the tyrosyl radical from inactive forms of the enzyme can be accomplished by addition of dioxygen to reduced R2.[231] The net reaction, described by eq 30, requires four electrons, three of which come

$$\text{Y122-H} + 2\text{Fe}^{\text{II}} + \text{O}_2 + \text{e}^- + \text{H}^+ \rightarrow \text{Y122}\cdot + \text{Fe}^{\text{III}}\text{–O–Fe}^{\text{III}} + \text{H}_2\text{O} \quad (30)$$

from the tyrosine and two ferrous ions and the fourth from another source. This fourth electron can be contributed by an external reductant such as ascorbate or by a third equivalent of ferrous ion.[238-240] Since ascorbate is capable of reducing ferric to ferrous ions,[241] it is possible that Fe(II) is always the electron donor. In the presence of excess ascorbate, however, ferric ion generated in the process is reduced before it can be detected to confirm this mechanism.

Further elaboration of the mechanism of tyrosyl radical formation has come from kinetic studies that have identified two spectroscopic intermediates.[239] The system lends itself nicely to kinetic analysis because of its many spectroscopic features. The tyrosyl radical has a strong visible absorption band at 412 nm, the (μ-oxo)diiron$^{\text{III}}$ core has absorption bands at 320 and 365 nm, and an intermediate (**U**) with an absorption maximum at 565 nm has been observed. A mutant Y122F, which lacks the key tyrosine residue and is therefore incapable of forming the active form of the enzyme, is also available.[239] When this mutant was used in the kinetic studies, **U** was still observed at 565 nm, but the band due to the stable tyrosyl radical at 412 nm was no longer present. This experiment proved that **U** could be generated independently from the tyrosyl residue of the active enzyme. The second intermediate (**X**) was discovered through freeze–quench EPR studies. A sharp, isotropic signal at $g = 2.00$ distinct from the tyrosyl radical signal was observed. This EPR spectrum exhibited quadrupolar broadening when ^{57}Fe was used, indicating that it was derived from a radical bound to the iron center. The EPR signal assigned to the tyrosyl radical grew in at the same rate that **X** disappeared. These observations were interpreted by the mechanism shown on the right hand side of Figure 18. The measured rate constants for each process indicated in the scheme are all kinetically competent. Intermediate **U** was originally assigned as a diferric peroxide species on the basis of comparison of its optical spectrum with those of several (μ-1,2-peroxo)diferric model compounds,[51,242] although a μ-1,1 structure has also been suggested.[176,243] These models are discussed in more detail below. An alternative assignment for this intermediate, supported by recent Mössbauer experiments,[244] is a protonated tryptophan cation radical, a species that has an optical absorbance maximum at 560 nm.[245] W48 is in a position suitable to partake in the reaction. In such a pathway, the diferric peroxide would still be a transient intermediate that decays into the diferric diradical enzyme species without being observed. The proposed radical ligand species (Z•) has not yet been assigned. Perhaps it is a coordinated oxyl radical, as proposed for the MMO hydroxylase in Figure 14.

Regardless of whether species **U** is a peroxide or a tryptophan radical, the mechanism shown in Figure 18 does not require a high-valent iron–oxo intermediate. Furthermore, freeze–quench Mössbauer experiments of intermediate **X** indicated a spin-coupled diferric site.[239] Most of the mechanisms for the decay of putative diferric peroxide intermediates invoke heterolytic O–O bond cleavage leading to a perferryl

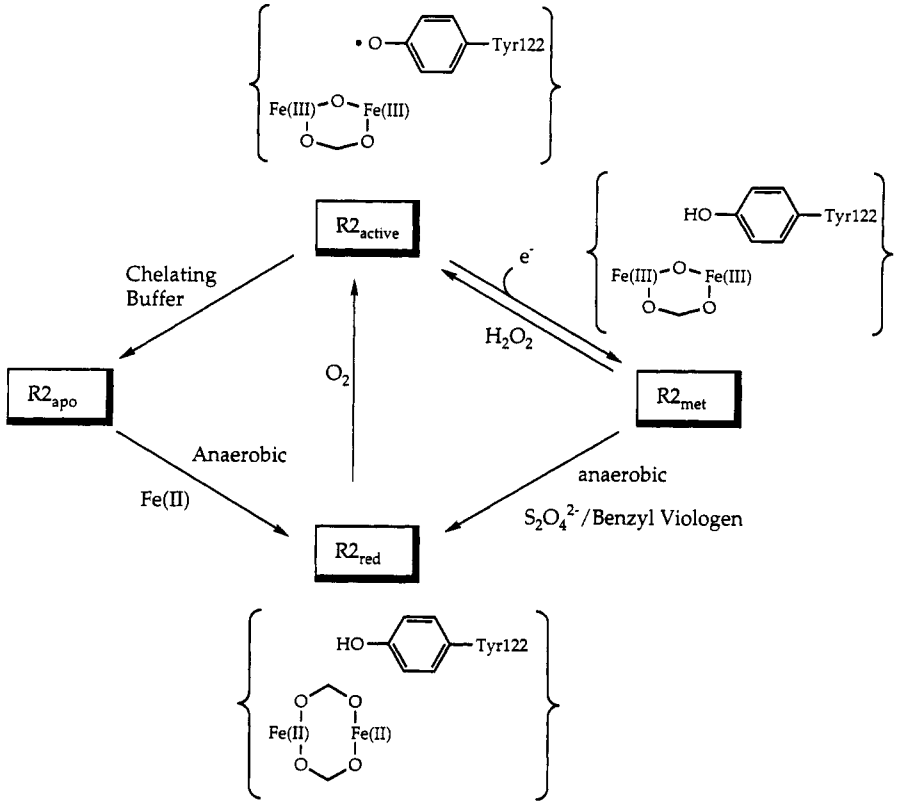

Figure 17. Redox states of the diiron core of ribonucleotide reductase from *E. coli*. (Adapted with permission from ref 240.)

Table 8. Spectroscopic Properties for the Different Forms of Ribonucleotide Reductase R2

		$R2_{red}$	$R2_{active}$	$R2_{met}$	ref(s)
Raman	ν_s(Fe–O–Fe), cm^{-1}		496	496	12
	ν_{as}(Fe–O–Fe), cm^{-1}		756	756	235
optical	λ, nm (ϵ, M^{-1} cm^{-1})		*a*	325 (9400) 370 (7200) 500 (800) 600 (300)	12
magnetics	$-J$, cm^{-1} [b]	10		110	12
Mössbauer	Fe1 δ, mm s^{-1}	1.26		0.53	12, 235
	Fe1 ΔE_Q, mm s^{-1}	3.13		1.66	12, 235
	Fe2 δ, mm s^{-1}			0.44	12
	Fe2 ΔE_Q, mm s^{-1}			2.45	12, 231
EPR	*g*		2 4.3	4.3	12

[a] Same transitions as $R2_{met}$ plus an additional band at 412 nm (ϵ = 4100 M^{-1} s^{-1}). [b] $\mathcal{H} = -2JS_1 \cdot S_2$.

species.[243,246,247] Support for this mechanism is based on experiments using peroxides, peracids, and other oxygen atom donors to activate metR2, a process that would bypass intermediate **U** of the dioxygen dependent reaction.[247] Resonance stabilization of the Fe^{V}–Fe^{III} species is afforded through the Fe^{IV}–O–Fe^{IV} form, as postulated for MMO (Figure 13). The two working hypotheses could be reconciled if the peroxo intermediate were to decay heterolytically to generate a ferryl species that rapidly afforded **X** by the influx of a single electron either from the tyrosine (pathway A, Figure 18) or from an external reductant (pathway B, Figure 18).[243] This concept leads to a difficult question regarding the dioxygen activation chemistry, namely, when do the electrons actually enter the system? Does the O–O bond break because an electron is added from an external source such as tyrosine, ascorbate, or a third mole of Fe(II) when excess iron is present, or does the diferric peroxide unit disproportionate, generating a species that abstracts an electron from whatever donor is closest? Future work is required to determine the true sequence of events. No structural evidence exists for a ferryl species in reactions of dioxygen with reduced RR R2 protein nor from ferrous model compounds (see below); however, if the decay of such a species were more rapid than its rate of formation, the chance of observing it spectroscopically would be small. Spectra assigned to a non-heme iron–oxo (ferryl) complex have been reported in the reaction of hydrogen peroxide with a ferric model compound,[248] although recent work indicates that the species is more complex than originally believed.[249]

The reaction of the reduced form of an R2 mutant, F208Y, with dioxygen provides additional detail about O_2 activation by ribonucleotide reductase.[216,250,251] In this mutant, a tyrosine replaces phenylalanine-208 in the hydrophobic pocket surrounding the dinuclear iron binding site. Upon addition of dioxygen, a strong visible absorption band at 720 nm appeared and the enzyme became inactivated. Crystallographic and chemical analyses proved that the mutant had tyrosine hydroxylase activity such that Y208 was oxidized to 3,4-dihydroxyphenylalanine (DOPA) upon exposure to dioxygen (Figure 19). It was postulated that decomposition of the diferric peroxide produced a ferryl species that activated Y208 by two-electron oxidation followed by nucleophilic attack of water or hydroxide ion or that Y208 had been directly oxygenated by an oxene mechanism.[251] These results imply that the chemistry used to generate the stable Y122 radical in the native enzyme is nonspecific and is directed by the

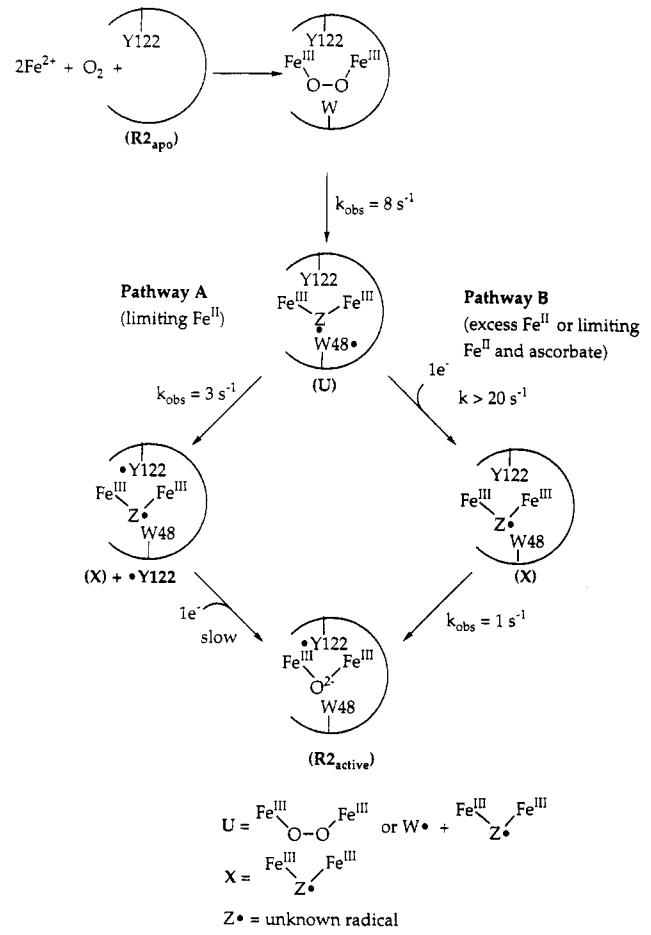

Figure 18. Proposed mechanism for the reconstitution and activation of *E. coli* ribonucleotide reductase by dioxygen. Intermediate U, observed by optical spectroscopy, has been postulated to be either a ferric peroxide species or a tryptophan cation radical. If U is the latter, the diferric peroxide species would probably be an unobserved precursor. (Adapted with permission from ref 239.)

relative positioning of reactive species in the active site. Attempts to trap hydroxyl radicals, potential electron shuttles during the reaction, have been unsuccessful and there is no evidence for OH• inactivation of the protein. Therefore, a direct electron-transfer mechanism from the iron center to the site of radical abstraction is preferred.

Having discussed the F208Y mutant and its interesting tyrosine oxidase activity, we conclude our treatment of the R2 protein with a few comments about how the structure of the metal center might affect the reactivity of its ferrous form with dioxygen. For Hr, it has been proposed that the hydrophobic nature of the core stabilizes a hydroperoxide diiron(III) adduct.[12] A similar situation probably contributes to the stability of the tyrosyl radical in the R2 site. The ability of the F208Y mutant RR to be hydroxylated, however, is consistent with the notion that its diiron site functionally resembles that of the MMO hydroxylase core more than that of Hr. MMO hydroxylase and RR have similar coordination spheres dominated by oxygen rather than histidine nitrogen donors. This coordination environment affects the reduction potentials of the iron atoms,[207] but it has not yet been shown unequivocally through model studies that oxygen donor atoms favor hydroxylation activity. In fact, many of the functional hydroxylation catalysts have pyridyl ligands or are inactive when pyridine is omitted from the solvent mixture.[252] In addition, the ability of the Hr structure to stabilize diferric hydroperoxide through internal hydrogen bonding does not seem to be possible in RR and may not be for the diiron site of MMO hydroxylase either. It is unclear at present whether the diiron(III) peroxide unit is stabilized in Hr because of the difficulty of oxidizing iron to the +4 state (redox related) or whether the Hr core simply does a more effective job of stabilizing the potentially reactive species, trapping it in a low energy, inactivated state.

C. Ferritin—A Polynuclear Iron Protein

Ferritins are a family of iron storage proteins found in many organisms. Detailed accounts of their chemistry and biology can be found in recent reviews.[253,254] Ferritins are composed of a mineral iron(III) oxide/hydroxide core, similar to ferrihydrate [$FeO(OH)\cdot H_2O$], containing up to 4500 iron atoms in microcrystalline particles approximately 65–70 Å in diameter surrounded by a protein shell. The ferritin protein provides an extremely soluble and concentrated store of intracellular ferric ions and is a fundamental component of iron homeostasis. The apoprotein from horse spleen Ft has been crystallographically characterized. It consists of

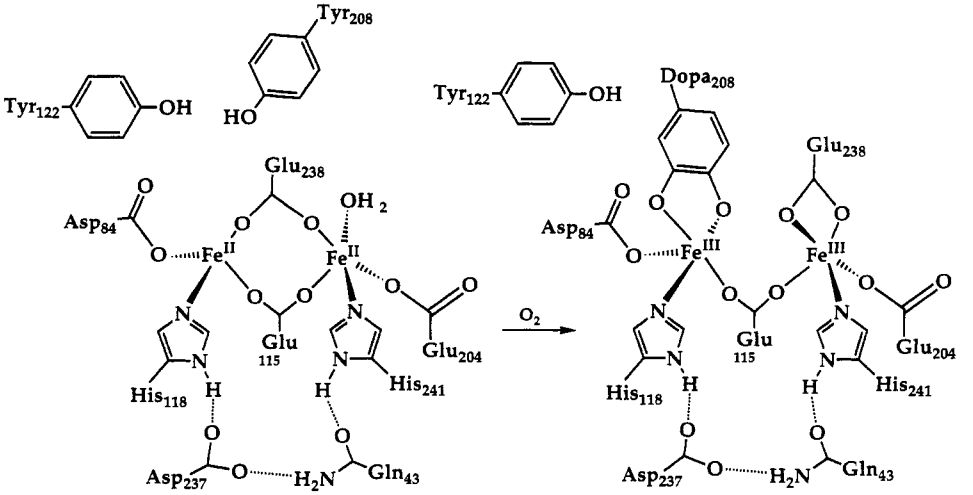

Figure 19. Proposed mechanism for the phenylalanine hydroxylase activity of the R2 F208Y mutant. The structure of the reduced form is a model adapted from the crystallographically characterized Mn(II) derivative of the native protein. (Reprinted from ref 251. Copyright 1993 American Chemical Society.)

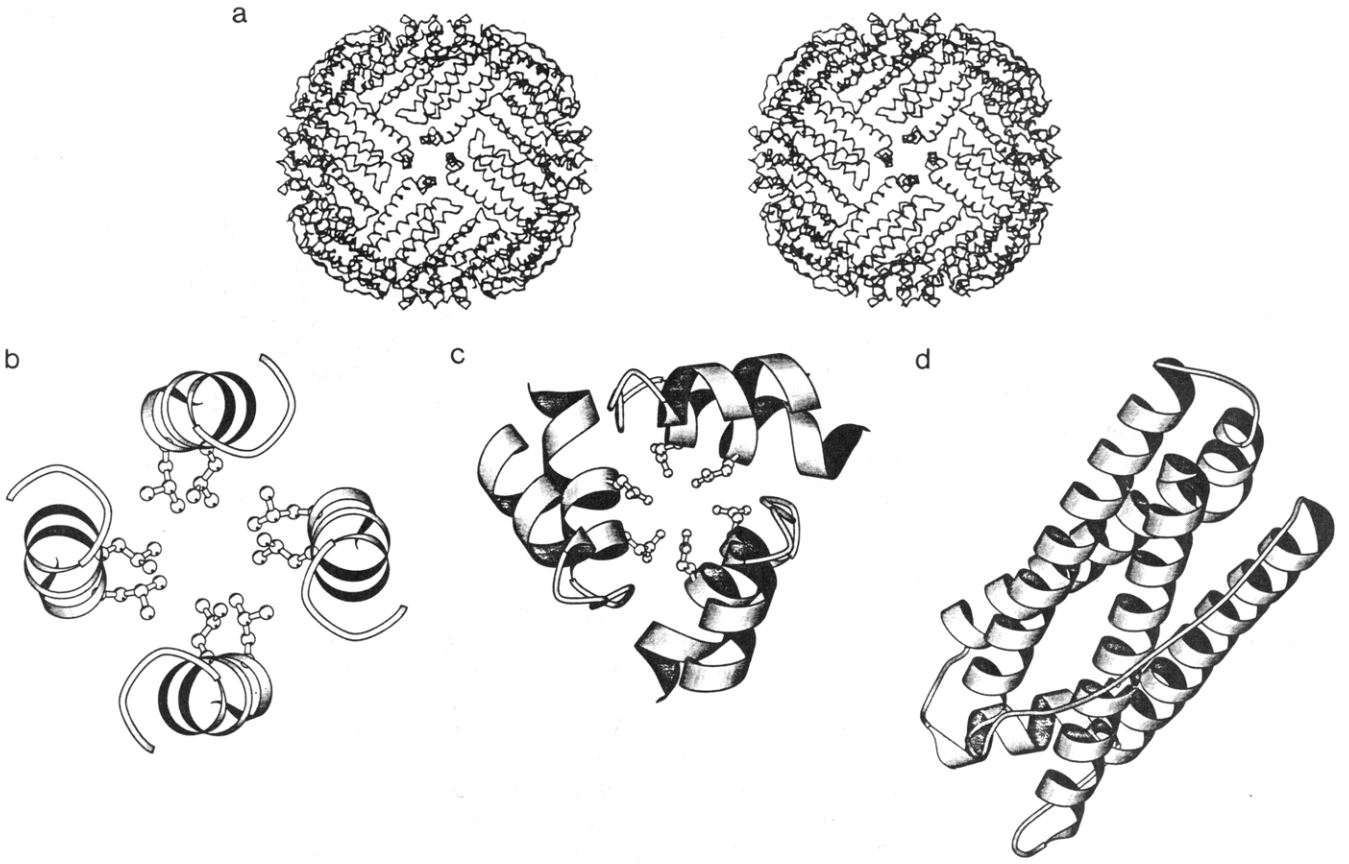

Figure 20. Structure of apoHoSF. (a) Stereoview of the quaternary structure viewed down the 4-fold axis. (Reprinted from ref 256. Copyright 1990 Plenum.) (b) MOLSCRIPT[363] diagram depicting the hydrophobic channel along the 4-fold symmetry axis. (c) MOLSCRIPT[363] diagram depicting the hydrophobic channel along the 3-fold symmetry axis. (d) MOLSCRIPT[363] ribbon representation of the structure of a single subunit.

24 subunits made up of H and L polypeptide chains, the ratio of which varies greatly from species to species.[253,254] In general, ferritins with a greater proportion of H subunits display more rapid iron uptake[255] while those composed predominantly of L subunits sequester greater quantities of iron in their cavity.[256] The structure of horse spleen apoFt is shown in Figure 20. The interior regions of the chains are predominantly hydrophobic with the exception of a conserved group of closely spaced hydrophilic residues located on the H polypeptides. Iron is generally assumed to bind apoFt as iron(II) that is catalytically oxidized at a center on the H subunits. It has been proposed that the conserved regions define the active site for this ferroxidase activity.[257-259] Iron(II) also binds to hydrophilic residues on the L chains, as evidenced by slow packing of apoLF, but the oxidation step involved in core formation is uncatalyzed. Recent X-ray structural analysis has revealed that the quaternary structure of Ft is preserved in other species.[259] Distinct channels in the protein coat have been postulated as entry points for diffusion of Fe(II) into the cavity.[260] The ferroxidase activity data support such potential roles for the channel, although other plausible entry routes have been discussed.[261] The oxidation of ferrous ions by dioxygen at such sites results in the initial deposition of the mineral core and is the focus of our present discussion. It should be noted that L chains in heterogeneous ferritins modulate the H-chain ferroxidase activity.[262] Therefore, the comparisons between species must be made with appropriate caution, especially when the H/L composition varies.

Early studies in vitro revealed that the only way to pack iron into ferritin was to supply Fe(II) and an oxidant.[263,264] In the case of partially loaded Ft, alternative oxidants could be employed, but only dioxygen was effective with the apoprotein.[253] The reaction proceeds by an oxidation-hydrolysis mechanism whereby ferrous ions are first oxidized to the ferric state and then packed into the crystalline core during a hydrolytic process. For complete loading of ferritin the stoichiometry is approximately $4Fe^{II}:1O_2$.[253] The stoichiometry of the oxidation reaction at low iron-loading levels appears variable, however, with reported values ranging from 1.5–4.0 $Fe^{II}:O_2$.[265] These disparate results for HoSF were explained by careful studies of the stoichiometry at different iron loading levels, from which a unifying explanation emerged.[265] In particular, there appear to be competing pathways, as illustrated in eqs 31–35 where eq 33 is the sum of eqs 31 and 32.

$$Fe^{2+} + O_2 + 2H_2O \rightarrow Fe^{3+}O(OH) + HO_2 + 2H^+ \quad (31)$$

$$Fe^{2+} + HO_2 + 2H_2O \rightarrow Fe^{3+}O(OH) + H_2O_2 + 2H^+ \quad (32)$$

$$2Fe^{2+} + O_2 + 4H_2O \rightarrow 2Fe^{3+}O(OH) + H_2O_2 + 4H^+ \quad (33)$$

$$4Fe^{2+} + O_2 + 6H_2O \rightarrow 4Fe^{3+}O(OH) + 8H^+ \quad (34)$$

$$Fe^{2+} + H_2O_2 + H_2O \rightarrow Fe^{3+}O(OH) + OH\cdot + 2H^+ \quad (35)$$

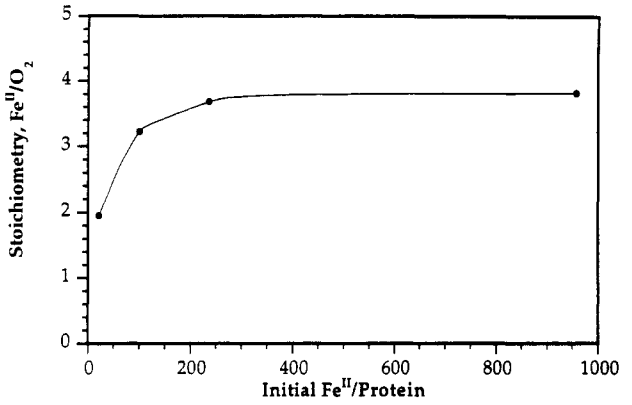

Figure 21. Stoichiometry of Fe^{II} uptake into apoHoSF measured as a function of initial iron loading. The conditions were as follows: 1 mM Fe^{II}, 1 μM to 42 μM apoferritin, 0.1 M MOPS, 0.15 M NaCl, pH 7.22, O_2/Fe^{II} ratio = 2.10. (Data taken from ref 265.)

At low iron loading, the stoichiometry of the oxidation is 2 mol of Fe(II) per mole of O_2 (eq 33), but under conditions of higher iron loading the ratio shifts to 4:1 (eq 34). This shift in stoichiometry can be seen quite clearly in Figure 21, where the stoichiometry is plotted as a function of iron loading for HoSF. At low iron(II) concentrations, where nucleation of the core occurs, a bimolecular reaction takes place between Fe(II) and O_2, generating a (μ-oxo)diiron(III) species and hydrogen peroxide. This pathway is discussed in detail below for it pertains to the catalytic ferroxidase activity of ferritin H chains. The second pathway for oxidation is proposed to be a heterogeneous reaction catalyzed on the surface of growing ferrihydrite crystallites. In this reaction, ferrous ions are stoichiometrically oxidized to ferric ions with the consumption of 4Fe(II) ions per dioxygen molecule, but much less is known about the details.[263,265]

The ferroxidase activity of ferritins has been studied by Mössbauer, EPR, and optical spectroscopy. A (μ-oxo)diiron(III) intermediate along the oxidation–hydrolysis pathway was detected by freeze–quench Mössbauer and UV difference experiments.[258,266,267] EPR studies on HoSF identified two intermediates, a mononuclear ferric species and a mixed-valence diiron(II,III) complex.[268] By optical spectroscopy, a ferric tyrosinate complex was observed in recombinant bullfrog erythrocyte H-ferritin (rHF).[259,269,270] The burst kinetics of the latter species were sufficiently fast to have precluded detection by the oximetry techniques employed in earlier studies.[262,271] Following the iron tyrosinate burst, a slow relaxation is observed (≈12 h for full relaxation) before a second burst of equal magnitude occurs. Together with structural and spectroscopic work on rHF mutants lacking the proposed ferrous binding sites on the H chains, these spectroscopic investigations led to a model for the initial phases of ferritin core formation, the nature of which is illustrated schematically in Figure 22. It should be noted that this model incorporates kinetic and spectroscopic data from homogeneous (rHF) and hetero-

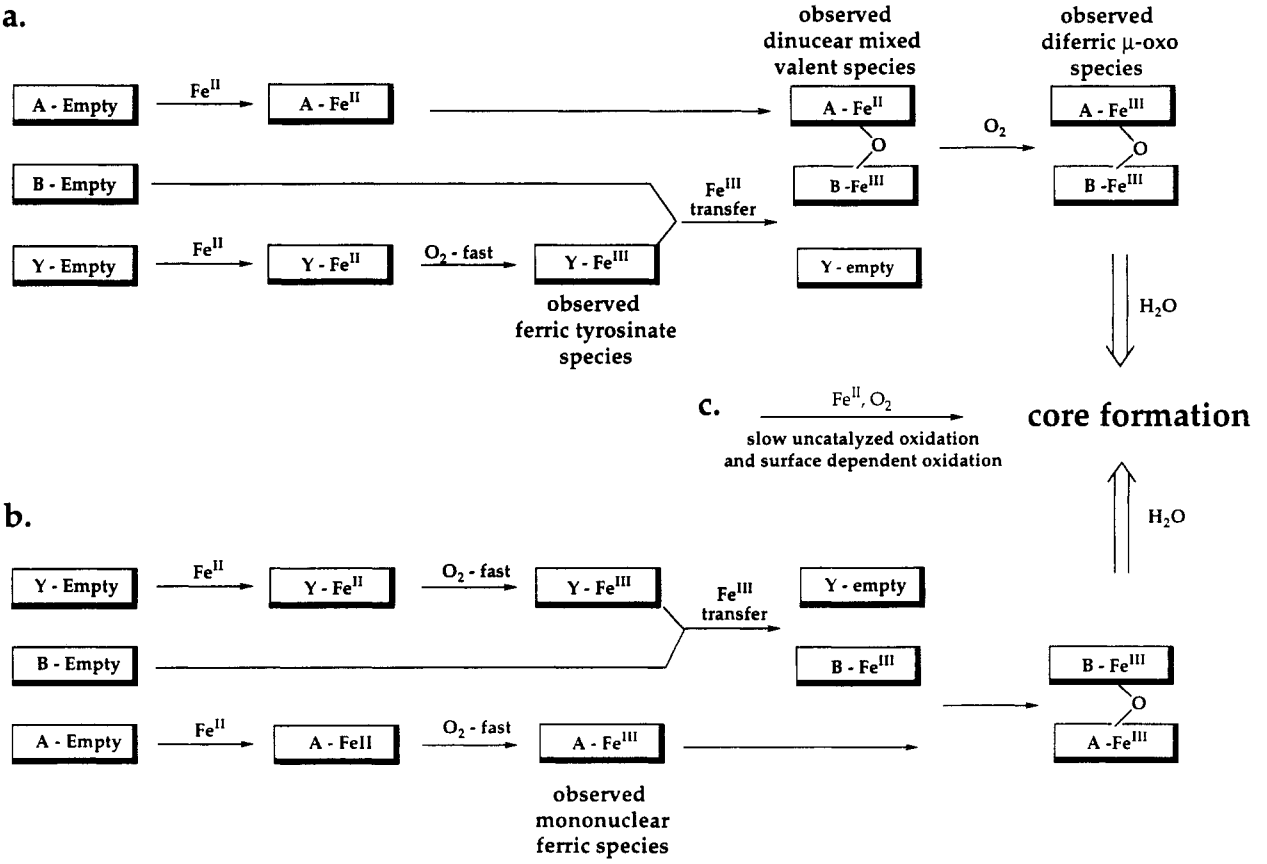

Figure 22. Diagrammatic representation of a model for the initial phases of ferritin loading via the ferroxidase center of H-chain ferritins based on spectroscopic data from rHF and HoSF, among others. A, B, and Y refer to the binding sites identified and discussed in the text. Site B is depicted as being empty, but an alternative mechanism could be drawn in which the iron transits from A to B before oxidation. The observed intermediates in core formation are noted. Pathway c refers to the major route of oxidation after the initial nucleation phase.

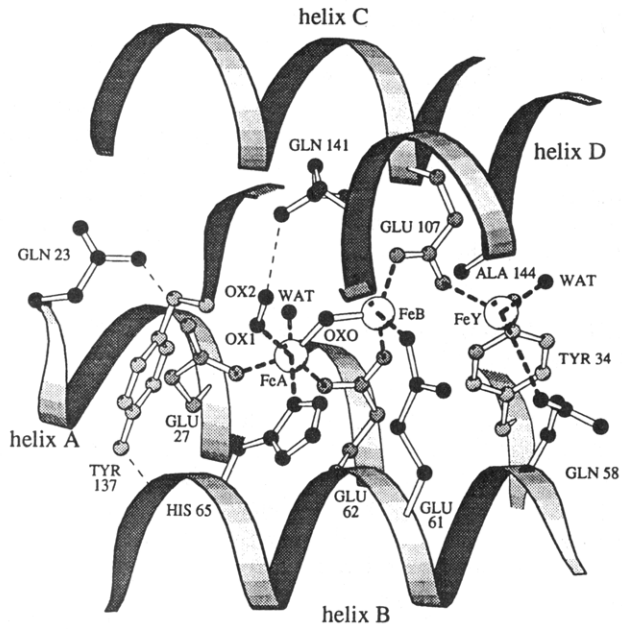

Figure 23. Identification of possible loci for the A, B, and Y iron-binding sites in recombinant H-chain ferritin.

geneous (H/L) ferritins as well as mutant H strains and may be a simplification of the actual events. It is useful nonetheless in helping to reconcile the differences observed in the varying ferritin systems currently under study.

There appear to be three specific sites for the binding of iron to Ft at low iron-loading levels, designated A, B, and Y. They were assigned, in part on the basis of the binding of Tb(III), an inhibitor of iron uptake,[253] to these locations in the crystal and are shown in Figure 23. Oxidation of iron(II) is proposed to occur at the A and Y sites. Kinetic studies using optical spectroscopy revealed the formation of a ferric tyrosinate complex that absorbed at 550 nm.[259,269,270] Initial burst kinetics monitored at this wavelength revealed much faster rates than for the formation of other intermediates in the ferritin loading reaction. This ferric tyrosinate species then decayed at a rate kinetically competent for the formation of the (μ-oxo)diiron(III) intermediate observed in the Mössbauer spectrum.[259] Site-directed mutagenesis experiments provided further support for these functional domains. Modification of any of the residues involved in stabilizing the dinuclear complex (FeA–FeB) resulted in significant losses in catalytic activity and recovery of L-chain-like behavior, as measured by optical spectroscopy.[259] Studies using oximetry to monitor the kinetics revealed that ferritin molecules mutated at site B (E61A, E64A, E67A) did not lose significant levels of ferroxidase activity, whereas site A mutants (E62K, H65G, K86Q) lost most of their activity.[262] Ferritins with mutations at both sites lost all of their ferroxidase activity.[262] Mutation of the tyrosine residue did not affect the formation of the dinuclear species or the total amount of Fe(II) oxidized, but the yield of total ferrihydrate was diminished.[259] As expected, the Y34F mutant did not display a tyrosine → iron(III) charge-transfer band at 550 nm prior to dimer formation. Since the mutation of tyrosine did not inhibit dimer formation, there must be alternative ways to catalyze ferrous ion oxidation, albeit more slowly than at the Y site. Possibly, all the iron is oxidized at

Table 9. Kinetic Parameters for the Ferroxidase Activity of rHF, HLF, and HoSF[a]

	rHF[b]	HLF[b]	HoSF[c]
K_{m,O_2}, μM	6 ± 2	60 ± 12	140 ± 30
$K_{m,Fe}$, μM	80 ± 10	50 ± 10	350 ± 10
$k_{cat\text{-}ox}$, s^{-1}	3.4 ± 0.2	0.52 ± 0.01	1.3 ± 0.06
$k_{cat\text{-}tyr}$, s^{-1}	920 ± 50[d]		
Fe^{II}/O_2	2.1 ± 0.1	<2.7 ± 0.1	2.0 ± 0.2[e]
E_a, kJ/mol	26.4 ● 0.1	67.3 ± 0.5	36.6 ± 1.3
$\Delta H^{\ddagger}$, kJ/mol	23.9 ± 0.1	64.8 ± 0.5	34.2 ± 1.3
$\Delta S^{\ddagger}$, J/mol K	−136.0 ± 0.4	−11.0 ± 1.6	−108 ± 5
ref	262	262	271

[a] rHF = recombinant H chain ferritin; HLF = human liver ferritin; HoSF = horse spleen ferritin. $k_{cat\text{-}ox}$ refers to oximetry measured k_{cat}. $k_{cat\text{-}tyr}$ refers to the k_{cat} for iron(III) tyrosinate formation. [b] Conditions: 0.1 M NaCl, 50 mM MOPS, pH 7.05, T = 20 °C. The composition of the HLF was 4% H and 96% L subunits. [c] Conditions as in footnote *a*, but the protein used consisted of 16% H and 84% L subunits. [d] Conditions: 0.2 M NaCl, 0.1 M MOPS, pH 7.0, T = 25 °C. Data point from ref 265. [e] Data point from ref 270.

Y and then migrates to the A and B sites in the wild-type rHF. A recycling time of approximately 12 h is required to see comparable initial burst effects, however.[270] This recovery time is not observed in other ferroxidase intermediates and supports a model in which parallel oxidation reactions at the A and Y sites are involved. Ferritin core packing also did not seem to be affected by mutation of the tyrosine residue. The distance between the A and Y sites is at least 7 Å, too long to be linked by a bridging ligand derived from a single dioxygen molecule. None of the current evidence requires simultaneous oxidation of the two ferrous ions, and oxidation by one-electron steps would explain the observations of mononuclear ferric complexes and mixed valence species.[268] All of these data are consistent with the chemical transformations discussed above (eqs 31–35).

Kinetic parameters for the ferroxidase activity of several apoferritin species have been measured and are compiled in Table 9. The activity of the human liver ferritin (HLF) species was substantially higher than expected on the basis of its subunit composition and the current understanding that catalytic ferroxidase activity derives from a site on the H subunit. The large negative activation entropy for both recombinant H-chain ferritin (rHF) and horse spleen ferritin (HoSF) suggest substantial ligand reorganization following iron(II) binding. From the kinetic studies, it was concluded that oxidation occurs via two one-electron steps, as previously shown in eqs 31–33.[262]

Attempts to observe superoxide or hydroxyl radicals during Ft core formation have been made by using spin-trapping agents.[265,272] Very low concentrations of trapped radicals were observed, but it was not possible to identify definitively the particular species. The low concentration, 1 trapped radical per 5000 Fe(II) atoms, was explained by noting that radical formation occurs within the protein shell, an environment favoring reaction of radical species with iron via Fenton and Haber–Weiss mechanisms.[60] One of the functional roles of the protein shell may be to react with the oxygen radicals so generated and prevent oxidative damage to other more sensitive biomolecules.[38,272] Because of the inability to trap superoxide ion as dissociated HO_2, a diferric peroxide intermediate was proposed. Such a

mechanism would imply that the dinuclear mixed-valent species results from the oxidation of iron(II) in site A followed by binding of Fe(II) at site B, rather than by transfer of iron(III) from the Y site as postulated by others.[254,258,259,269,270]

Few reliable kinetic studies on the rate of packing iron into partially loaded ferritin are currently available, partly because of the multiple steps and competing pathways for core formation. Since these pathways depend upon the extent of iron loading, it is difficult to evaluate the published data. Individual intermediates have been studied by different techniques, and a particularly good kinetic investigation on ferritin-catalyzed iron oxidation has appeared.[273] One especially significant finding from this study was the observation that phosphate anions greatly accelerated the rates of ferrous ion oxidation, intermediate decay, and core formation. The phosphate-dependent oxidation acceleration is reminiscent of the autoxidation reactions of aqua–iron(II) species discussed previously and might arise for similar reasons. The rate of the ferroxidase-catalyzed reaction is several orders of magnitude more rapid than the uncatalyzed reaction, however. Alternatively, phosphate ions might facilitate the formation of core particle crystallites, and the effect of phosphate on the oxidation reaction may simply be to clear out ferric intermediates from the catalytic sites.[273]

A final point concerning the ferritin core loading reaction is the fate of the oxygen atoms derived from the dioxygen molecule. Labeling studies using $^{18}O_2$ have conclusively shown that, under both high (1200–1900 Fe/molecule) and low (220–240 Fe/molecule) loading conditions, the oxygen atoms from dioxygen do not appear in the ferritin core with greater than 3–4% efficiency.[274] Thus, the hydrolysis step leading to ferrihydrite formation is distinct from the oxidation process. In a separate study at low iron concentrations, it was shown that hydrogen peroxide was released during the oxidation process on the basis of the ability of catalase to alter the Fe^{II}:O_2 stoichiometry of the reaction from 2:1 to 4:1.[265] Since the oxygen atoms from dioxygen are lost to diffusible hydrogen peroxide, this finding supports the premise that the oxygen atom in the (μ-oxo)diiron(III) intermediate as well as the oxide ions in the ferrihydrite core result from hydrolysis or protonolysis of the ferric peroxide species. A question that might be raised at this point is why is the ferric peroxide intermediate formed in the early stages of ferritin core deposition unstable toward loss of hydrogen peroxide, whereas a similar species in oxyHr is perfectly stable? One possibility is that the nonpolar nature of the peroxide coordination environment in Hr retards release of the HOO^- anion, whereas the hydrated environment within the ferritin core leads to protonolysis of the hydrogen peroxide.[12,253] Furthermore, there does not appear to be any clear mechanism for the stabilization of the hydroperoxide. A related question is why, under low iron-packing conditions, is O_2 not converted to water but instead departs as hydrogen peroxide?

If this oxidation reaction occurs in independent one-electron steps at the A and Y sites, superoxide ion might also be produced. Since HoSF has weak superoxide dismutase activity, free O_2^- produced will be converted to dioxygen and hydrogen peroxide before detection.[271] When superoxide was added to apoFt, the SOD activity converted it to dioxygen before iron(II) oxidation was observed. Therefore, the inability to observed free superoxide does not preclude its generation. Addition of exogenous bovine SOD had no effect on either the kinetics of O_2 consumption or iron oxidation, and it was postulated that O_2^- produced remained bound to iron or was dismutated before leaving the confines of the ferritin shell.[271]

D. Bleomycin—A Metallopeptide with Biological Activity

Bleomycin (BLM) is an anticancer antibiotic used clinically in the treatment of squamous cell carcinomas and malignant lymphomas.[275] Its structure is shown in Figure 24. Studies using synthetic analogs have helped to define functional roles for the three domains of BLM, the central one of which, consisting of a pyrimidine, a β-aminoalanine and a β-hydroxyimidazole, is involved in metal binding.[276,277] The other domains are thought to facilitate DNA binding and the specificity of uptake by cells.[276–278] Although BLM strongly coordinates many transition metal ions, it is the ferrous complex that is considered to be the functional form of the drug.[279–281] In the presence of dioxygen, ferrous BLM is transformed into "activated-BLM" that is capable of DNA strand scission.[282–285] Activated-BLM can also oxygenate substrates such as olefins and phosphines.[286–292] A primary step in the chemistry leading to DNA damage is abstraction of the 4′-hydrogen atom of the deoxyribose ring. Transformation of ferrous-BLM into the activated-BLM is less well understood, but the process is relevant to mechanisms discussed above for non-heme iron enzymes. Features of this reaction are also found in the dioxygen chemistry of nonbiological ferrous complexes, as discussed in the next section.

Structural information about the ferrous and ferric forms of bleomycin is based on analogy to the copper(II), zinc(II), and cobalt(III) derivatives which have been characterized by X-ray crystallography (Cu) and NMR spectroscopy (Zn, Co).[276,293] Since the X-ray structure determination was carried out on a peptide precursor of BLM, and not the final antibiotic, it lacks information about the potential metal-binding roles of the sugar and bithiazole moieties.[293,294] Spectroscopic similarities between the copper derivative of the peptide precursor and the parent molecule, however, suggest that the former is a valid model.[295] As indicated in Figure 24b, the ligands in the equatorial plane afford a coordination environment that resembles porphyrin systems. In fact, the spectroscopic and reactivity properties of metal BLM derivatives are often compared to those of heme systems, especially chloroperoxidase.[286] The comparison extends to axial ligand effects so prominent in tuning the chemistry of iron porphyrins.[44,276] Although the saccharide portion of the molecule is usually neglected in discussions of BLM metal ion binding, this domain might have a functional role in the activation of dioxygen.[296] Weaker EPR signals and reduced reactivity toward DNA for the deglyco-BLM versus native BLM under identical conditions were attributed to diminished stability of the activated BLM. Moreover, the deglyco-BLM–Fe^{III} complex did not

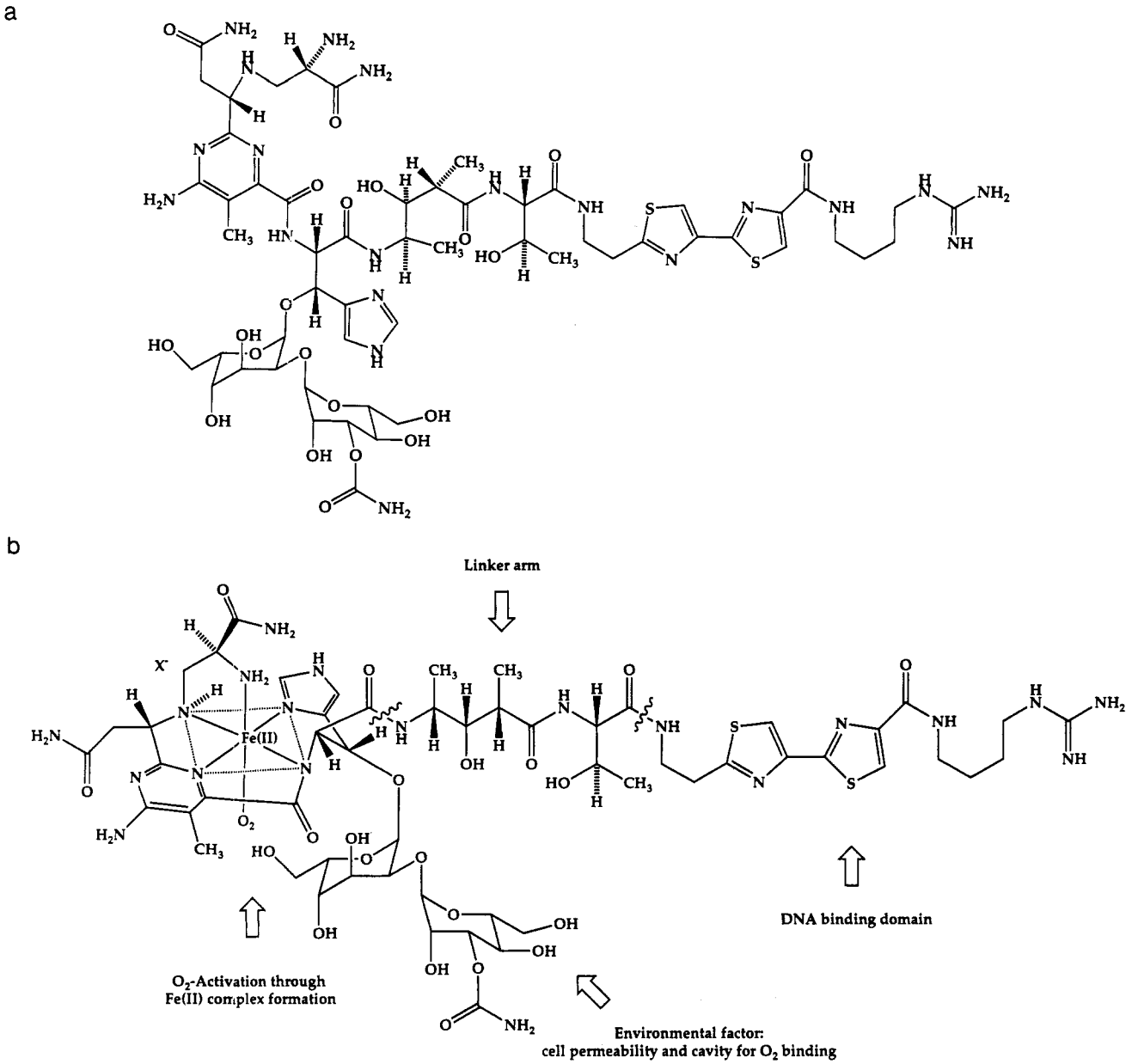

Figure 24. (a) Structure of bleomycin-B_2, where the B_2 refers to the nature of the specific terminal amine attached to the bithiazole moiety and (b) the proposed structure for BLM–Fe^{II}–O_2. (Adapted with permission from ref 290.)

undergo the pH-dependent high spin to low spin transition that occurred in the parent Fe^{III}–BLM complex.[296] It was therefore suggested that the sugar residues provide stabilizing hydrogen-bonding interactions with the dioxygen moiety of activated BLM, but further work is required to test this hypothesis.

BLM has proved to be a remarkable system for studying reactions of non-heme iron(II) with dioxygen because of the ability to characterize several intermediates, first observed through a combination of EPR and visible spectroscopic studies.[282,283] These species and their relationships to one another are shown diagramatically in Figure 25 together with the relevant spectroscopic parameters. In the ferrous form, the BLM complex can reversibly bind several dioxygen analogs (NO, CO, RNC) in a manner similar to iron–porphyrin complexes.[283] The initial reaction of the Fe^{II}–BLM complex with dioxygen results in the formation of a pink, EPR-silent species. It forms according to the rate law shown in eq 36 with a $t_{1/2}$ of 0.2 s at 2 °C.[282] The rate of this reaction is independent of pH from 6–8 and, from Mössbauer studies, the pink intermediate was proposed to be a Fe^{III}–superoxide complex.[285] A

$$\frac{d[\mathbf{c}]}{dt} = k_1[Fe^{II}\text{–BLM}][O_2] \qquad (36)$$

second intermediate (**c**′), having an indistinguishable optical spectrum but a different EPR spectrum from that of **c**, has been reported.[297] It is not clear what the relationship between these two species is, but since they both decompose to the same product, it is possible that they are coordination isomers of one another, where the mode of O_2 bonding affects both the stability and EPR parameters. This intermediate (**c**) can also be intercepted by the addition of nucleophiles such as ethyl isocyanide, which can bind the ferric center, leading to the displacement of dioxygen and formation of a completely inactive ferrous–BLM–isocyanide complex.[284] The ability of ethyl isocyanide to affect the bleomycin chemistry only occurs at this stage of the reaction; once the dioxygen has been reduced to the

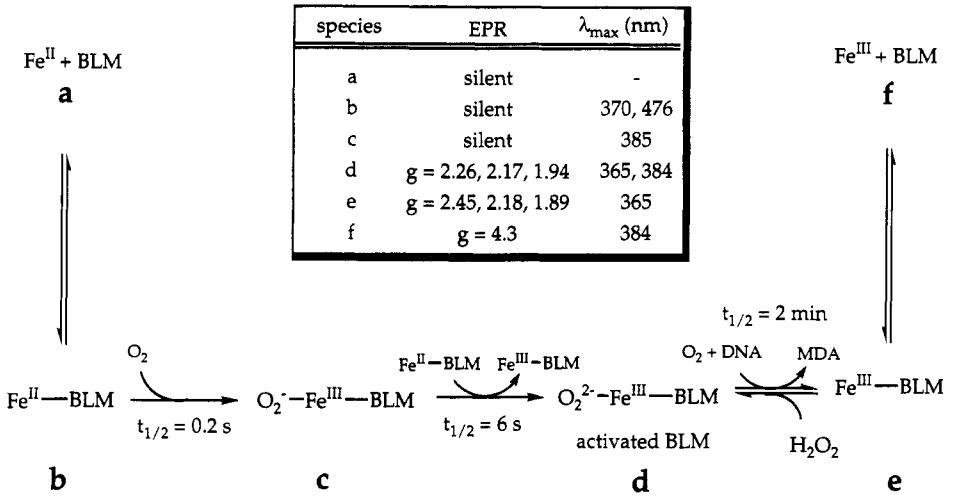

Figure 25. Proposed mechanism for the activation of Fe^{II}–BLM. (Adapted with permission from ref 284.)

peroxide level, the energy barrier for reoxidizing it to O_2 is prohibitive. The decay of **c**, which has a half-life of 6 s and follows the rate law in eq 37, affords activated-

$$\frac{d[\text{activated-BLM}]}{dt} = k_2[\mathbf{c}] \qquad (37)$$

BLM.[284] This species appears to be a one-electron-reduced form of **c** and has been designated a ferric peroxide.[284,285] The Mössbauer and EPR studies definitively rule out an Fe(IV) assignment, since these spectra require the iron center to have an odd number of electrons.[284,285] The electron donor needed to form activated BLM in the absence of reducing agents has been proposed to be another equivalent of Fe^{II}–BLM.[282,284] The use of a second ferrous ion to effect the thermodynamically preferred two-electron reduction of dioxygen is similar to the autoxidation reactions of ferrous ions discussed above as well as the mechanism of tyrosyl radical formation in RR. This reaction is influenced slightly by the presence of DNA, as revealed by EPR studies on ^{57}Fe-enriched samples, indicating direct interaction between the product, activated-BLM, and DNA.[284] As an alternative to the dioxygen route, activated BLM can also be generated by addition of H_2O_2 to Fe^{III}–BLM in a manner analogous to the peroxide shunt mechanism of iron–porphyrin and MMO systems.[40,222,276,298,299]

In the absence of DNA, activated-BLM undergoes autoxidation, leading to complete inactivation within several minutes.[284] The resulting species can be only partially reconstituted by addition of ferrous iron. This behavior contrasts with that of the ferric BLM product resulting from the reaction of activated BLM with DNA which, upon addition of fresh ferrous ions, is fully functional.[284] The stoichiometry of this autoxidation reaction, starting from ferrous iron, is 4 mol of Fe(II) per mole O_2 consumed, once again similar to the oxidation reactions of aquated iron(II).[300] When $^{18}O_2$ is used, the label is found almost quantitatively in water, showing that the active species undergoes inactivation via a ligand oxidation rather than an oxygenation process. Were metallo-BLM to decompose by self-hydroxylation, labeled oxygen would be incorporated into the molecule and less would appear in the water. Oxygenation followed by hydrolysis is not ruled out, however.[300]

In the presence of DNA, activated BLM immediately initiates cleavage chemistry by abstracting the 4′-H atom of the ribose ring. With the use of [4′-^{3}H]DNA, kinetic isotope measurements revealed this reaction to be involved in the rate-determining step.[301] The sugar radical then decomposes as indicated in Figure 26 to form free nucleic acid bases or base propenals.[295] The oxygen molecule in pathway a of Figure 26 has been distinguished from dioxygen involved in BLM activation by pulse chase experiments.[276,302] The overall DNA cleavage reaction follows Michaelis–Menten kinetics with a K_m = 1.8 mM and V_{max} = 5000 mol min^{-1} Fe(II).[303] It has a half-life of 8 s, making the formation of activated BLM kinetically competent to carry out the reaction.

Early work proposed hydroxyl radicals or superoxide ion to be the active species involved in BLM-mediated DNA degradation,[283,304,305] but such a mechanism seems unlikely on the basis of the low yields of trapped hydroxyl radicals and the inability of small molecule superoxide dismutases to intercept the chemistry.[306] More recently,[295] the reaction has been envisioned to occur by a rebound mechanism similar to that proposed for cytochrome P-450.[40,298] Further evidence has cast doubt on this hypothesis, however. Whereas cytochrome P-450 and its models incorporate oxygen atoms from O_2 into the substrate, the products of BLM cleavage receive their oxygen atom from solvent water under anaerobic conditions using H_2O_2 as the activating agent.[307] A rebound mechanism need not be invoked in this chemistry. For the hydrogen abstraction step to be rate determining, formation of the proposed ferryl ion must be faster than abstraction and therefore it would be expected to build up to some steady-state concentration. A ferryl species has never been observed spectroscopically, however.[292] If the oxygen atoms of activated-BLM were exchanging with solvent, the rebound mechanism would still be plausible, but experiments have shown that such is not the case.[292]

When provided with an alternative substrate to DNA, BLM oxidation chemistry ensues in a manner similar to that of cytochrome P-450 and its models. Another similarity between Fe–BLM-catalyzed oxidation chemistry and P-450 systems is the ability to initiate the chemistry with a variety of alternative oxidants and oxo-transfer agents in place of dioxygen and a reduc-

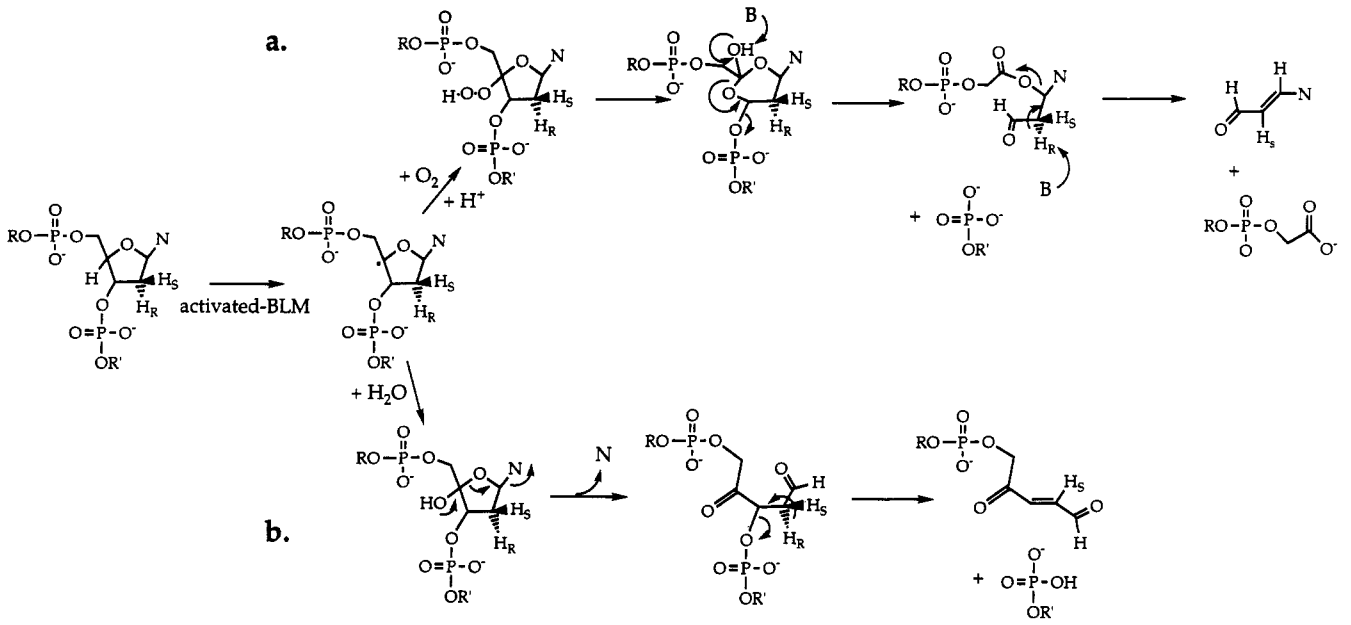

Figure 26. Proposed mechanism for the degradation of DNA by activated-BLM. Pathway ***a*** predominates under aerobic conditions and ***b*** under anaerobic conditions. (Adapted with permission ref ref 276.)

tant.[288,295] It should be noted, however, that the distribution of products is not always identical for the dioxygen reactions and these shunt pathways. This point is clearly illustrated by studies using *cis*-stilbene.[288] The dioxygen-promoted reaction yields solely benzaldehyde with complete incorporation of isotopic label. Hydrogen peroxide affords predominantly the *cis*-epoxide, and other oxo-transfer agents (PhIO, $NaIO_4$, ROOH) yield a mixture of the *cis*- and *trans*-epoxide, benzyl phenyl ketone, and benzaldehyde. Furthermore, the isotopic distribution of the products is a function of the reductant used to initiate the reaction. These results imply that a bleomycin ferryl species can be generated, but raises serious concerns as to whether the oxo-transfer agents follow the same chemical mechanism as the dioxygen reaction. To generate 2 equiv of labeled benzaldehyde from stilbene and dioxygen, a cyclic peroxide is likely to be a key intermediate.[276] This intermediate cannot form under anaerobic conditions, and the mechanistic pathway will certainly be altered. Activated bleomycin might be capable of decomposing to a ferryl species, but for the case of stilbene oxidation at least, it appears that a dioxygen insertion reaction is operative.

The above discussion has presented evidence that argues against the involvement of a ferryl-induced rebound mechanism or diffusible oxygen-derived radicals in the reaction of BLM with DNA. The challenge is to provide a plausible mechanism that fits all the observed data. It is still possible that activated-BLM decomposes to generate a ferryl intermediate that effects the chemistry by hydrogen atom abstraction in such a way that the substrate (or DNA) radicals produced react faster with water than with the Fe^{IV}–OH unit. One of the roles of the protein in P-450 systems might be to prevent such a water molecule from interacting with substrate radicals, but porphyrin model systems no bulkier than BLM exist which afford products attributed to ferryl species formed by the same mechanism. Direct reaction of a BLM ferric peroxide intermediate with DNA has rarely been invoked, but is one of the remaining contenders. When viewed with the benefit of information provided by studies of the small molecule catalysts, such as the Gif system discussed below, it seems possible that such a species may be reactive enough to catalyze the observed DNA degradation chemistry. In fact, early work on the Gif systems proposed ferryl intermediates before they were excluded by subsequent experimental work.[308,309]

IV. Reactions of Biomimetic Iron(II) Complexes with Dioxygen

The systems discussed in this section were devised in various attempts to mimic the biological structures and functions described above. We present this work in three subsections according to the relative stability of the oxygenated species formed in the initial reaction of a ferrous precursor with dioxygen. The first section treats the most stable complexes, which form dioxygen adducts detected spectroscopically, usually at low temperature. A summary of the spectroscopic data on these compounds is provided in Table 10. The second section covers autoxidations of model compounds, reactions having transient intermediates but which do not function to hydroxylate a substrate molecule. The last section discusses systems known to oxidize a hydrocarbon for which iron–dioxygen species have been inferred on the basis of the measured catalytic properties. We make no attempt to include every catalytic reaction involving ferrous–dioxygen chemistry, for such a treatment would be prohibitively broad. Instead, we present selected reactions, chosen to illustrate the general scope, breadth, and versatility of ferrous–dioxygen systems as oxidation catalysts. Reactions of hydrogen peroxide or superoxide ion with ferric complexes to form active oxygenation species are not explicitly treated, although they are mentioned in a few cases where the information was found to be insightful.

Table 10. Visible and Raman Spectroscopy of the Dioxygen Adducts of Non-Heme Iron Model Compounds

compound	solvent	λ_{max}, nm (ϵ, M^{-1} cm^{-1})	ν(Fe–O)(^{18}O)	ν(O–O)(^{18}O)	binding mode	ref
1	THF	534 (1590)		853	μ^4	48
2/O_2	toluene/pyridine 99:1	529				310
4/O_2	acetone/pyridine/water (3:1:1)	523 (3200)				313
10b	water	540 (187)				327
12b	toluene	679 (3454)	418 (409)	876 (827)	μ-1,2	50
14a/H_2O_2	water	560 (2200)	476 (457)	895 (854)	μ-1,2	336
15b	CH_2Cl_2	588 (1500)	476 (460)	900 (850)	μ-1,2	51
16b	CH_2Cl_2/DMSO 9:1, v/v	562 (3200)			μ-1,2	51
16b	CH_2Cl_2/DMSO 8:2, v/v	572 (2060)	453, 481 (444)	877, 893 (834)	μ-1,2	51
$[Fe_2\{HB(3,5\text{-}iPr_2pz)_3\}_2(OBz)(OH)]/O_2$	pentane	$\approx$ 700				335
$[Fe_2(5\text{-Me-HXTA})(O_2)(OAc)]^{2-}$	DMSO or MeOH	480 (2370)	n.o.	884	μ-1,2	375
$[Fe(Ph_3PO)_4]_2(O_2)$	MeCN	576 (3540)	n.o.	884[a]	μ-1,2	376
$[Fe(OEP)O_2]^-$			n.o.	806 (759)	η^2	377
$[Fe(EDTAH)O_2]^{3-}$	water	520 (530)	n.o.	815 (794)	η^2	81
oxyHr	water	500 (2300)	503 (480)	844 (797)	η^1	366

[a] Raman spectrum taken in the solid state as a KCl mull.

A. Stable Dioxygen Adducts

1. Pseudo-Heme Systems

Several mononuclear non-heme ferrous complexes in this class have been synthesized as models for the chemistry of porphyrin systems (Figure 27). Some bind dioxygen to form relatively stable mononuclear or dinuclear adducts.[310–315] Geometric information about these dioxygen adducts is not available and even their exact coordination modes are not well known. All but one of these compounds contain a N_4 donor macrocyclic ligand occupying the equatorial positions of the octahedral ferrous ion in the absence of dioxygen. Such a rigid planar coordination geometry is uncommon among non-heme systems, as manifest by the structural features of the biological molecules discussed above. Unlike the porphyrins, however, these macrocyclic ligands are not fully conjugated, a property that may destabilize the ferryl species. In this respect their reactivity may be more comparable to non-heme iron centers.

Some of the complexes shown in Figure 27 bind O_2 reversibly. Even these reversible systems undergo irreversible autoxidation, however (eq 38). This instability is minimized at low temperatures where the reversible binding of dioxygen still takes place.

$$LFe^{II} + O_2 \rightleftharpoons LFe^{III}\text{–}O_2^- \xrightarrow{\text{slow}} \text{irreversible oxidation} \quad (38)$$

Early workers[310] approached the construction of a non-heme iron reversible dioxygen carrier by the strategy that proved successful for heme analogs.[316–318] In the latter systems, the dioxygen adducts decompose in a bimolecular reaction involving a (μ-1,2-peroxo)-diiron(III) porphyrinato complex that has been thoroughly characterized.[319,320] By constructing ligands with sufficient geometric bulk to prevent formation of the peroxide-bridged diiron(III) complex, such as capped or picket fence porphyrins,[317,321,322] the desired 1:1 adduct was stabilized. In a similar manner, sterically encumbered non-heme ligands and their respective ferrous complexes (**2** and **3**, Figure 27) were prepared having two different pocket depths (5 and 2.2 Å respectively). As expected, in the presence of pyridine as an axial base, the more sterically crowded ligand afforded reversible dioxygen binding at temperatures below −50 °C. A 1:1 stoichiometry was demonstrated by dioxygen uptake experiments, and the adduct exhibited an optical band at 529 nm. Unfortunately, neither resonance Raman nor Mössbauer spectroscopy was used to characterize this compound, but its presumed mononuclear nature is consistent with the presence of a ferric–superoxide unit similar to that of Hb and synthetic iron–porphyrin–dioxygen complexes.[4] Compound **3**, having a shallower pocket, was rapidly and irreversibly autoxidized at −78 °C with the consumption of 0.5 equiv of O_2.[310] Clearly, ligand control of the environment around the dioxygen binding site attenuates the reactivity of the adducts.

The comparison of the reactivity of these two compounds, similar in all respects except for the depth of their O_2-binding pockets, reveals the importance of steric constraints in determining the course of the reaction of dioxygen with ferrous complexes. A second example of this property is afforded by the mononuclear cyclidene complexes.[313–315] Unlike the previous molecules, which had a simple cleft, these ligands are bicyclic, enclosing pockets of defined size based upon the length of the R^1 spacer (compounds **4**–**8**, Figure 27). Because of their versatility and ease of substitution at the different sites, iron complexes of these cyclidenes display a range of chemical reactions, for which complete and up-to-date reviews can be found elsewhere.[323,324]

Upon exposure of **4** to dioxygen at low temperature, an optical absorption band around 520 nm appears as well as less intense features in the 500–650-nm region.[313] The spectrum is quite similar to that of **2** discussed above. Gas uptake experiments revealed the new species to be a 1:1 adduct, which was diamagnetic and EPR silent.[313] This complex can best be formulated as a low-spin ferric superoxide complex. The effect of axial bases on its dioxygen affinity parallels that of the porphyrin dioxygen carriers, with $Cl^- < py < 1\text{-MeIm}$.[313] When steric bulk was added to the R2 and R3 sites while maintaining a constant R1 bridge, the autoxidation process was retarded without affecting the

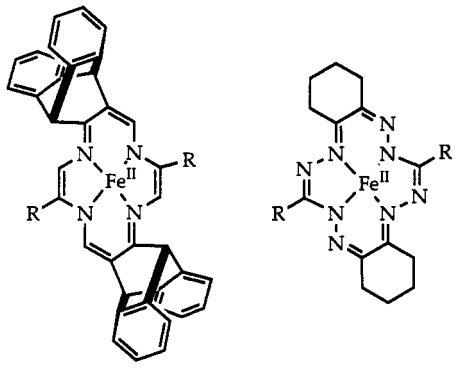

2 3

R = $(CH_2)_7CH_3$

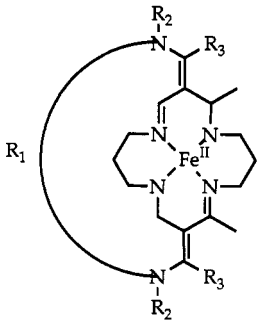

4: R_1 = m-xylylene, R_2 = Me, R_3 = Me
5: R_1 = m-xylylene, R_2 = benzyl, R_3 = phenyl
6: $R_1 = (CH_2)_3$, R_2 = Me, R_3 = Me
7: $R_1 = (CH_2)_4$, R_2 = Me, R_3 = phenyl
8: $R_1 = (CH_2)_5$, R_2 = Me, R_3 = phenyl

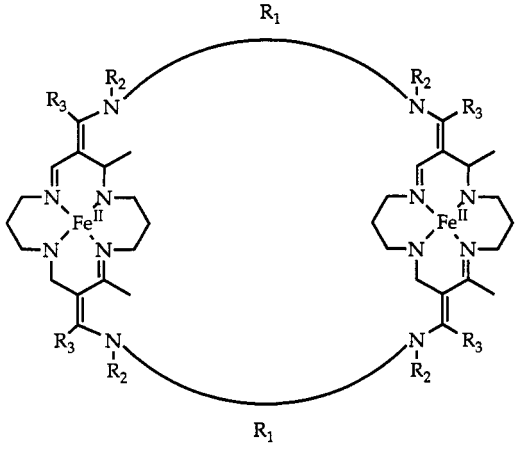

9: R_1 = m-xylylene, $(CH_2)_2$, $(CH_2)_3$, $(CH_2)_4$ among others
R_2 = H, R_3 = Me

Figure 27. Pseudo-heme ferrous complexes **2–9** which bind dioxygen to form stable adducts.

oxygen binding properties of the molecule.[314] The most stable adduct was formed with compound **5**, which bound dioxygen reversibly even at room temperature because of its slow ($t_{1/2}$ = 24 h) autoxidation process. The thermodynamic values for the reaction of this complex with dioxygen are $\Delta H = -17.5 \pm 0.4$ kcal/mol, $\Delta S = -76 \pm 2$ eu, $K_{O_2} = 0.050$ $Torr^{-1}$.[314] Although the reaction enthalpy is similar to values for Hr, the entropy is significantly more negative for this model compound. Such a large negative reaction entropy is consistent with the properties of other "lacunar" metal complexes.[314]

Because the autoxidation rate could be altered without changing the dioxygen binding properties of the iron center, this system provided a unique opportunity to carry out comparative mechanistic studies of the autoxidation and dioxygen binding reactions of the ferrous complexes. A series of ferrous cyclidene complexes with different exterior R groups and pocket sizes, including some with pockets too small for O_2 binding, was investigated.[323,325,326] For systems capable of binding dioxygen in the pocket, usually **4**, it was concluded that a ferric–peroxide species formed during autoxidation and that parallel, competing inner- and outer-sphere redox processes were involved. The binding and autoxidation reactions are shown in eqs 39 and 40, and the rate law derived from this competition is given in eq 41. Potential chemical routes to the peroxide species are listed in eqs 42–45.[323,326] An EPR

$$LFe^{II} + O_2 \overset{K_{O_2}}{\rightleftharpoons} LFe^{III}\text{–}O_2^- \quad (39)$$

$$LFe^{II} + O_2 \overset{k'}{\rightarrow} LFe^{III} + O_2^- \quad (40)$$

$$\text{rate}_{\text{autox}} = \frac{k'[Fe^{II}][O_2]}{1 + K_{O_2}[O_2]} \quad (41)$$

$$LFe^{II} + HO_2 \rightarrow LFe^{III}\text{–}(HO_2^-) \quad (42)$$

$$LFe^{III}\text{–}(O_2^-) + HO_2 \rightarrow LFe^{III}\text{–}(HO_2^-) + O_2 \quad (43)$$

$$LFe^{II} + HO_2 \rightarrow LFe^{III} + HO_2^- \quad (44)$$

$$LFe^{III} + HO_2^- \rightarrow LFe^{III}\text{–}(HO_2^-) \quad (45)$$

spectral feature at $g = 2.00$ was assigned to the peroxide complex for experiments conducted in acetonitrile/

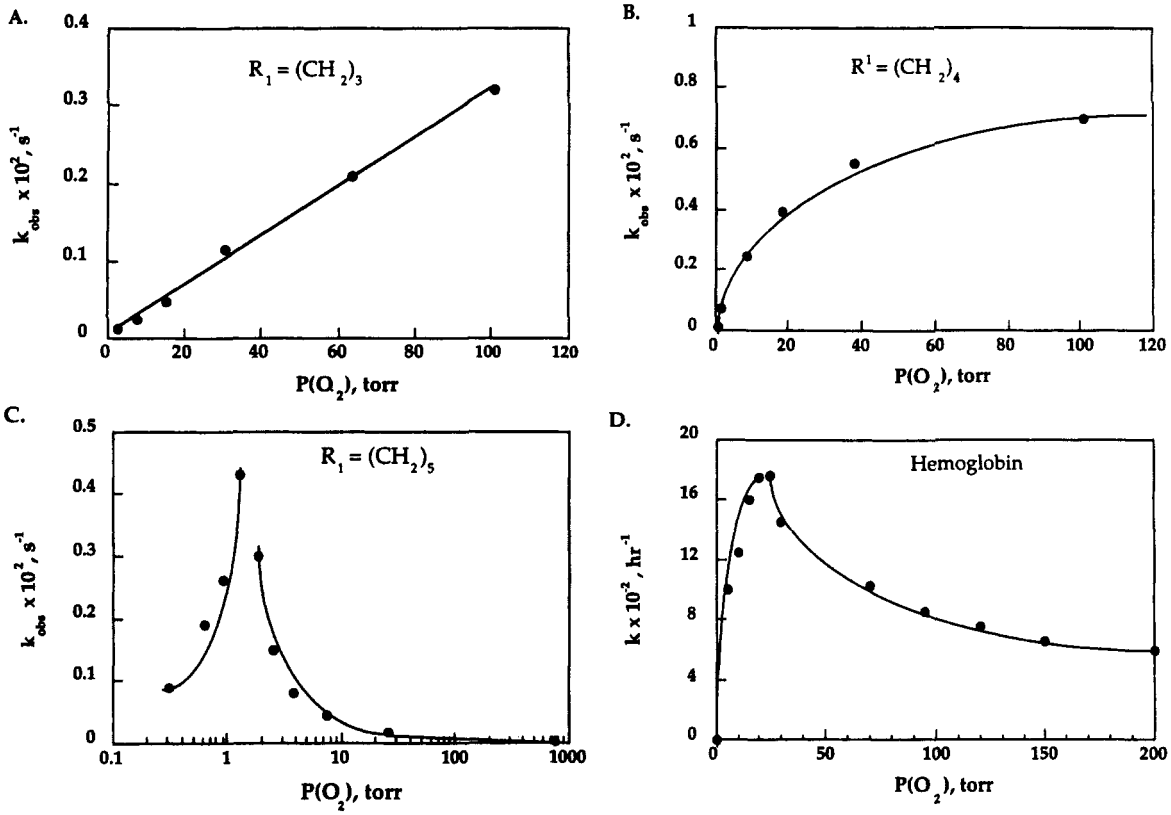

Figure 28. Plots of the observed rate constants for autoxidation as a function of dioxygen pressure for (A) compound 6, (B) compound 7, (C) compound 8, and (D) hemoglobin. (Reprinted from ref 325. Copyright 1993 American Chemical Society.)

pyridine/water and acetonitrile/1-MeIm solutions.[323] This signal was not observed in certain other solvent systems, however, and it is not clear whether the proposed intermediate was simply more reactive under such conditions, and therefore not observed, or whether its formation was somehow solvent specific. Although the process outlined for the autoxidation of 4 is chemically reasonable, spectroscopic evidence for the existence of the peroxide is weak.

In the work just discussed, it was postulated that the autoxidation step occurs by a separate pathway, parallel to the route leading to reversible dioxygen binding. The nature of this parallel reaction was approached by studying the effect of cavity size on autoxidation.[325] The species compared in this study were the tri-, tetra-, and the pentamethylene-bridged cyclidene compounds 6–8 (Figure 27). The cavity sizes in these complexes are such that the smallest does not even allow O_2 to approach the iron center, whereas the largest allows access of both O_2 and solvent molecules. The effect of dioxygen concentration on the rates of autoxidation was dramatically different among these three systems, as shown graphically in Figure 28.[325] These results are consistent with the interpretation that autoxidation is a parallel pathway to dioxygen binding for the $(CH_2)_3$ (6) and $(CH_2)_4$ (7) cases (eqs 39–41). For the trimethylene-bridged compound, K_{O_2} approaches zero and the rate law for autoxidation simplifies to a pseudo-first-order reaction. The extremely complicated behavior for the $(CH_2)_5$ complex (8), as for Hb, is explained by a solvent-dependent competition for the dioxygen binding site (eqs 46–48). Since the cavity in the $(CH_2)_4$ species (7) is only large enough to allow dioxygen access, solvent competition is removed and normal saturation behavior is observed.

$$LFe^{II} + S \underset{k_{-1}}{\overset{k_1}{\rightleftharpoons}} LFe^{II}\text{–}S \tag{46}$$

$$LFe^{II}\text{–}S + O_2 \xrightarrow{k_2} LFe^{III}\text{–}S + O_2^- \tag{47}$$

$$\text{rate} = \frac{k_1(k_2/k_{-1})[Fe^{II}][S][O_2]}{(k_2/k_{-1})K_{O_2}[O_2]^2 + \{(k_2/k_{-1}) + K_{O_2}\}[O_2] + 1} \tag{48}$$

As a final note on the reversible O_2-binding behavior of the cyclidene complexes, we mention the dinuclear variant, compound 9 (Figure 27).[315] Complexes of this ligand undergo a different reaction with dioxygen, one not necessarily based on metal coordination. The two ferrous ions are separated by 8–15 Å, depending on the length of the linker arms, and the iron atoms are postulated to act completely independently.[315] Superoxide is produced in the reaction but does not appear to coordinate to the metal ions. Autoxidation severely hampers the study of this system. To minimize this side reaction, very low oxygen tension was used to prevent the buildup of appreciable quantities of O_2^-. Interestingly, dioxygen binding in these dinuclear cyclidenes showed an inverse first-order dependence on the concentration of added nitrogenous base. Since no metal-binding site was required for the electron-transfer event, this result probably reflects changes in the redox properties of the ferrous center that accompany the base on/off equilibrium. For example, addition of excess pyridine to acetonitrile solutions shifted the Fe(II,III) couple by approximately −100 mV. Addition of 1-MeIm shifted it by −300 mV, the more

negative value arising from stronger binding to iron(III) than to iron(II) of imidazole relative to pyridine. In less coordinating solvents, the magnitude of the pyridine-initiated shift of the redox potentials was greatly enhanced.[315] Since the ferrous form of the complex is stabilized by the binding of a base, the driving force for the outer-sphere redox reaction is diminished, accounting for the inverse order in base concentration.

Although the effects of added base are well defined in reactions of porphyrins with dioxygen,[44] in non-porphyrin systems they are more difficult to observe and to rationalize. For heme iron the base effect results from coordination at the proximal site, trans to the dioxygen binding position. The composition of the coordination spheres varies greatly among non-heme iron oxygenases and oxygen carriers, whereas variations in the ligand environment in porphyrin systems occur mainly in the axial sites. Therefore, in the non-heme systems, there are more states than simply base-on and base-off such that both the basicity of the ligand and its position in the coordination sphere will affect the reactivity of the iron site. The consequences of these considerations are largely unknown at present, however.

2. Non-Heme Systems

Very few ferrous complexes having non-porphyrin ligands react with dioxygen to form stable adducts.[35,50-52,242,327-330] Several claimed dioxygen adducts[331-334] could not be substantiated or were proved to be incorrect.[35] Unlike the pseudo-heme model complexes, all of these adducts appear to be peroxo rather than superoxo species. This behavior parallels that of heme versus non-heme dioxygen carrier proteins. For diiron complexes, this result was not unexpected, but the formation of stable dinuclear peroxides from mononuclear iron(II) precursors was a surprise, although very similar bridging peroxide motifs had been observed as intermediates in the chemistry of porphyrin models with dioxygen.[319,320] Figure 29 displays the known or postulated structures of diiron(II) complexes and their corresponding (μ-peroxo)diiron(III) adducts to be discussed in this section.

When compound **10a** was exposed to dioxygen,[327] a violet species **10b** formed having λ_{max} = 540 nm (ϵ = 187 M^{-1} cm^{-1}). The adduct irreversibly decayed at room temperature over a period of 5 h. For the corresponding ligand in which the pyridine ring was replaced by an aliphatic amine **11a** the dioxygen adduct was much shorter lived.[327] Upon exposure to dioxygen a red-purple adduct **11b** formed, but immediately faded as the colorless oxidized end product was generated.[327] Kinetic studies of the formation of **10b** indicated a process first order in both [O_2] and [LFe^{II}] and polarographic studies of dioxygen uptake revealed a stoichiometry of 2Fe:1O_2. The kinetic results were adequately fit by a simple two-step mechanism for the formation of the complex, where the first step is rate limiting. The rate constant for this reaction in water, (I = 0.2 M, pH 8.0) at 25 °C is (1.4 ± 0.2) × 10^2 M^{-1} s^{-1}.[327] The reaction was sensitive to pH, showing a 6-fold rate increase over the pH range 8.0–9.5. No explanation for this behavior was provided.

Another mononuclear complex that binds dioxygen and rapidly forms a dinuclear peroxide adduct is **12a**.[50,52] The precursor is a 5-coordinate ferrous ion bound to a

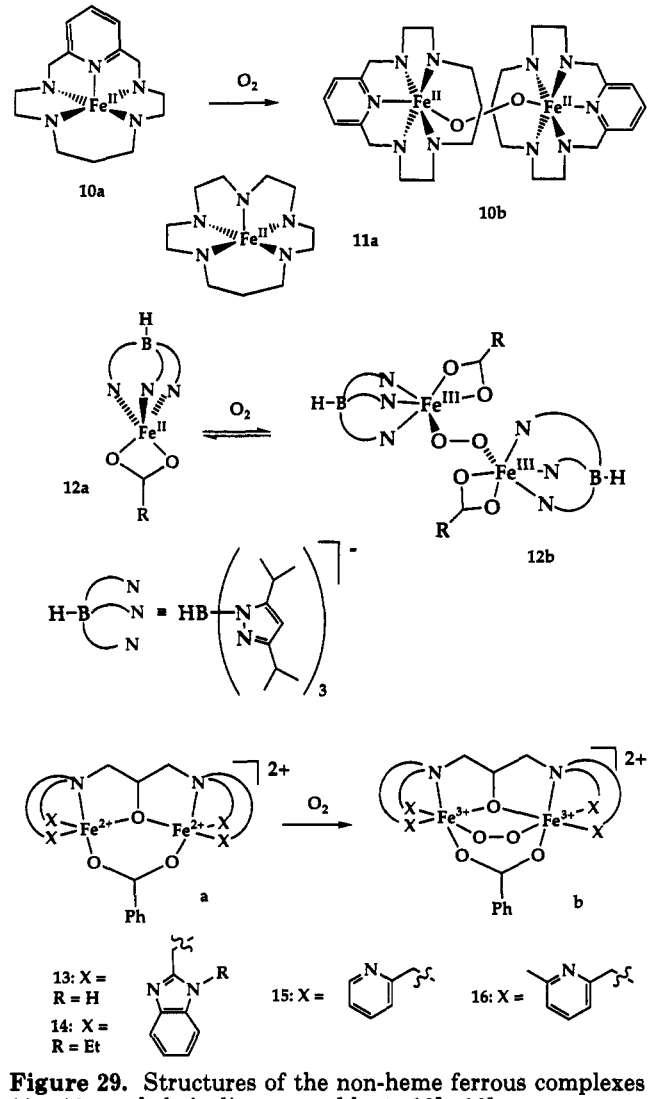

Figure 29. Structures of the non-heme ferrous complexes **10a–16a** and their dioxygen adducts **10b–16b**.

sterically demanding tridentate, facially coordinating ligand {HB(3,5-$iPr_2pz)_3$} and a chelating carboxylate ligand. The structure of the precursor has been crystallographically determined. On exposure to dioxygen in non-coordinating solvents at temperatures below −20 °C, **12a** reacts to form a dark blue-green (λ_{max} = 680 nm) 2:1 dioxygen adduct, **12b**.[50] Below −50 °C, the binding is irreversible, but between −50 and −20 °C, the ferrous starting material can be regenerated by application of vacuum or purging with an inert gas.[50,52] This system can be cycled at least 10 times with only minimal loss of activity. In coordinating solvents, **12b** is not formed at any temperature.[50]

The nature of the 2:1 adduct has been studied by a variety of physical methods in an attempt to determine its structure.[52] The resonance Raman spectrum revealed an O–O stretching band at 876 cm^{-1}, in the region for peroxide, and the assignment was supported by $^{18}O_2$ isotope shifts.[50] Unlike the pseudo-heme dioxygen adducts discussed above, this product was paramagnetic (S = $^5/_2$) and exhibited modest (J = −33 cm^{-1}) antiferromagnetic coupling. EXAFS data supported the assignment of the structure as a (μ-1,2-peroxo)diiron(III) unit with a dihedral angle at the O–O bond of approximately 90° and an Fe–Fe distance of 4.3–4.4 Å.[52] Dinuclear ferrous derivatives of **12a** also bind dioxygen, but the adducts appear to be less stable.[335]

It is unclear whether solution equilibria lead to the formation of the same dioxygen adduct or whether the species are structurally different.

Compound **12b** is one of the more robust non-heme iron dioxygen complexes. Its autoxidation must be slow to explain reversible O_2 binding. The steric bulk of the hydrotris(diisopropylpyrazolyl)borate is probably responsible for the added stability, the reasons being similar to those discussed above for the phenyl- and benzyl-substituted cyclidene complexes. The electronic properties of the carboxylate ligand do not significantly affect the chemistry; changing the carboxylate ligand shifted the broad charge transfer band of the dioxygen adduct slightly, but did not alter its temperature sensitivity.[52]

A final class of stable ferric dioxygen adducts to be discussed form in the reaction of dioxygen with ferrous complexes of ligands derived from *N,N,N',N'*-X_4-2-hydroxy-1,3-diaminopropane, where X is one of several nitrogeneous bases. Most extensively studied are complexes where X = 2-benzimidazolylmethyl (HPTB) (**13a**), (*N*-ethyl-2-benzimidazolyl)methyl (Et-HPTB) (**14a**), 2-pyridylmethyl (HPTP) (**15a**) and (6-methyl-2-pyridyl)methyl (HPTMP) (**16a**). As a series, the diferrous compounds **13–16** nicely illustrate how ligand alterations can affect the reactivity of the metal center.

The first dioxygen adduct generated for this class was with the HPTB system.[328] The starting material was reportedly $[Fe^{II}_2(HPTB)Cl_5]$, but was largely uncharacterized. Later studies of the oxygenation reactions employed μ-carboxylato analogs.[51,336] The bridging carboxylate group renders the model more biomimetic, although an alkoxo bridge has not yet been observed in a non-heme iron protein. The steric bulk of the benzimidazolyl rings prevented coordination of a second carboxylate to the dinuclear ferrous center, providing some indication of the crowding around the iron atoms.

At low temperature (T < −80 °C), the HPTP–, HPTMP–, and Et-HPTB–diiron(II) complexes all formed stable dioxygen adducts quite readily. Only the HPTMP adduct exhibited reversible behavior, however, with $P_{1/2}$ = 42 Torr (CF_3COO^- complex) and 6 Torr ($PhCOO^-$ complex) at −35 °C in CH_2Cl_2.[329,330] The Et-HPTB complex is relatively symmetric, having two 5-coordinate square pyramidal ferrous ions.[51,242] The more sterically demanding HPTMP complex, on the other hand, is solvated and has one octahedral and one square pyramidal iron atom. The higher coordination number results in a lengthening of the Fe–N bonds and helps alleviate the steric clash. This asymmetric solvation probably indicates more flexibility for this complex than for **13a**, a property that could facilitate the binding of small molecules to the metal center.

The three complexes differ not only in the degree to which formation of their O_2 adducts is reversible, but also in the stability of the adducts toward irreversible decomposition. Compound **14b** is indefinitely stable in methylene chloride or acetonitrile at −60 °C and forms transiently at room temperature before decomposing.[51] Formation of the HPTMP adduct **16b** is reversible at −20 °C, and the product is completely stable at −60 °C.[329] The HPTP–O_2 adduct **15b** is exceedingly reactive, however, and cannot be formed at −40 °C in MeCN or at −80 °C in CH_2Cl_2.[51,329] The addition of small amounts of DMSO or other polar aprotic solvents has a stabilizing influence on this entire series of dioxygen complexes, although the reason for this effect is currently unknown.[51]

The chemical reactivities of the diiron(III) peroxide species have been studied only preliminarily. Substoichiometric oxo transfer to PPh_3 occurred for all three compounds, with the HPTP complex showing the greatest activity.[51,329] The degree of oxo-transfer capability follows the relative temperature stabilities of the adducts (HPTP > HPTMP > Et-HPTB, HPTB). The HPTP complex can also oxidize phenols, but none of these complexes shows any propensity to hydroxylate or oxygenate substrates such as alkanes, which are much poorer oxo transfer acceptors.[51,337] The lack of oxo-transfer reactivity of **14b** contrasts with a report in which $[Fe^{III}_2(HPTB)(OH)]^{4+}$ was able to catalyze the oxidation of 2,4-di-*tert*-butylphenol to 3,5-di-*tert*-butylcatechol by hydrogen peroxide.[22] Presumably, quite similar diferric peroxide complexes are present in both reactions, although the carboxylate ligand is absent in the reported catalytic system. Reinvestigation of the latter may be required to resolve the inconsistency.

Recently, a kinetic investigation of the reactions of **14a–16a** with dioxygen has been undertaken.[338] The first step of the reaction, formation of the (μ-peroxo)-diiron(III) species, was studied by stopped-flow spectroscopy at low temperature. The results revealed a much larger activation barrier for the reaction of **16a** with O_2 relative to the other two compounds. The significantly larger activation enthalpy and less negative entropy of activation arise from a postulated internal ligand rearrangement required to open a coordination site for dioxygen.

Peroxide derivatives of **13–16** were formed from the reaction of the diiron(III) species with hydrogen peroxide.[21,22,29,328,336] The wavelengths of the absorption maxima often differed slightly from those of complexes formed in the reaction of the diiron(II) complexes with O_2, however.[21,51,328] The variations might arise from solvent system differences, since addition of aqueous hydrogen peroxide introduces protons that are not present in the dioxygen reactions carried out in dry, aprotic organic solvents.

B. Non-Catalytic Oxidation of Iron(II) Complexes Following Unstable Dioxygen Adduct Formation

The oxidation kinetics of a well-characterized model compound, $[Fe^{II}(Me_3TACN)_2(OH)(OAc)_2](ClO_4)_2$ (**17a**), which does not form a stable peroxide adduct have recently been investigated.[192] The reaction is shown in eq 49. The goal of this work was to elucidate intrinsic factors involved in the oxidation of dinuclear iron(II) centers similar to those found in the biological systems but without the surrounding protein sheath. The reaction consumed 0.5 molar equiv of dioxygen, all of which was used to form the oxo bridge in the product, as verified by ^{18}O-labeling experiments.[192] The kinetics of the oxidation reaction could be explained by proposing a preequilibrium step that afforded an open coordination site prior to dioxygen binding. In particular, the order in dioxygen depended upon the choice

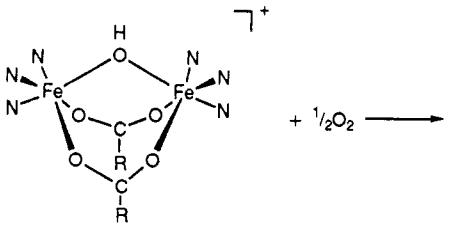

17a

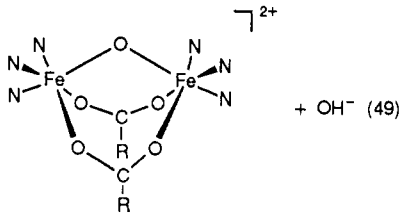

17b

+ OH⁻ (49)

of solvent. In chloroform, the rate law followed eq 50, with a first-order dependence on $[O_2]$, whereas in methanol, the reaction was independent of dioxygen concentration (eq 51). This behavior was readily

$$\text{rate} = k_{exp}[O_2][\mathbf{17a}]^2 \quad (50)$$

$$\text{rate} = k_{exp}[\mathbf{17a}]^2 \quad (51)$$

explained by proposing an equilibrium for **17a** in which a carboxylate ligand shifts from bidentate bridging to monodentate terminal with concomitant coordination of methanol to the site vacated on one of the ferrous ions. This intermediate accounts for the more rapid rate of oxidation in methanol compared to chloroform. The transition state was postulated to be a mixed-valent tetranuclear η^2,η^2-peroxide-bridged complex[192] (Figure 3j). Such a tetranuclear species, besides accounting for the kinetic data, has precedence in the only structurally characterized non-heme iron–peroxide model complex.[48] The tetranuclear intermediate is presumed to be the complex in which the critical O–O bond cleavage step occurs, but since its formation and not its decomposition was the rate-limiting step, direct observation of bond scission was not possible.

The results of this study recall one of the main findings of the iron–EDTA oxidation studies,[74] namely, that coordination of dioxygen to the metal is required. In reactions of **17a** with dioxygen, the need for a vacant coordination site is manifest by equilibria that precede the actual oxidation steps. The kinetic behavior of this complex is very different from that of the non-heme diiron proteins, where the diiron cores cannot approach one another to form the tetranuclear peroxide-bridged intermediate. The decomposition of this intermediate is analogous to the decay of iron porphyrin intermediates postulated to form during their reactions with dioxygen.[319,320]

The lesson learned from this kinetic study is one recognized by porphyrin chemists many years ago. To mimic the biological reactions, bulky ligands must be employed to avoid the kinetically favored bimolecular decay pathway. Dinucleating ligands provide some of the stability and bulk required, but many of the existing diiron(II) complexes in this class contain non-biomimetic bridges such as alkoxides or aryloxides. Moreover, in complexes of these dinucleating ligands, the RO^- bridge impedes access of O_2 to the dinuclear core from the direction typically found in proteins such as Hr. The search for alternative dinucleating ligands is an area of active research.

C. Catalytic Hydroxylation Reactions with Fe(II) and O_2 Involving Transient Fe–O_2 Intermediates

In many oxidations, the active species are too short-lived to be observed. In some cases, information on the active oxidants can be obtained indirectly from kinetics investigations, the distribution of products, or the identification of a decomposition product. Even when the spectroscopic signature of a species formed during the reaction can be monitored, it must be demonstrated to be on the reaction pathway. Unless the intermediate can be synthesized separately and shown to be capable of entering the reaction in the absence of its precursors, its proposed role is not definitively established.

The chemistry discussed in this section uses the reaction of dioxygen with a ferrous compound to oxygenate or oxidize an organic substrate in a catalytic manner. Commonly employed substrates include cyclohexane, cyclohexanol, cyclohexene, adamantane, and *cis*-stilbene. Information about the mechanism is gathered from relative reactivity at primary, secondary, and tertiary aliphatic carbon positions, the ratio of alcohol to ketone products, the ability to form epoxides from alkenes, and isomerization taking place during the reaction. Together these features provide clues about the transient oxygen species involved in the reaction mechanism.

1. Udenfriend's Reaction

A catalytic system for synthesizing phenols, catechols, and epoxides using ferrous ions, EDTA, ascorbic acid, and dioxygen at neutral pH was first reported by Udenfriend.[339] This reaction has been well studied because of its similarity to that of many mononuclear monooxygenases. The actual species responsible for the activity, however, is still being debated 40 years after the original discovery.[340–344] The reaction is mechanistically related to many of the autoxidations of chelated iron(II) discussed above (eqs 21 and 22). Two features differentiate the autoxidation and catalytic reactions, however. The first is the presence of a substrate, which reacts with one of the activated dioxygen intermediates, and the second is the presence of ascorbate, which reduces the ferric ions back to their ferrous form, closing the catalytic cycle. The oxidation and reduction phases of the reaction can be separated on the basis of work investigating the catalytic oxidation of ascorbate by dioxygen and iron.[241,345,346] In the absence of an oxidizable substrate, Udenfriend's reaction and the catalytic oxidation of ascorbate are identical. Iron(II) chelates are autoxidized to their iron(III) form, which then are reduced back to iron(II) by an intermediate iron(III)–ascorbate complex. This similarity is analogous to the coupled and uncoupled reactions discussed above for the pterin- and α-ketoglutarate-dependent enzymes. No evidence was found for a complex between ferrous ions and ascorbate.[346,347] Instead, ferric ions produced by oxidation of iron(II) interact with ascorbate in a separate reaction, leading to the reduction of the iron. Udenfriend's catalytic

cycle can therefore be roughly approximated by eqs 52 and 53, where the former is the functional step and the

$$2LFe^{II} + O_2 + ArH + 2H^+ \rightarrow 2LFe^{III} + ArOH + H_2O \quad (52)$$

$$2LFe^{III} + AscH_2 \rightarrow 2LFe^{II} + dAsc + 2H^+ \quad (53)$$

latter reactivates the catalyst. Further support for the functional separation of these steps is the ability to substitute alternative reductants for ascorbic acid, a property also shared by many biological systems.[341,348] The efficiency of the Udenfriend reaction is extremely poor, however, often affording oxidized product yields of 5–10% on the basis of reductant.[340] Since the active oxidant is extremely reactive, a rate constant of $k = (3.9 \pm 0.6) \times 10^9$ M^{-1} s^{-1} having been measured for the Udenfriend reaction on thymine,[344] the low yield is probably based on a nonproductive reaction with solvent or, more likely, autoxidation of the reductant. This problem is circumvented in biological systems by rendering the iron(II) center inactive in the absence of bound substrate and through the use of a separate reductase protein (see above discussion).

The active species in Udenfriend's reaction may or may not involve free hydroxyl radicals. The general methods used to approach this issue are to run parallel Fenton reactions, while attempting to trap the radical, or observe a rearranged substrate probe. The assumption here is that Fenton chemistry generates only free hydroxyl radicals and that a significant decrease in the amount of radical-generated products would indicate an alternative mechanism for Udenfriend's reaction. Product distribution studies revealed the presence of additional species formed in the Fenton chemistry and the ratios of common products formed by the two reactions were different.[340,341,349] It was therefore concluded that the active oxidant in Udenfriend's reaction was not the same one as in Fenton chemistry. On the other hand, use of a radical quenching technique to examine the effects of alcohols on the two systems gave identical results.[344] None of these investigations is totally convincing, however. Product distributions can be influenced by extremely small variations in reaction conditions or contaminants and, just because two chemical species are quenched at the same rate, does not necessarily mean that the reactive species are identical.

2. Gif Chemistry

One of the most studied catalytic reactions is the so-called Gif system.[309,350,351] Although there are many varieties of Gif chemistry, some using oxidants other than dioxygen, there are several (Gif^{III}, Gif^{IV}, and Gif-Orsay) which rely on the reaction of ferrous iron with dioxygen in a pyridine/acetic acid solvent. Some systems thought to use H_2O_2 as the oxygen donor were subsequently found to utilize dioxygen. When run under an atmosphere of $^{18}O_2$, the products contained exclusively ^{18}O-labeled oxygen.[352] In spite of extensive work on these systems, many of the mechanistic details remain murky. The structures of several intermediates proposed in the following discussion are quite speculative and have not been observed directly. They have been proposed in the primary literature to explain the observed products and isotopic distributions. The postulated mechanisms should therefore be viewed as working hypotheses.

Gif catalysts react with alkanes, affording primarily ketones along with small amounts of alcohols and other minor products, depending on the conditions. Furthermore, the preference for secondary over tertiary carbons has been measured to be as high as 22:1, but more typically the ratio is around 1.[309] A key piece of information regarding the nature of the Gif reaction was the observation of a cyclohexyl hydroperoxide intermediate.[308,352] In the absence of an oxidant, this hydroperoxide decomposed in the presence of catalyst to form the observed ratio of products. Since the hydroperoxide affords both the major and minor products, it must lie along the reaction pathway at a point that precedes the divergence of products into alcohols and ketones. Mechanistic studies on other alkane activation systems employing iron catalysts have also proposed the intermediate formation of alkyl hydroperoxides and/or metal bound alkyl peroxides.[353,354] As currently formulated, the Gif mechanism does not involve direct reaction of dioxygen with a ferrous species in any of the mechanistically important steps (Figure 30); instead, O_2 oxidizes the Fe(II) precatalyst to a (μ-oxo)diiron(III) compound and hydrogen peroxide. These species then continue as if hydrogen peroxide and ferric ion were added initially.[36,309,355] Recent work, discussed below, may require that these Gif mechanistic proposals be altered, however.[252,356]

The picolinate (PA) and dipicolinate (DPA) systems, termed oxygenated Fenton reagents,[351,357] are quite similar to the Gif chemistry. The reactions are run in pyridine/acetic acid solutions with comparable product distributions, although the yields are higher. Instead of using Fe(III) and peroxide, as in the Gif^{II} system, the PA and DPA reactions employ Fe(II) and hydrogen peroxide. Anaerobically, this mixture would be expected to undergo basic Fenton chemistry,[60] generating pyridyl or substrate radicals from hydroxyl radical. In the presence of dioxygen, however, the reaction is drastically modified.[252,351,356] Instead of cyclohexylpyridine being the primary product when cyclohexane is used as the substrate, cyclohexanone is produced.[356] The relative reaction rates of ferrous material with dioxygen and peroxide were measured, revealing a 1000-fold kinetic preference for reaction with the latter.[356] It was therefore proposed that a ferrous–hydroperoxide species reacts with dioxygen before decomposing via Fenton chemistry. A scheme delineating this hypothesis is shown in Figure 31. The active agent for hydrogen abstraction in this system is the ferric–peroxy–superoxide complex which, by analogy to Gif chemistry, leads to formation of a metallo–alkyl peroxide, the decomposition of which yields products. Minor products can arise from simple Fenton chemistry or alternative modes of peroxide decomposition.

The Gif mechanism should be re-analyzed in light of these results and the $^{18}O_2$-labeling studies discussed above. The dioxygen affinity of ferrous ions is considerably greater than that of ferric complexes. Biological systems that carry out such hydroxylations with iron usually require the reduced state of the enzyme. In one mechanism (Figure 30), oxygenation results from

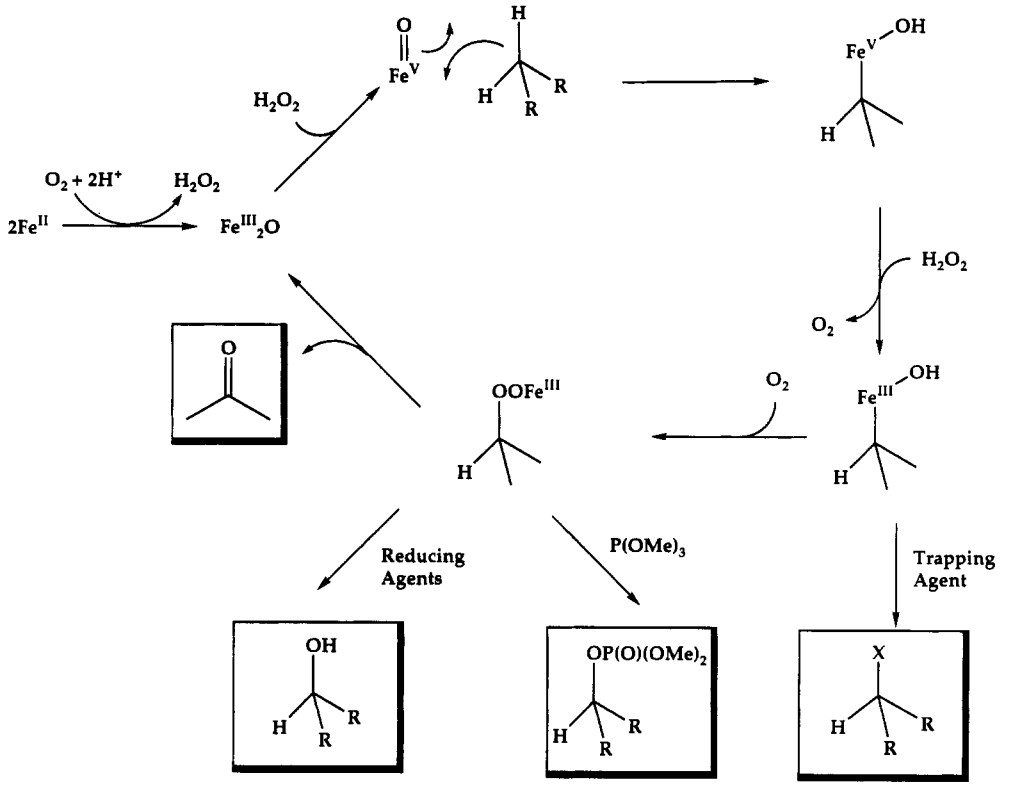

Figure 30. Proposed mechanism for the catalytic cycle of Gif oxidations. (Adapted with permission from ref 309.)

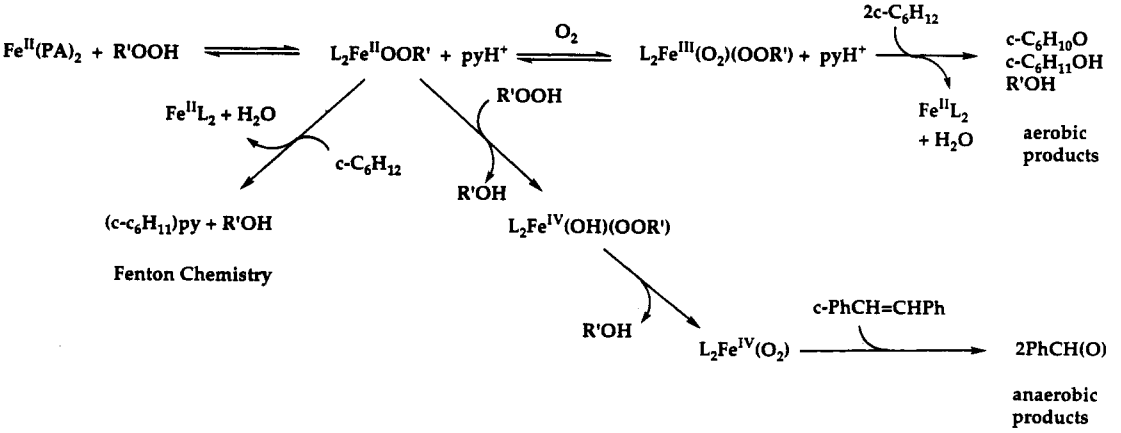

Figure 31. Proposed mechanism for the oxidation of alkanes by $Fe^{II}(PA)_2$. (Adapted with permission from ref 356.)

dioxygen insertion into the iron–carbon bond of an organometallic intermediate. Insertion reactions of this type are precedented in organometallic chemistry, but alternative routes to a metallo–alkyl peroxide species, such as the one in Figure 31, can be envisioned and must be explored further. Whether one of these mechanisms, or some totally different route, is eventually accepted will have to await more detailed study of the reactions. To aid in that process, better defined catalysts will be helpful. The number of potentially equilibrating species in the parent Gif reactions is large, and elucidation of any rational mechanism is likely to be difficult until the system is simplified. The use of PA and DPA provides some stability for the metal complex resulting from chelation effects, and presumably the ligands remain coordinated during catalysis. These complexes are therefore a step toward better characterization of these reactions. As the full reaction schemes from the published work indicate, however, the chemistry still has little specificity and slight changes in conditions lead to new and different products.[356]

In the absence of peroxide, the ferrous compound $Fe^{II}(DPAH)_2$, will also react catalytically with dioxygen to convert cyclohexane to cyclohexanone. It has been postulated that the reaction results from in situ generation of hydrogen peroxide as shown in eq 54.[252]

$$[Fe^{II}(DPAH)_2] + O_2 \rightleftharpoons [(DPAH)(DPA)Fe^{IV}(OOH)] + L_2Fe^{II} \rightarrow HOOH + 2[(DPA)(DPAH)Fe^{III}] \quad (54)$$

Support for this mechanism, which is inconsistent with the common dinuclear intermediate observed for the autoxidation of porphyrins and several non-heme iron compounds discussed above,[319,320,327] comes from electrochemical experiments where a (μ-oxo)diiron(III) species, the normal product of the diferrous reaction pathway, is not observed. It is unclear why this complex

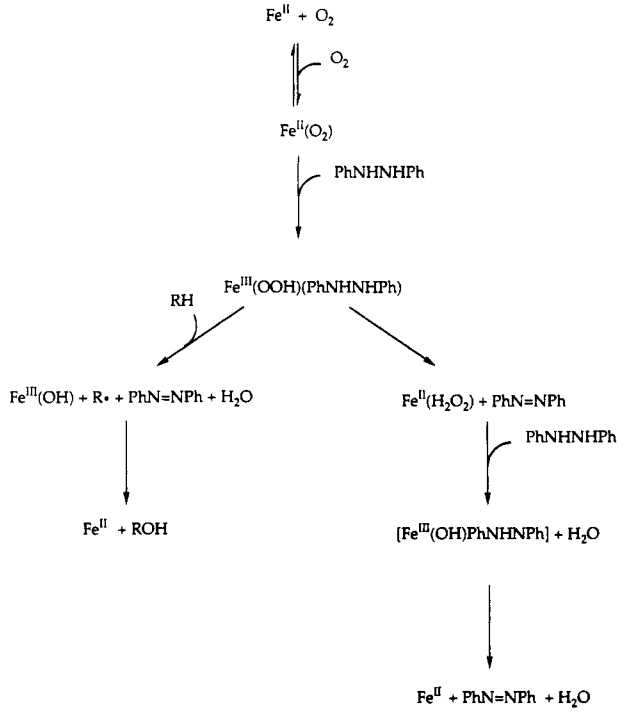

Figure 32. Proposed mechanism for the oxidation of alkanes by Mimoun's system. (Reprinted from ref 359. Copyright 1988 Pergamon.)

reacts with dioxygen differently from other typical ferrous complexes or why the commonly observed and thermodynamically stable (μ-oxo)diiron(III) species is not formed.

3. Mimoun's System

Whereas Udenfriend's reaction can be written as two distinct steps, oxidation and reactivation as discussed above, a separate class of oxidations has been described in which an iron species coordinates simultaneously to both dioxygen and the reducing agent. As a result, more concerted redox steps can be envisioned. Several of the biological systems discussed employ a similar strategy in which multienzyme or multisubunit aggregates join the oxidizing and reducing functionalities. The interactions between subunits can then control the biochemistry to time the influx of electrons and avoid wasteful consumption of reductant. A model system of this type, capable of hydroxylating alkanes, alkenes, and arenes, was first described by Mimoun[358] although other similar systems are known. The reaction is written in eq 55, where diphenylhydrazine is reduced

$$\mathrm{RH + PhNHNHPh + O_2} \xrightarrow[\mathrm{PhCOOH}]{\mathrm{Fe^{II}\ cat.}} \mathrm{ROH + PhN{=}NPh + H_2O} \quad (55)$$

to diazobenzene concomitant with substrate oxidation. This system tends to give alcohols rather than ketones and, like many other catalytic systems, is characterized by low yields and small turnover numbers.[359] As expected, the system exerts less control over the autoxidation of the reductant than its biological counterparts and greater than stoichiometric consumption of reductant is usually observed. The secondary/tertiary oxidation ratio is typically around 1.[359]

Kinetic studies of this system have led to the proposal that an iron–hydroperoxide–hydrazine complex is the active species in the hydroxylation chemistry.[359] Electrochemical studies of Fe^{II}/diphenylhydrazine/hydrogen peroxide solutions support this finding, revealing that, in the presence of the disubstituted hydrazine, normal Fenton chemistry is subverted by an alternative reaction that leads to catalytic monooxygenation.[360] A proposed mechanistic scheme derived from kinetic studies is presented in Figure 32, but unfortunately no spectroscopic evidence has been obtained for any of the postulated intermediates. Structurally similar intermediates with different formal oxidation states are invoked in a [Fe^{II}(DPAH)$_2$]-catalyzed system, where diphenylhydrazine was used as the reductant.[361] In the latter study, greater oxidative selectivity was observed compared to Fenton chemistry. Much work remains to be done on systems of this kind before their reactivity is fully understood or the chemistry is rendered synthetically useful.

V. Conclusions and Future Directions

The foregoing discussion reveals the diversity of biochemical and biomimetic oxygenation reactions carried out by non-heme iron centers. Our understanding of these reactions is far from complete and examples of contradictory and confusing results have been included to illustrate the nature of the debate on the mechanisms of these reactions.

Over the past few years, the greatest advances have been in understanding the chemistry of dinuclear iron cores in Hr, RR, and MMO as well as their small molecule models. The extensive structural and spectroscopic detail available for these three proteins has helped to unravel their individual reaction mechanisms, and we are beginning to understand why Hr reacts differently from RR and MMO. The lower coordination numbers, preponderance of oxygen versus nitrogen donor atoms and possibly the involvement of amino acid-derived radicals in RR, and perhaps MMO, activate dioxygen for O–O bond cleavage. Another key factor may be that Hr, like Hb and Mb, has a well-defined site for monodentate binding of O_2, whereas both RR and MMO have the potential to form bridging peroxides. Perhaps such a species is a required precursor for oxygenation reactions in non-heme proteins.

As a whole, there is less structural information available about mononuclear systems, and this area deserves more attention. Like MMO and RR, the coordination environments of the mononuclear non-heme iron enzymes are flexible, with multiple sites of attachment for small molecules. The systems exhibit features that do not appear to play an important role in the chemistry of the dinuclear enzymes. The ability of substrates to activate the iron site toward dioxygen is of particular interest because the nonspecific oxidation of the reductant is one of the major drawbacks in most model catalytic hydroxylation reactions. In the enzymes, this property prevents the oxidation of the iron center when substrate is absent. In dinuclear systems such as MMO, binding of the other components and possibly the substrate can affect the hydroxylase reactivity. Understanding the structural changes at the iron center that occur upon substrate and coupling protein binding will lead to more sophisticated design

of model compounds and small molecule catalysts, allowing the greater tuning of the dioxygen reactivity of the ferrous ion.

For the modeling chemist, these systems provide a particular challenge. On the one hand, extreme bulk seems to be necessary to prevent the unwanted bimolecular decay reactions of the active intermediates. At the same time, the ligand cannot be so sterically encumbered that dioxygen cannot bind; moreover, there must be room for a substrate to approach the active species. To accomplish these seemingly contradictory aims with anything less than a protein is a daunting task, but one that might be surmountable through the application of innovative ligand design. The functional models for the catalytic hydroxylation reactions currently have little resemblance to their biogenic progenitors. The path toward the marriage of structural and functional modeling lies ahead.

VI. Acknowledgments

We wish to thank all of our colleagues who generously provided us with preprints of their unpublished work and for their helpful discussions: D. H. R. Barton, D. H. Busch, N. D. Chasteen, T. J. Collins, M. Fontecave, S. Gorun, P. M. Harrison, K. D. Karlin, N. Kitajima, J. Klinman, Y. Nishida, L. Que, Jr., J. Sanders-Loehr, D. T. Sawyer, A. E. Shilov, B.-M. Sjöberg, J. Stubbe, M. Suzuki, E. C. Theil, and J. S. Valentine. We would especially like to acknowledge J. M. Berg and P. M. Harrison for their assistance in preparing figures of the enzyme active sites and K. E. Liu, A. Masschelein, and K. L. Taft for their insightful comments on early drafts of this manuscript. This work was supported by grants from the National Institutes of Health.

VII. Abbreviations

1-MeIm	1-methylimidazole
2-KG	2-oxoglutarate, α-ketoglutarate
5-Me-HXTA	*N,N'*-(2-hydroxy-5-methyl-1,3-xylylene)bis(*N*-carboxymethylglycine)
ACV	δ-[5-amino-5-(hydroxycarbonyl)pentanoyl]-L-cysteinyl-D-valine
$AscH_2$	ascorbic acid
BLM	bleomycin
dAsc	dehydroascorbate
DMSO	dimethyl sulfoxide
DNA	deoxyribonucleic acid
DOPA	dihydroxyphenylalanine
DPA	dipicolinate
DPAH	dipicolinic acid
EDTA	ethylenediaminetetraacetate
ENDOR	electron nuclear double resonance
EPR	electron paramagnetic resonance
Et-HPTB	*N,N,N',N'*-tetrakis(*N*-ethyl-2-benzimidazolylmethyl)-2-hydroxy-1,3-diaminopropane
EXAFS	extended X-ray absorption fine structure
FAD	flavin adenine dinucleotide
H_2BP	dihydrobiopterin
H_4BP	tetrahydrobiopterin
$HB(3,5\text{-}iPr_2pz)_3$	hydrotris(3,5-diisopropylpyrazol-1-yl)borate
Hb	hemoglobin
HLF	human liver ferritin
HoSF	horse spleen ferritin
HPTB	*N,N,N',N'*-tetrakis(2-benzimidazolylmethyl)-2-hydroxy-1,3-diaminopropane
HPTMP	*N,N,N',N'*-tetrakis[(6-methylpyrid-2-yl)methyl]-2-hydroxy-1,3-diaminopropane
HPTP	*N,N,N',N'*-tetrakis(2-pyridylmethyl)-2-hydroxy-1,3-diaminopropane
Hr	hemerythrin
IPNS	isopenicillin N synthase
KIE	kinetic isotope effect
Mb	myoglobin
MCD	magnetic circular dichroism
MeCN	acetonitrile
Me_3TACN	1,4,7-trimethyl-1,4,7-triazacyclononane
MMO	methane monooxygenase
MOPS	4-morpholinepropanesulfonic acid
NADH	nicotinamide adenine dinucleotide
NHE	normal hydrogen electrode
NMR	nuclear magnetic resonance
OAc	acetate
OBz	benzoate
OEP	octaethylporphyrin
PA	picolinate
PAH	phenylalanine hydroxylase
4,5-PCD	protocatechuate 4,5-dioxygenase
PhIO	iodosylbenzene
py	pyridine
PMO	putidamonooxin (4-methylbenzoate *O*-demethylase)
rHF	recombinant H chain ferritin
rLF	recombinant L chain ferritin
RMS	root mean squared
RR	ribonucleotide reductase
SOD	superoxide dismutase
TH	thymine hydroxylase
TRP	tryptophan hydroxylase

VIII. References

(1) *Iron-Sulfur Proteins*; Lovenberg, W., Ed.; Academic: New York, 1977; Vols. 1–3.
(2) *Iron-Sulfur Proteins*; Spiro, T. G., Ed.; Wiley and Sons: New York, 1982; Vol. 4.
(3) *Heme Proteins*; Eichhorn, G. L., Marzilli, L. G., Eds.; Elsevier: New York, 1988; Vol. 7.
(4) Rifkind, J. M. *Adv. Inorg. Biochem.* **1988**, *7*, 155–244.
(5) Holm, R. H.; Ciurli, S.; Weigel, J. A. *Prog. Inorg. Chem.* **1990**, *38*, 1–74.
(6) Springer, B. A.; Sligar, S. G.; Olson, J. S.; Phillips, G. N., Jr. *Chem. Rev.* **1994**, *94*, 699–714 (this issue).
(7) Janssen, D. B.; Grobben, G.; Hoekstra, R.; Oldenhuis, R.; Witholt, B. *Appl. Microbiol. Biotechnol.* **1988**, *29*, 392–399.
(8) Janssen, D. B.; Witholt, B. In *Metal Ions in Biological Systems*; Sigel, H., Sigel, A., Eds.; Marcel Dekker: New York, 1992; Vol. 28, pp 299–327.
(9) *Methane and Methanol Utilizers*; Murrell, J. C., Dalton, H., Eds.; Plenum: New York, 1992.
(10) Fennell, D. E.; Nelson, Y. M.; Underhill, S. E.; White, T. E.; Jewell, W. J. *Biotechnol. Bioeng.* **1993**, *42*, 859–872.
(11) Lippard, S. J. *Angew. Chem., Int. Ed. Engl.* **1988**, *27*, 344–361.
(12) Sanders-Loehr, J. In *Iron Carriers and Iron Proteins*; Loehr, T. M., Ed.; VCH: New York, 1989; Vol. 5, pp 373–466.
(13) Que, L., Jr.; True, A. E. *Prog. Inorg. Chem.* **1990**, *38*, 97–200.
(14) Vincent, J. B.; Olivier-Lilley, G. L.; Averill, B. A. *Chem. Rev.* **1990**, *90*, 1447–1467.
(15) Kurtz, D. M., Jr. *Chem. Rev.* **1990**, *90*, 585–606.
(16) Howard, J. B.; Rees, D. C. In *Advances in Protein Chemistry*; Anfinsen, C. B., Edsall, J. T., Richards, F. M., Eisenberg, D. S., Eds.; Academic: New York, 1991; Vol. 42, pp 199–280.
(17) Wilkins, R. G. *Chem. Soc. Rev.* **1992**, *21*, 171–178.
(18) Que, L., Jr. In *Bioinorganic Catalysis*; Reedijk, J., Ed.; Marcel Dekker: New York, 1993; pp 347–393.
(19) McClune, G. J.; Fee, J. A.; McCluskey, G. A.; Groves, J. T. *J. Am. Chem. Soc.* **1977**, *99*, 5220–5222.
(20) Shirazi, A.; Goff, H. M. *J. Am. Chem. Soc.* **1982**, *104*, 6318–6322.
(21) Nishida, Y.; Takeuchi, M.; Shimo, H.; Kida, S. *Inorg. Chim. Acta* **1984**, *96*, 115–119.
(22) Nishida, Y.; Takeuchi, M. *Z. Naturforsch.* **1987**, *42b*, 52–54.
(23) Balch, A. L. *Inorg. Chim. Acta* **1992**, *198–200*, 297–307.
(24) Nishida, Y.; Nasu, M.; Akamatsu, T. *Z. Naturforsch.* **1992**, *47b*, 115–120.
(25) Funk, M. O., Jr.; Carroll, R. T.; Thompson, J. F.; Sands, R. H.; Dunham, W. R. *J. Am. Chem. Soc.* **1990**, *112*, 5375–5376.
(26) Que, L., Jr. *Adv. Inorg. Biochem.* **1983**, *5*, 167–199.
(27) Que, L., Jr. In *Iron Carriers and Iron Proteins*; Loehr, T. M., Ed.; VCH: New York, 1989; Vol. 5, pp 467–524.

(28) Nishida, Y.; Yamada, K.; Furuhashi, A. *Z. Naturforsch.* **1990**, *45b*, 1433–1436.
(29) Nishida, Y.; Yoshizawa, K.; Takahashi, S.; Watanabe, I. *Z. Naturforsch.* **1992**, *47c*, 209–214.
(30) Fridovich, I. *Adv. Enzymol.* **1986**, *58*, 61–97.
(31) Fox, B. G.; Shanklin, J.; Somerville, C.; Münck, E. *Proc. Natl. Acad. Sci. U.S.A.* **1993**, *90*, 2486–2490.
(32) Minotti, G.; Aust, S. D. *J. Biol. Chem.* **1987**, *262*, 1098–1104.
(33) Ursini, F.; Maiorino, M.; Hochstein, P.; Ernster, L. *Free Radical Biol. Med.* **1989**, *6*, 31–36.
(34) Valentine, J. S. *Chem. Rev.* **1973**, *73*, 235–245.
(35) Jones, R. D.; Summerville, D. A.; Basolo, F. *Chem. Rev.* **1979**, *79*, 139–179.
(36) Simandi, L. I. *Catalytic Activation of Dioxygen by Metal Complexes*; Kluwer Academic: Dordrecht, 1992; Vol. 13.
(37) Foote, C. S. *Acc. Chem. Res.* **1968**, *1*, 104–110.
(38) Halliwell, B.; Gutteridge, J. M. C. *Biochem. J.* **1984**, *219*, 1–14.
(39) Halliwell, B.; Gutteridge, J. M. C. *Arch. Biochem. Biophys.* **1986**, *246*, 501–514.
(40) Ortiz de Montellano, P. R. In *Cytochrome P-450*; Ortiz de Montellano, P. R., Ed.; Plenum: New York, 1985; pp 217–271.
(41) Dawson, J. H.; Sono, M. *Chem. Rev.* **1987**, *87*, 1255–1276.
(42) Dolphin, D.; Forman, A.; Borg, D. C.; Fajer, J.; Felton, R. H. *Proc. Natl. Acad. Sci. U.S.A.* **1971**, *68*, 614–618.
(43) Traylor, T. G.; Lee, W. A.; Stynes, D. V. *J. Am. Chem. Soc.* **1984**, *106*, 755–764.
(44) Yamaguchi, K.; Watanabe, Y.; Morishima, I. *J. Am. Chem. Soc.* **1993**, *115*, 4058–4065.
(45) Nordlund, P.; Dalton, H.; Eklund, H. *FEBS Lett.* **1992**, *307*, 257–262.
(46) Rosenzweig, A. C.; Frederick, C. A.; Lippard, S. J.; Nordlund, P. *Nature* **1993**, *366*, 537–543.
(47) Holmes, M. A.; Trong, I. L.; Turley, S.; Sieker, L. C.; Stenkamp, R. E. *J. Mol. Biol.* **1991**, *218*, 583–593.
(48) Micklitz, W.; Bott, S. G.; Bentsen, J. G.; Lippard, S. J. *J. Am. Chem. Soc.* **1989**, *111*, 372–374.
(49) *Bioinorganic Chemistry of Copper*; Karlin, K. D., Tyeklár, Z., Eds.; Chapman Hall: New York, 1993.
(50) Kitajima, N.; Fukui, H.; Moro-oka, Y.; Mizutani, Y.; Kitagawa, T. *J. Am. Chem. Soc.* **1990**, *112*, 6402–6403.
(51) Dong, Y.; Menage, S.; Brennan, B. A.; Elgren, T. E.; Jang, H. G.; Pearce, L. L.; Que, L., Jr. *J. Am. Chem. Soc.* **1993**, *115*, 1851–1859.
(52) Kitajima, N.; Tamura, N.; Amagai, H.; Fukui, H.; Moro-oka, Y.; Mizutani, Y.; Kitagawa, T.; Methur, R.; Heerwegh, K.; Reed, C. A.; Randall, C. R.; Que, L., Jr.; Tatsumi, K. *J. Am. Chem. Soc.*, submitted for publication.
(53) Kurtz, D. M., Jr.; Shriver, D. F.; Klotz, I. M. *J. Am. Chem. Soc.* **1976**, *98*, 5033–5035.
(54) Kurtz, D. M., Jr.; Shriver, D. F.; Klotz, I. M. *Coord. Chem. Rev.* **1977**, *24*, 145–178.
(55) Goddard, W. A., III; Olafson, B. D. *Proc. Natl. Acad. Sci. U.S.A.* **1975**, *72*, 2335–2339.
(56) Abramowitz, S.; Acquista, N.; Levin, I. W. *Chem. Phys. Lett.* **1977**, *50*, 423–426.
(57) Chang, S.; Blyholder, G.; Fernandez, J. *Inorg. Chem.* **1981**, *20*, 2813–2817.
(58) *McGraw-Hill Dictionary of Scientific Technological Terms*; Parker, S. P., Ed.; McGraw-Hill, Inc.: New York, 1989.
(59) Weiss, J. *J. Chim. Phys.* **1951**, *48*, 6–10.
(60) Walling, C. *Acc. Chem. Res.* **1975**, *8*, 125–131.
(61) Brown, E. R.; Mazzarella, J. D. *J. Electroanal. Chem.* **1987**, *222*, 173–192.
(62) Weiss, J. *Experientia* **1953**, *9*, 61–62.
(63) Taube, H. *Science* **1984**, *226*, 1028–1036 and references therein.
(64) George, P. *J. Chem. Soc.* **1954**, 4349–4359.
(65) Cher, M.; Davidson, N. *J. Am. Chem. Soc.* **1955**, *77*, 793–798.
(66) Huffman, R. E.; Davidson, N. *J. Am. Chem. Soc.* **1956**, *78*, 4836–4842.
(67) Macejevskis, B.; Dokuchaeva, A. N.; Liepina, L. *Latv. PSR Zinat. Akad. Vestis Kim. Ser.* **1965**, *4*, 453–460; *Chem. Abstr.* **1966**, *64*, 2786d.
(68) McBain, J. W. *J. Phys. Chem.* **1901**, *5*, 623–638.
(69) Posner, A. M. *Trans. Faraday Soc.* **1953**, *49*, 382–388.
(70) Lamb, A. B.; Elder, L. W. *J. Am. Chem. Soc.* **1931**, *53*, 137–163.
(71) King, J.; Davidson, N. *J. Am. Chem. Soc.* **1958**, *80*, 1542–1545.
(72) Pound, J. R. *J. Phys. Chem.* **1939**, *43*, 969–980.
(73) Hammond, G. S.; Wu, C.-H. S. In *Adv. Chem. Ser.*; Gould, R. F., Ed.; American Chemical Society: Washington, DC, 1968; Vol. 77, pp 186–207.
(74) Kurimura, Y.; Ochiai, R.; Matsuura, N. *Bull. Chem. Soc. Jpn.* **1968**, *41*, 2234–2239.
(75) Purmal, A. P.; Skurlatov, Y. I.; Travin, S. O. *Izv. Akad. Nauk SSSR, Ser. Khim.* **1980**, *3*, 492–497.
(76) Ng, F. T. T.; Henry, P. M. *Can. J. Chem.* **1980**, *58*, 1773–1779.
(77) Nishida, Y.; Yoshizawa, K.; Takahashi, S. *J. Chem. Soc., Chem. Commun.* **1991**, 1647–1648.
(78) Burkitt, M. J.; Gilbert, B. C. *Free Radical Res. Commun.* **1991**, *14*, 107–123.
(79) Lind, M. D.; Hoard, J. L.; Hamor, M. J.; Hamor, T. A.; Hoard, J. L. *Inorg. Chem.* **1964**, *3*, 34–43.
(80) Kosaka, H.; Katsuki, Y.; Shiga, T. *Arch. Biochem. Biophys.* **1992**, *293*, 401–408.
(81) Ahmad, S.; McCallum, J. D.; Shiemke, A. K.; Appelman, E. H.; Loehr, T. M.; Sanders-Loehr, J. *Inorg. Chem.* **1988**, *27*, 2230–2233.
(82) Fridovich, I. *Annu. Rev. Biochem.* **1975**, *44*, 147–159.
(83) Veldink, G.; Vliegenthart, J. F. G. *Adv. Inorg. Biochem.* **1984**, *6*, 139–161.
(84) Axcell, B. C.; Geary, P. J. *Biochem. J.* **1975**, *146*, 173–183.
(85) Bernhardt, F.-H.; Heymann, E.; Traylor, P. S. *Eur. J. Biochem.* **1978**, *92*, 209–223.
(86) Bernhardt, F.-H.; Meisch, H.-U. *Biochem. Biophys. Res. Commun.* **1980**, *93*, 1247–1253.
(87) Adrian, W.; Bernhardt, F.-H.; Bill, E.; Gersonde, K.; Heymann, E.; Trautwein, A. X.; Twilfer, H. *Hoppe-Seyler's Z. Physiol. Chem.* **1980**, *361*, 211.
(88) Bernhardt, F.-H.; Kuthan, H. *Eur. J. Biochem.* **1981**, *120*, 547–555.
(89) Bill, E.; Bernhardt, F.-H.; Trautwein, A. X. *Eur. J. Biochem.* **1981**, *121*, 39–46.
(90) Twilfer, H.; Bernhardt, F.-H.; Gersonde, K. *Eur. J. Biochem.* **1981**, *119*, 595–602.
(91) Bernhardt, F.-H.; Nastainczyk, W.; Seydewitz, V. *Eur. J. Biochem.* **1977**, *72*, 107–115.
(92) Bernhardt, F.-H.; Erdin, N.; Staudinger, H.; Ullrich, V. *Eur. J. Biochem.* **1973**, *35*, 126–134.
(93) Twilfer, H.; Bernhardt, F.-H.; Gersonde, K. *Eur. J. Biochem.* **1985**, *147*, 171–176.
(94) Bill, E.; Bernhardt, F.-H.; Trautwein, A. X.; Winkler, H. *Eur. J. Biochem.* **1985**, *147*, 177–182.
(95) Wende, P.; Pfleger, K.; Bernhardt, F.-H. *Biochem. Biophys. Res. Commun.* **1982**, *104*, 527–532.
(96) Hayaishi, O.; Nozaki, M.; Abbott, M. T. In *The Enzymes*; Boyer, P. D., Ed.; Academic: New York, 1975; Vol. 12, pp 119–189.
(97) Lipscomb, J. D.; Orville, A. M. In *Metal Ions in Biological Systems*; Sigel, H., Sigel, A., Eds.; Marcel Dekker: New York, 1992; Vol. 28, pp 243–298.
(98) Que, L., Jr.; Kolanczyk, R. C.; White, L. S. *J. Am. Chem. Soc.* **1987**, *109*, 5373–5380.
(99) Cox, D. D.; Que, L., Jr. *J. Am. Chem. Soc.* **1988**, *110*, 8085–8092.
(100) Jang, H. G.; Cox, D. D.; Que, L., Jr. *J. Am. Chem. Soc.* **1991**, *113*, 9200–9204.
(101) Arciero, D. M.; Lipscomb, J. D.; Huynh, B. H.; Kent, T. A.; Münck, E. *J. Biol. Chem.* **1983**, *258*, 14981–14991.
(102) Zimmermann, R.; Huynh, B. H.; Münck, E.; Lipscomb, J. D. *J. Chem. Phys.* **1978**, *69*, 5463–5467.
(103) Arciero, D. M.; Lipscomb, J. D. *J. Biol. Chem.* **1986**, *261*, 2170–2178.
(104) Arciero, D. M.; Orville, A. M.; Lipscomb, J. D. *J. Biol. Chem.* **1985**, *260*, 14035–14044.
(105) Mabrouk, P. A.; Orville, A. M.; Lipscomb, J. D.; Solomon, E. I. *J. Am. Chem. Soc.* **1991**, *113*, 4053–4061.
(106) Harris, W. R.; Carrano, C. J.; Cooper, S. R.; Sofen, S. R.; Avdeef, A. E.; McArdle, J. V.; Raymond, K. N. *J. Am. Chem. Soc.* **1979**, *101*, 6097–6104.
(107) Heistand, R. H., II; Lauffer, R. B.; Fikrig, E.; Que, L., Jr. *J. Am. Chem. Soc.* **1982**, *104*, 2789–2796.
(108) Shiman, R. In *Folates and Pterins*; Blakley, R. L., Benkovic, S. J., Eds.; Wiley and Sons: New York, 1985; Vol. 2, pp 179–250.
(109) Dix, T. A., Benkovic, S. J. *Acc. Chem. Res.* **1988**, *21*, 101–107.
(110) Blakley, R. L.; Benkovic, S. J. *Folates and Pterines*; Wiley and Sons: New York, 1985; Vol. 2.
(111) Dix, T. A.; Benkovic, S. J. *Biochemistry* **1985**, *24*, 5839–5846.
(112) Dix, T. A.; Bollag, G. E.; Domanico, P. L.; Benkovic, S. J. *Biochemistry* **1985**, *24*, 2955–2958.
(113) Nakata, H.; Fujisawa, H. *Biochim. Biophys. Acta* **1980**, *614*, 313–327.
(114) Pember, S. O.; Villafranca, J. J.; Benkovic, S. J. *Biochemistry* **1986**, *25*, 6611–6619. (a) See, however: Carr, R. T.; Benkovic, S. J. *Biochemistry* **1993**, *32*, 14132–14138.
(115) Martínez, A.; Abeygunawardana, C.; Haavik, J.; Flatmark, T.; Mildvan, A. S. *Biochemistry* **1993**, *32*, 6381–6390.
(116) Storm, C. B.; Kaufman, S. *Biochem. Biophys. Res. Commun.* **1968**, *32*, 788–793.
(117) Webber, S.; Harzer, G.; Whiteley, J. M. *Anal. Biochem.* **1980**, *106*, 63–72.
(118) Rhoads, R. E.; Udenfriend, S. *Proc. Natl. Acad. Sci. U.S.A.* **1968**, *60*, 1473–1478.
(119) Cardinale, G. J.; Rhoads, R. E.; Udenfriend, S. *Biochem. Biophys. Res. Commun.* **1971**, *43*, 537–543.
(120) Hanauske-Abel, H. M.; Günzler, V. *J. Theor. Biol.* **1982**, *94*, 421–455.
(121) Kivirikko, K. I.; Myllylä, R.; Pihlajaniemi, T. *FASEB J.* **1989**, *3*, 1609–1617.
(122) Majamaa, K.; Günzler, V.; Hanauske-Abel, H. M.; Myllylä, R.; Kivirikko, K. I. *J. Biol. Chem.* **1986**, *261*, 7819–7823.
(123) Nietfeld, J. J.; De Jong, L.; Kemp, A. *Biochim. Biophys. Acta* **1982**, *704*, 321–325.
(124) Popenoe, E. A.; Aronson, R. B.; Van Slyke, D. D. *Arch. Biochem. Biophys.* **1969**, *133*, 286–292.
(125) Halme, J.; Kivirikko, K. I.; Simons, K. *Biochim. Biophys. Acta* **1970**, *198*, 460–470.

(126) Hobza, P.; Hurych, J.; Zahradník, R. *Biochim. Biophys. Acta* **1973**, *304*, 466–472.
(127) De Jong, L.; Albracht, S. P. J.; Kemp, A. *Biochim. Biophys. Acta* **1982**, *704*, 326–332.
(128) Nietfeld, J. J.; Kemp, A. *Biochim. Biophys. Acta* **1981**, *657*, 159–167.
(129) Majamaa, K.; Hanauske-Abel, H. M.; Günzler, V.; Kivirikko, K. I. *Eur. J. Biochem.* **1984**, *138*, 239–245.
(130) Myllylä, R.; Majamaa, K.; Günzler, V.; Hanauske-Abel, H. M.; Kivirikko, K. I. *J. Biol. Chem.* **1984**, *259*, 5403–5405.
(131) Myllylä, R.; Kuutti-Savolainen, E.-R.; Kivirikko, K. I. *Biochem. Biophys. Res. Commun.* **1978**, *83*, 441–448.
(132) Yu, R.; Kurata, T.; Arakawa, N. *Agric. Biol. Chem.* **1988**, *52*, 721–728.
(133) Majamaa, K.; Turpeenniemi-Hujanen, T. M.; Latipää, P.; Günzler, V.; Hanauske-Abel, H. M.; Hassinen, I. E.; Kivirikko, K. I. *Biochem. J.* **1985**, *229*, 127–133.
(134) Chiou, Y.-M.; Que, L., Jr. *J. Am. Chem. Soc.* **1992**, *114*, 7567–7568.
(135) Chiou, Y.-M.; Que, L., Jr. *J. Inorg. Biochem.* **1993**, *51*, 127.
(136) Tuderman, L.; Myllylä, R.; Kivirikko, K. I. *Eur. J. Biochem.* **1977**, *80*, 341–348.
(137) Warn-Cramer, B. J.; Macrander, L. A.; Abbott, M. T. *J. Biol. Chem.* **1983**, *258*, 10551–10557.
(138) Thornburg, L. D.; Lai, M.-T.; Wishnok, J. S.; Stubbe, J. *Biochemistry* **1993**, *32*, 14023–14033.
(139) Baldwin, J. E. In *Recent Advances in the Chemistry of β-Lactam Antibiotics*; Bentley, P. H., Southgate, R., Eds.; Royal Society of Chemistry: London, 1989; pp 1–22.
(140) Baldwin, J. E.; Bradley, M. *Chem. Rev.* **1990**, *90*, 1079–1088.
(141) Baldwin, J. E. *J. Heterocycl. Chem.* **1990**, *27*, 71–78.
(142) White, R. L.; John, E.-M. M.; Baldwin, J. E.; Abraham, E. P. *Biochem. J.* **1982**, *203*, 791–793.
(143) Bainbridge, Z. A.; Scott, R. I.; Perry, D. *J. Chem. Tech. Biotechnol.* **1992**, *55*, 233–238.
(144) Chen, V. J.; Orville, A. M.; Harpel, M. R.; Frolik, C. A.; Surerus, K. K.; Münck, E.; Lipscomb, J. D. *J. Biol. Chem.* **1989**, *264*, 21677–21681.
(145) Orville, A. M.; Chen, V. J.; Kriauciunas, A.; Harpel, M. R.; Fox, B. G.; Münck, E.; Lipscomb, J. D. *Biochemistry* **1992**, *31*, 4602–4612.
(146) Ming, L.-J.; Que, L., Jr.; Kriauciunas, A.; Frolik, C. A.; Chen, V. J. *Inorg. Chem.* **1990**, *29*, 1111–1112.
(147) Ming, L.-J.; Que, L., Jr.; Kriauciunas, A.; Frolik, C. A.; Chen, V. J. *Biochemistry* **1991**, *30*, 11653–11659.
(148) Scott, R. A.; Wang, S.; Eidsness, M. K.; Kriauciunas, A.; Frolik, C. A.; Chen, V. J. *Biochem.* **1992**, *31*, 4596–4601.
(149) Randall, C. R.; Zang, Y.; True, A. E.; Que, L., Jr.; Charnock, J. M.; Garner, C. D.; Fujishima, Y.; Schofield, C. J.; Baldwin, J. E. *Biochemistry* **1993**, *32*, 6664–6673.
(150) Samson, S. M.; Chapman, J. L.; Belagaje, R.; Queener, S. W.; Ingolia, T. D. *Proc. Natl. Acad. Sci. U.S.A.* **1987**, *84*, 5705–5709.
(151) Kriauciunas, A.; Frolik, C. A.; Hassell, T. C.; Skatrud, P. L.; Johnson, M. G.; Holbrook, N. L.; Chen, V. J. *J. Biol. Chem.* **1991**, *266*, 11779–11788.
(152) Baldwin, J. E.; Adlington, R. M.; Domayne-Hayman, B. P.; Knight, G.; Ting, H.-H. *J. Chem. Soc., Chem. Commun.* **1987**, 1661–1663.
(153) Baldwin, J. E.; Adlington, R. M.; Bradley, M.; Norris, W. J.; Turner, N. J.; Yoshida, A. *J. Chem. Soc., Chem. Commun.* **1988**, 1125–1128.
(154) Baldwin, J. E.; Adlington, R. M.; Bradley, M.; Turner, N. J.; Pitt, A. R. *J. Chem. Soc., Chem. Commun.* **1989**, 978–981.
(155) Baldwin, J. E.; Bradley, M.; Turner, N. J.; Adlington, R. M.; Pitt, A. R.; Sheridan, H. *Tetrahedron* **1991**, *47*, 8203–8222.
(156) Baldwin, J. E.; Bradley, M.; Turner, N. J.; Adlington, R. M.; Pitt, A. R.; Derome, A. E. *Tetrahedron* **1991**, *47*, 8223–8242.
(157) Baldwin, J. E.; Lynch, G. P.; Schofield, C. J. *J. Chem. Soc., Chem. Commun.* **1991**, 736–738.
(158) Baldwin, J. E.; Adlington, R. M.; Marquess, D. G.; Pitt, A. R.; Russell, A. T. *J. Chem. Soc., Chem. Commun.* **1991**, 856–858.
(159) Baldwin, J. E.; Lynch, G. P.; Schofield, C. J. *Tetrahedron* **1992**, *48*, 9085–9100.
(160) Nonhebel, D. C. *Chem. Soc. Rev.* **1993**, 347–359.
(161) Baldwin, J. E.; Adlington, R. M.; Flitsch, S. L.; Ting, H.-H.; Turner, N. J. *J. Chem. Soc., Chem. Commun.* **1986**, 1305–1308.
(162) Wilkins, R. G.; Harrington, P. C. *Adv. Inorg. Biochem.* **1983**, *5*, 51–85.
(163) Stenkamp, R. E. *Chem. Rev.* **1994**, *94*, 715–726 (this issue).
(164) Stenkamp, R. E.; Sieker, L. C.; Jensen, L. H.; McCallum, J. D.; Sanders-Loehr, J. *Proc. Natl. Acad. Sci. U.S.A.* **1985**, *82*, 713–716.
(165) Sheriff, S.; Hendrickson, W. A.; Smith, J. L. *Life Chem. Rep. Suppl. Ser.* **1983**, *1*, 305–308.
(166) Stenkamp, R. E.; Sieker, L. C.; Jensen, L. H. *J. Am. Chem. Soc.* **1984**, *106*, 618–622.
(167) Sheriff, S.; Hendrickson, W. A.; Smith, J. L. *J. Mol. Biol.* **1987**, *197*, 273–296.
(168) Holmes, M. A.; Stenkamp, R. E. *J. Mol. Biol.* **1991**, *220*, 723–737.
(169) Sheriff, S.; Hendrickson, W. A.; Stenkamp, R. E.; Sieker, L. C.; Jensen, L. H. *Proc. Natl. Acad. Sci. U.S.A.* **1985**, *82*, 1104–1107.
(170) Dunn, J. B. R.; Shriver, D. F.; Klotz, I. M. *Proc. Natl. Acad. Sci. U.S.A.* **1973**, *70*, 2582–2584.
(171) Dunn, J. B. R.; Shriver, D. F.; Klotz, I. M. *Biochemistry* **1975**, *14*, 2689–2695.
(172) Shiemke, A. K.; Loehr, T. M.; Sanders-Loehr, J. *J. Am. Chem. Soc.* **1986**, *108*, 2437–2443.
(173) Reem, R. C.; McCormick, J. M.; Richardson, D. E.; Devlin, F. J.; Stephens, P. J.; Musselman, R. L.; Solomon, E. I. *J. Am. Chem. Soc.* **1989**, *111*, 4688–4704.
(174) Sanders-Loehr, J.; Wheeler, W. D.; Shiemke, A. K.; Averill, B. A.; Loehr, T. M. *J. Am. Chem. Soc.* **1989**, *111*, 8084–8093.
(175) Kaminaka, S.; Takizawa, H.; Handa, T.; Kihara, H.; Kitagawa, T. *Biochemistry* **1992**, *31*, 6997–7002.
(176) Solomon, E. I.; Zhang, Y. *Acc. Chem. Res.* **1992**, *25*, 343–352.
(177) Bates, G.; Brunori, M.; Amiconi, G.; Antonini, E.; Wyman, J. *Biochemistry* **1968**, *7*, 3016–3020.
(178) De Waal, D. J. A.; Wilkins, R. G. *J. Biol. Chem.* **1976**, *251*, 2339–2343.
(179) Petrou, A. L.; Armstrong, F. A.; Sykes, A. G.; Harrington, P. C.; Wilkins, R. G. *Biochim. Biophys. Acta* **1981**, *670*, 377–384.
(180) Zimmer, J. R.; Tachi-iri, Y.; Takizawa, H.; Handa, T.; Yamamura, T.; Kihara, H. *Biochim. Biophys. Acta* **1986**, *874*, 174–180.
(181) Tachi'iri, Y.; Ichimura, K.; Yamamura, T.; Satake, K.; Kurita, K.; Nagamura, T.; Kihara, H. *Eur. Biophys. J.* **1990**, *18*, 9–16.
(182) Wilkins, P. C.; Wilkins, R. G. *Coord. Chem. Rev.* **1987**, *79*, 195–214.
(183) Klotz, I. M.; Klotz, T. A. *Science* **1955**, *121*, 477–480.
(184) Clark, P. E.; Webb, J. *Biochemistry* **1981**, *20*, 4628–4632.
(185) Armstrong, G. D.; Sykes, A. G. *Inorg. Chem.* **1986**, *25*, 3135–3139.
(186) Alberding, N.; Lavalette, D.; Austin, R. H. *Proc. Natl. Acad. Sci. U.S.A.* **1981**, *78*, 2307–2309.
(187) Zhang, J.-H.; Kurtz, D. M., Jr. *Biochemistry* **1991**, *30*, 9121–9125.
(188) Matsukawa, S.; Mawatari, K.; Yoneyama, Y.; Kitagawa, T. *J. Am. Chem. Soc.* **1985**, *107*, 1108–1113.
(189) Bradić, Z.; Conrad, R.; Wilkins, R. G. *J. Biol. Chem.* **1977**, *252*, 6069–6075.
(190) Chaudhuri, P.; Wieghardt, K.; Nuber, B.; Weiss, J. *Angew. Chem., Int. Ed. Engl.* **1985**, *24*, 778–779.
(191) Hartman, J.; Rardin, L.; Chaudhuri, P.; Pohl, K.; Wieghardt, K.; Nuber, B.; Weiss, J.; Papaefthymiou, G.; Frankel, R.; Lippard, S. *J. Am. Chem. Soc.* **1987**, *109*, 7387–7396.
(192) Feig, A. L.; Masschelein, A.; Lippard, S. J. To be submitted for publication.
(193) Dalton, H. In *Advances in Applied Microbiology*; Academic: New York, 1980; Vol. 26, pp 71–87.
(194) Anthony, C. *The Biochemistry of Methylotrophs*; Academic: New York, 1982.
(195) Ruzicka, F.; Huang, D.-S.; Donnelly, M. I.; Frey, P. A. *Biochemistry* **1990**, *29*, 1696–1700.
(196) Priestley, N. D.; Floss, H. G.; Froland, W. A.; Lipscomb, J. D.; Williams, P. G.; Morimoto, H. *J. Am. Chem. Soc.* **1992**, *114*, 7561–7562.
(197) Lee, S.-K.; Fox, B. G.; Froland, W. A.; Lipscomb, J. D.; Münck, E. *J. Am. Chem. Soc.* **1993**, *115*, 6450–6451. (a) Lee, S.-K.; Nesheim, J. C.; Lipscomb, J. D. *J. Biol. Chem.* **1993**, *268*, 21569–21577.
(198) Liu, K. E.; Johnson, C. C.; Newcomb, M.; Lippard, S. J. *J. Am. Chem. Soc.* **1993**, *115*, 939–947.
(199) Liu, K. E.; Feig, A. L.; Goldberg, D. P.; Watton, S. P.; Lippard, S. J. In *Applications of Enzyme Biotechnology*; Kelly, J. W., Ed.; Plenum: New York, 1993; pp 301–320.
(200) Green, J.; Dalton, H. *Biochem. J.* **1989**, *259*, 167–172.
(201) Fox, B. G.; Froland, W. A.; Dege, J. E.; Lipscomb, J. D. *J. Biol. Chem.* **1989**, *264*, 10023–10033.
(202) Liu, K. E.; Lippard, S. J. *J. Biol. Chem.* **1991**, *266*, 12836–12839; 24859.
(203) Froland, W. A.; Andersson, K. K.; Lee, S.-K.; Liu, Y.; Lipscomb, J. D. *J. Biol. Chem.* **1992**, *267*, 17588–17597.
(204) Lund, J.; Dalton, H. *Eur. J. Biochem.* **1985**, *147*, 291–296.
(205) Lund, J.; Woodland, M. P.; Dalton, H. *Eur. J. Biochem.* **1985**, *147*, 297–305.
(206) Fox, B. G.; Lipscomb, J. D. In *Biological Oxidation Systems*; Reddy, C. C., Ed.; Academic: New York, 1990; Vol. 1, pp 367–388.
(207) Rosenzweig, A. C.; Feng, X.; Lippard, S. J. In *Applications of Enzyme Biotechnology*; Kelly, J. W., Baldin, T. O., Eds.; Plenum: New York, 1991; pp 69–85.
(208) DeWitt, J. G.; Bentsen, J. G.; Rosenzweig, A. C.; Hedman, B.; Green, J.; Pilkington, S.; Papaefthymiou, G. C.; Dalton, H.; Hodgson, K. O.; Lippard, S. J. *J. Am. Chem. Soc.* **1991**, *113*, 9219–9235.
(209) Green, J.; Dalton, H. *J. Biol. Chem.* **1985**, *260*, 15795–15801.
(210) Ericson, A.; Hedman, B.; Hodgson, K. O.; Green, J.; Dalton, H.; Bentsen, J. G.; Beer, R. H.; Lippard, S. J. *J. Am. Chem. Soc.* **1988**, *110*, 2330–2332.
(211) Fox, B. G.; Surerus, K. K.; Münck, E.; Lipscomb, J. D. *J. Biol. Chem.* **1988**, *263*, 10553–10556.
(212) DeRose, V. J.; Liu, K. E.; Kurtz, D. M., Jr.; Hoffman, B. M.; Lippard, S. J. *J. Am. Chem. Soc.* **1993**, *115*, 6440–6441.
(213) Thomann, H.; Bernardo, M.; McCormick, J. M.; Pulver, S.; Andersson, K. K.; Lipscomb, J. D.; Solomon, E. I. *J. Am. Chem. Soc.* **1993**, *115*, 8881–8882.
(214) DeGrado, W. F. *Adv. Protein Chem.* **1988**, *39*, 51–124.
(215) Cohen, C.; Parry, D. A. D. *Proteins: Struct., Funct., Genet.* **1990**, *7*, 1–15.
(216) Åberg, A. Thesis, Stockholm University, 1993.

(217) Nordlund, P.; Åberg, A.; Eklund, H.; Regnström, K.; Hajdu, J. Submitted for publication.
(218) Woodland, M. P.; Patil, D. S.; Cammack, R.; Dalton, H. *Biochim. Biophys. Acta* **1986**, *873*, 237–242.
(219) Rardin, R. L.; Tolman, W. B.; Lippard, S. J. *New J. Chem.* **1991**, *15*, 417–430.
(220) Paulsen, K. E.; Liu, Y.; Fox, B. G.; Lipscomb, J. D.; Münck, E.; Stankovich, M. T. *Biochemistry* **1994**, *33*, 713–722.
(221) Green, J.; Dalton, H. *J. Biol. Chem.* **1989**, *264*, 17698–17703.
(222) Andersson, K. K.; Froland, W. A.; Lee, S.-K.; Lipscomb, J. D. *New J. Chem.* **1991**, *15*, 411–415.
(223) Wilkins, P. C.; Dalton, H.; Podmore, I. D.; Deighton, N.; Symons, M. C. R. *Eur. J. Biochem.* **1992**, *210*, 67–72.
(224) Newcomb, M. Wayne State University, personal communications, 1993.
(225) Deighton, N.; Podmore, I. D.; Symons, M. C. R.; Wilkins, P. C.; Dalton, H. *J. Chem. Soc., Chem. Commun.* **1991**, 1086–1088.
(226) Ton-That, H.; Magnus, K. A. *J. Inorg. Biochem.* **1993**, *51*, 65.
(227) Jiang, Y.; Wilkins, P. C.; Dalton, H. *Biochim. Biophys. Acta* **1993**, *1163*, 105–112.
(228) Liu, K. E.; Lippard, S. J. Unpublished results.
(229) Tyeklár, Z.; Karlin, K. D. In *Dioxygen Activation and Homogeneous Catalytic Oxidation*; Simándi, L. I., Ed.; Elsevier Science: Amsterdam, 1991; pp 237–248.
(230) Tian, G.; Berry, J. A.; Klinman, J. P. *Biochemistry* **1994**, *33*, 226–234.
(231) Atkin, C. L.; Thelander, L.; Reichard, P.; Lang, G. *J. Biol. Chem.* **1973**, *248*, 7464–7472.
(232) Eriksson, S.; Sjöberg, B.-M. In *Allosteric Enzymes*; CRC: Boca Raton, FL, 1989; pp 189–215.
(233) Stubbe, J. In *Advances in Enzymology and Related Areas of Molecular Biology*; Meister, A., Ed.; John Wiley and Sons: New York, 1990; Vol. 63, pp 349–420.
(234) Stubbe, J. *J. Biol. Chem.* **1990**, *265*, 5329–5332.
(235) Fontecave, M.; Nordlund, P.; Eklund, H.; Reichard, P. In *Advances in Enzymology and Related Areas of Molecular Biology*; Meister, A., Ed.; Wiley and Sons: New York, 1992; Vol. 65, pp 147–183.
(236) Nordlund, P.; Sjöberg, B.-M.; Eklund, H. *Nature* **1990**, *345*, 593–598.
(237) Nordlund, P.; Eklund, H. *J. Mol. Biol.* **1993**, *232*, 123–164.
(238) Ochiai, E.-I.; Mann, G. J.; Gräslund, A.; Thelander, L. *J. Biol. Chem.* **1990**, *265*, 15758–15761.
(239) Bollinger, J. M., Jr.; Edmondson, D. E.; Huynh, B. H.; Filley, J.; Norton, J. R.; Stubbe, J. *Science* **1991**, *253*, 292–298.
(240) Elgren, T. E.; Lynch, J. B.; Juarez-Garcia, C.; Münck, E.; Sjöberg, B.-M.; Que, L., Jr. *J. Biol. Chem.* **1991**, *266*, 19265–19268.
(241) Taqui Khan, M. M.; Martell, A. E. *J. Am. Chem. Soc.* **1967**, *89*, 4176–4185.
(242) Menage, S.; Brennan, B. A.; Juarez-Garcia, C.; Münck, E.; Que, L., Jr. *J. Am. Chem. Soc.* **1990**, *112*, 6423–6425.
(243) Ling, J. Thesis, Oregon Graduate Institute of Science, 1993.
(244) Stubbe, J., et al. Manuscript in preparation.
(245) Bollinger, J. M., Jr.; Ravi, N., Tong, W. H.; Edmondson, D. E.; Huynh, B. H.; Stubbe, J. *J. Inorg. Biochem.* **1993**, *51*, 6.
(246) Sahlin, M.; Sjöberg, B.-M.; Backes, G.; Loehr, T.; Sanders-Loehr, J. *Biochem. Biophys. Res. Commun.* **1990**, *167*, 813–818.
(247) Fontecave, M.; Gerez, C.; Atta, M.; Jeunet, A. *Biochem. Biophys. Res. Commun.* **1990**, *168*, 659–664.
(248) Leising, R. A.; Brennan, B. A.; Que, L., Jr.; Fox, B. G.; Münck, E. *J. Am. Chem. Soc.* **1991**, *113*, 3988–3990.
(249) Que, L., Jr. University of Minnesota, personal communications, 1994.
(250) Ormö, M.; deMaré, F.; Regnström, K.; Åberg, A.; Sahlin, M.; Ling, J.; Loehr, T. M.; Sanders-Loehr, J.; Sjöberg, B.-M. *J. Biol. Chem.* **1992**, *267*, 8711–8714.
(251) Åberg, A.; Ormö, M.; Nordlund, P.; Sjöberg, B.-M. *Biochemistry* **1993**, *32*, 9845–9850.
(252) Kang, C.; Sobkowiak, A.; Sawyer, D. T. *Inorg. Chem.* **1994**, *33*, 79–82.
(253) Harrison, P. M.; Lilley, T. H. In *Iron Carriers and Iron Proteins*; Loehr, T. M., Ed.; VCH: New York, 1989; Vol. 5, pp 123–238.
(254) Theil, E. C. In *Advances in Enzymology and Related Areas of Molecular Biology*; Meister, A., Ed.; John Wiley and Sons: New York, 1990; Vol. 63, pp 421–450.
(255) Wagstaff, M.; Worwood, M.; Jacobs, A. *Biochem. J.* **1978**, *173*, 969–977.
(256) Artymiuk, P. J.; Bauminger, E. R.; Harrison, P. M.; Lawson, D. M.; Nowik, I.; Treffry, A.; Yewdall, S. J. In *Iron Biominerals*; Frankel, R. B., Blakemore, R. P., Eds.; Plenum: New York, 1990; pp 269–294.
(257) Levi, S.; Luzzago, A.; Cesareni, G.; Cozzi, A.; Franceschinelli, F.; Albertini, A.; Arosio, P. *J. Biol. Chem.* **1988**, *263*, 18086–18092.
(258) Treffry, A.; Hirzmann, J.; Yewdall, S. J.; Harrison, P. M. *FEBS Lett.* **1992**, *302*, 108–112.
(259) Harrison, P. M.; Bauminger, E. R.; Hechel, D.; Hodson, N. W.; Nowik, I.; Treffry, A.; Yewdall, S. J. In *Iron and Iron Protein Conference*; Israel, in press.
(260) Harrison, P. M.; Bauminger, E. R.; Hechel, D.; Hodson, N. W.; Nowik, I.; Treffry, A.; Yewdall, S. J. In *Iron and Iron Protein Conference*; Israel, 1993; in press and references therein.
(261) Lawson, D. M.; Artymiuk, P. J.; Yewdall, S. J.; Smith, J. M. A.; Livingstone, J. C.; Treffry, A.; Luzzago, A.; Levi, S.; Arosio, P.; Cesareni, G.; Thomas, C. D.; Shaw, W. V.; Harrison, P. M. *Nature* **1991**, *349*, 541–544.
(262) Sun, S.; Arosio, P.; Levi, S.; Chasteen, N. D. *Biochemistry* **1993**, *32*, 9362–9369.
(263) Macara, I. G.; Hoy, T. G.; Harrison, P. M. *Biochem. J.* **1972**, *126*, 151–162.
(264) Treffry, A.; Sowerby, J. M.; Harrison, P. M. *FEBS Lett.* **1979**, *100*, 33–36.
(265) Xu, B.; Chasteen, N. D. *J. Biol. Chem.* **1991**, *266*, 19965–19970.
(266) Bauminger, E. R.; Harrison, P. M.; Nowick, I.; Treffry, A. *Biochemistry* **1989**, *28*, 5486–5493.
(267) Bauminger, E. R.; Harrison, P. M.; Hechel, D.; Nowik, I.; Treffry, A. *Biochim. Biophys. Acta* **1991**, *1118*, 48–58.
(268) Hanna, P. M.; Chen, Y.; Chasteen, N. D. *J. Biol. Chem.* **1991**, *266*, 886–893.
(269) Waldo, G. S.; Ling, J.; Sanders-Loehr, J.; Theil, E. C. *Science* **1993**, *259*, 796–798.
(270) Waldo, G. S.; Theil, E. C. *Biochemistry* **1993**, *32*, 13262–13269.
(271) Sun, S.; Chasteen, N. D. *J. Biol. Chem.* **1992**, *267*, 25160–25166.
(272) Grady, J. K.; Chen, Y.; Chasteen, N. D.; Harris, D. C. *J. Biol. Chem.* **1989**, *264*, 20224–20229.
(273) Cheng, Y. G.; Chasteen, N. D. *Biochemistry* **1991**, *30*, 2947–2953.
(274) Mayer, D. E.; Rohrer, J. S.; Schoeller, D. A.; Harris, D. C. *Biochemistry* **1983**, *22*, 876–880.
(275) Umezawa, H. In *Bleomycin: Chemical, Biochemical and Biological Aspects*; Hecht, S. M., Ed.; Springer-Verlag: New York, 1979; pp 24–36.
(276) Stubbe, J.; Kozarich, J. W. *Chem. Rev.* **1987**, *87*, 1107–1136.
(277) Petering, D. H.; Byrnes, R. W.; Antholine, W. E. *Chem.-Biol. Interact.* **1990**, *73*, 133–182.
(278) Hamamichi, N.; Natrajan, A.; Hecht, S. M. *J. Am. Chem. Soc.* **1992**, *114*, 6278–6291.
(279) Sausville, E. A.; Peisach, J.; Horwitz, S. B. *Biochem. Biophys. Res. Commun.* **1976**, *73*, 814–822.
(280) Sausville, E. A.; Peisach, J.; Horwitz, S. B. *Biochemistry* **1978**, *17*, 2740–2746.
(281) Sausville, E. A.; Stein, R. W.; Peisach, J.; Horwitz, S. B. *Biochemistry* **1978**, *17*, 2746–2754.
(282) Burger, R. M.; Horwitz, S. B.; Peisach, J.; Wittenberg, J. B. *J. Biol. Chem.* **1979**, *254*, 12299–12302.
(283) Burger, R. M.; Peisach, J.; Blumberg, W. E.; Horwitz, S. B. *J. Biol. Chem.* **1979**, *254*, 10906–10912.
(284) Burger, R. M.; Peisach, J.; Horwitz, S. B. *J. Biol. Chem.* **1981**, *256*, 11636–11644.
(285) Burger, R. M.; Kent, T. A.; Horwitz, S. B.; Münck, E.; Peisach, J. *J. Biol. Chem.* **1983**, *258*, 1559–1564.
(286) Padbury, G.; Sligar, S. S. *J. Biol. Chem.* **1985**, *260*, 7820–7823.
(287) Heimbrook, D. C.; Mulholland, R. L., Jr.; Hecht, S. M. *J. Am. Chem. Soc.* **1986**, *108*, 7839–7840.
(288) Heimbrook, D. C.; Carr, S. A.; Mentzer, M. A.; Long, E. C.; Hecht, S. M. *Inorg. Chem.* **1987**, *26*, 3835–3836.
(289) Padbury, G.; Sligar, S. G.; Labeque, R.; Marnett, L. J. *Biochemistry* **1988**, *27*, 7846–7852.
(290) Suga, A.; Sugiyama, T.; Otsuka, M.; Ohno, M.; Sugiura, Y.; Maeda, K. *Tetrahedron* **1991**, *47*, 1191–1204.
(291) Dawson, D. Y.; Hudson, S. E.; Mascharak, P. K. *J. Inorg. Biochem.* **1992**, *47*, 109–117.
(292) Sam, J. W.; Peisach, J. *Biochemistry* **1993**, *32*, 1488–1491.
(293) Dabrowiak, J. C. *Adv. Inorg. Biochem.* **1982**, *4*, 69–113.
(294) Iitaka, Y.; Nakamura, H.; Nakatani, T.; Muraoka, Y.; Fujii, A.; Takita, T.; Umezawa, H. *J. Antibiot.* **1978**, *31*, 1070–1072.
(295) Stubbe, J.; Kozarich, J. W. *Chem. Rev.* **1987**, *87*, 1107–1136 and references therein.
(296) Kénani, A.; Bailly, C.; Helbecque, N.; Catteau, J.-P.; Houssin, R.; Bernier, J.-L.; Hénichart, J.-P. *Biochem. J.* **1988**, *253*, 497–504.
(297) Sugiura, Y.; Kikuchi, T. *J. Antibiot.* **1978**, *31*, 1310–1312.
(298) McMurry, T. J.; Groves, J. T. In *Cytochrome P-450*; Ortiz de Montellano, P., Ed.; Plenum: New York, 1985; pp 1–28.
(299) Natrajan, A.; Hecht, S. M.; van der Marel, G. A.; van Boom, J. H. *J. Am. Chem. Soc.* **1990**, *112*, 3997–4002.
(300) Barr, J. R.; van Atta, R. B.; Natrajan, A.; Hecht, S. M.; van der Marel, G. A.; van Boom, J. H. *J. Am. Chem. Soc.* **1990**, *112*, 4058–4060.
(301) Wu, J. C.; Stubbe, J.; Kozarich, J. W. *Biochemistry* **1985**, *24*, 7569–7573.
(302) McGall, G. H.; Rabow, L. E.; Stubbe, J.; Kozarich, J. W. *J. Am. Chem. Soc.* **1987**, *109*, 2836–2837.
(303) Caspary, W. J.; Niziak, C.; Lanzo, D. A.; Friedman, R.; Bachur, N. R. *Mol. Pharmacol.* **1979**, *16*, 256–260.
(304) Lown, J. W.; Sim, S.-K. *Biochem. Biophys. Res. Commun.* **1977**, *77*, 1150–1157.
(305) Oberley, L. W.; Buettner, G. R. *FEBS Lett.* **1979**, *97*, 47–49.
(306) Rodriguez, L. O.; Hecht, S. M. *Biochem. Biophys. Res. Commun.* **1982**, *104*, 1470–1476.
(307) Rabow, L. E.; McGall, G. H.; Stubbe, J.; Kozarich, J. W. *J. Am. Chem. Soc.* **1990**, *112*, 3203–3208.
(308) Barton, D. H. R.; Csuhai, E.; Doller, D.; Balavoine, G. *J. Chem. Soc., Chem. Commun.* **1990**, 1787–1789.

(309) Barton, D. H. R.; Doller, D. *Acc. Chem. Res.* **1992**, *25*, 504–512.
(310) Baldwin, J. E.; Huff, J. *J. Am. Chem. Soc.* **1973**, *95*, 5757–5759.
(311) Collamati, I.; Ercolani, C.; Rossi, G. *Inorg. Nucl. Chem. Lett.* **1976**, *12*, 799–802.
(312) Collamati, I. *Inorg. Chim. Acta* **1979**, *35*, L303–L304.
(313) Herron, N.; Busch, D. H. *J. Am. Chem. Soc.* **1981**, *103*, 1236–1237.
(314) Herron, N.; Cameron, J. H.; Neer, G. L.; Busch, D. H. *J. Am. Chem. Soc.* **1983**, *105*, 298–301.
(315) Herron, N.; Schammel, W. P.; Jackels, S. C.; Grzybowski, J. J.; Zimmer, L. L.; Busch, D. H. *Inorg. Chem.* **1983**, *22*, 1433–1440.
(316) Collman, J. P.; Gagne, R. R.; Reed, C. A.; Halbert, T. R.; Lang, G.; Robinson, W. T. *J. Am. Chem. Soc.* **1975**, *97*, 1427–1439.
(317) Almog, J.; Baldwin, J. E.; Dyer, R. L.; Peters, M. *J. Am. Chem. Soc.* **1975**, *97*, 227–228.
(318) Collman, J. P. *Acc. Chem. Res.* **1977**, *10*, 265–272.
(319) Chin, D.-H.; La Mar, G. N.; Balch, A. L. *J. Am. Chem. Soc.* **1980**, *102*, 4344–4350.
(320) Paeng, I. R.; Shiwaku, H.; Nakamoto, K. *J. Am. Chem. Soc.* **1988**, *110*, 1995–1996.
(321) Almog, J.; Baldwin, J. E.; Huff, J. *J. Am. Chem. Soc.* **1975**, *97*, 228–229.
(322) Collman, J. P. *Acc. Chem. Res.* **1977**, *10*, 265–272 and references therein.
(323) Sauer-Masarwa, A.; Dickerson, L. D.; Herron, N.; Busch, D. H. *Coord. Chem. Rev.* **1993**, *128*, 117–137.
(324) Busch, D. H.; Alcock, N. W. *Chem. Rev.* **1994**, *94*, 585–623 (this issue).
(325) Dickerson, L. D.; Sauer-Masarwa, A.; Herron, N.; Fendrick, C. M.; Busch, D. H. *J. Am. Chem. Soc.* **1993**, *115*, 3623–3626.
(326) Sauer-Masarwa, A.; Herron, N.; Fendrick, C. M.; Busch, D. H. *Inorg. Chem.* **1993**, *32*, 1086–1094.
(327) Kimura, E.; Kodama, M.; Machida, R.; Ishizu, K. *Inorg. Chem.* **1982**, *21*, 595–602.
(328) Sakurai, T.; Kaji, H.; Nakahara, A. *Inorg. Chim. Acta* **1982**, *67*, 1–5.
(329) Hayashi, Y.; Suzuki, M.; Uehara, A.; Mizutani, Y.; Kitagawa, T. *Chem. Lett.* **1992**, 91–94.
(330) Hayashi, Y.; Suzuki, M.; Uehara, A.; Mizutani, Y.; Kitagawa, T. Submitted for publication.
(331) Drake, J. F.; Williams, R. J. P. *Nature* **1958**, *182*, 1084.
(332) Davies, R. C. Thesis, Wadham College, Oxford, 1963.
(333) McClellan, W. R.; Benson, R. E. *J. Am. Chem. Soc.* **1966**, *88*, 5165–5169.
(334) McKee, V.; Nelson, S. M.; Nelson, J. *J. Chem. Soc., Chem. Commun.* **1976**, 225–226.
(335) Kitajima, N.; Tamura, N.; Tanaka, M.; Moro-oka, Y. *Inorg. Chem.* **1992**, *31*, 3342–3343.
(336) Brennan, B.; Chen, Q.; Juarez-Garcia, C.; True, A. E.; O'Connor, C. J.; Que, L., Jr. *Inorg. Chem.* **1991**, *30*, 1937–1943.
(337) Holm, R. H.; Donahue, J. P. *Polyhedron* **1993**, *12*, 571–589.
(338) Feig, A. L.; Lippard, S. J. Unpublished results.
(339) Udenfriend, S.; Clark, C. T.; Axelrod, J.; Brodie, B. B. *J. Biol. Chem.* **1954**, *208*, 731–739.
(340) Hamilton, G. A.; Workman, R. J.; Woo, L. *J. Am. Chem. Soc.* **1964**, *86*, 3390–3391.
(341) Hamilton, G. A. *J. Am. Chem. Soc.* **1964**, *86*, 3391–3392.
(342) Hamilton, G. A. In *Molecular Mechanisms of Dioxygen Activation*; Hayaishi, O., Ed.; Academic: New York, 1974; pp 405–451.
(343) Kochi, J.; Sheldon, R. A. *Metal-catalyzed Oxidations of Organic Compounds*; Academic: New York, 1981.
(344) Ito, S.; Ueno, K.; Mitarai, A.; Sasaki, K. *J. Chem. Soc., Perk. Trans. 2* **1993**, 255–259.
(345) Taqui Khan, M. M.; Martell, A. E. *J. Am. Chem. Soc.* **1967**, *89*, 7104–7111.
(346) Hamed, M. Y.; Silver, J.; Wilson, M. T. *Inorg. Chim. Acta* **1983**, *80*, 237–244.
(347) Hamed, M. Y.; Keypour, H.; Silver, J.; Wilson, M. T. *Inorg. Chim. Acta* **1988**, *152*, 227–231.
(348) Hamilton, G. A. *Adv. Enzymol.* **1969**, *32*, 55–96.
(349) Norman, R. O. C.; Radda, G. K. *Proc. Chem. Soc.* **1962**, 138.
(350) Sawyer, D. T.; Kang, C.; Qiu, A.; Sobkowiak, A. In *5th International Symposium on Redox Mechanisms and Interfacial Properties of Molecules of Biological Importance*; Schultz, F. A., Taniguchi, I., Eds.; The Electrochemical Society: Pennington, NJ, 1993; pp 216–231.
(351) Sawyer, D. T.; Kang, C.; Llobet, A.; Redman, C. *J. Am. Chem. Soc.* **1993**, *115*, 5817–5818.
(352) Barton, D. H. R.; Bévière, S. D.; Chavasiri, W.; Csuhai, E.; Doller, D.; Liu, W.-G. *J. Am. Chem. Soc.* **1992**, *114*, 2147–2156.
(353) Fish, R. H.; Konings, M. S.; Oberhausen, K. J.; Fong, R. H.; Yu, W. M.; Christou, G.; Vincent, J. B.; Coggin, D. K.; Buchanan, R. M. *Inorg. Chem.* **1991**, *30*, 3002–3006.
(354) Fish, R. H.; Oberhausen, K. J.; Chen, S.; Richardson, J. F.; Pierce, W.; Buchanan, R. M. *Catal. Lett.* **1993**, *18*, 357–365.
(355) Barton, D. H. R.; Doller, D. In *Dioxygen Activation and Homogeneous Catalytic Oxidation*; Simándi, L. I., Ed.; Elsevier: New York, 1991; Vol. 66, pp 1–10.
(356) Kang, C.; Redman, C.; Cepak, V.; Sawyer, D. T. *Bioorg. Med. Chem.* **1993**, *1*, 125–140.
(357) Barton, D. H. R.; Sawyer, D. T. In *The Activation of O_2 and Homogeneous Catalytic Oxidation*; Barton, D. H. R., Martell, A. E., Sawyer, D. T., Eds.; Plenum: New York, 1993; pp 1–7.
(358) Mimoun, H.; Seree de Roch, I. *Tetrahedron* **1975**, *31*, 777–784.
(359) Davis, R.; Durrant, J. L. A.; Khan, M. A. *Polyhedron* **1988**, *7*, 425–438.
(360) Sawyer, D. T.; Sugimoto, H.; Calderwood, T. S. *Proc. Natl. Acad. Sci. U.S.A.* **1984**, *81*, 8025–8027.
(361) Sheu, C.; Sawyer, D. T. *J. Am. Chem. Soc.* **1990**, *112*, 8212–8214.
(362) Sawyer, D. T. In *Oxygen Complexes and Oxygen Activation by Transition Metals*; Martell, A. E., Sawyer, D. T., Eds.; Plenum: New York, 1988; pp 131–148.
(363) Kraulis, P. *J. Appl. Crystallogr.* **1991**, *24*, 946–950.
(364) Harrison, P. M.; Andrews, S. C.; Ford, G. C.; Smith, J. M. A.; Treffry, A.; White, J. L. In *Iron Transport in Microbes, Plants and Animals*; Winkelmann, G., van der Helm, D., Neilands, J. B., Eds.; VCH: New York, 1987; pp 445–498.
(365) Que, L., Jr.; Lipscomb, J. D.; Zimmermann, R.; Münck, E.; Orme-Johnson, N. R.; Orme-Johnson, W. H. *Biochim. Biophys. Acta* **1976**, *452*, 320–334.
(366) Shiemke, A. K.; Loehr, T. M.; Sanders-Loehr, J. *J. Am. Chem. Soc.* **1984**, *106*, 4951–4956.
(367) Antonini, E.; Brunori, M. *Hemoglobin and Myoglobin and Their Reactions with Ligands*; North-Holland: Amsterdam, 1971.
(368) Brunori, M.; Schuster, T. M. *J. Biol. Chem.* **1969**, *244*, 4046–4053.
(369) Gibson, Q. H. *J. Biol. Chem.* **1970**, *245*, 3285–3288.
(370) de Waal, A.; de Jong, L.; Hartog, A. F.; Kemp, A. *Biochemistry* **1985**, *24*, 6493–6499.
(371) Fox, B. G.; Hendrich, M. P.; Surerus, K. K.; Andersson, K. K.; Froland, W. A.; Lipscomb, J. D.; Münck, E. *J. Am. Chem. Soc.* **1993**, *115*, 3688–3701.
(372) Hendrich, M. P.; Münck, E.; Fox, B. G.; Lipscomb, J. D. *J. Am. Chem. Soc.* **1990**, *112*, 5861–5865.
(373) Fox, B. G.; Liu, Y.; Dege, J. E.; Lipscomb, J. D. *J. Biol. Chem.* **1991**, *266*, 540–550.
(374) Paulsen, K. E.; Liu, Y.; Fox, B. G.; Stankovich, M. T.; Lipscomb, J. D.; Münck, E. *J. Inorg. Biochem.* **1993**, *51*, 307.
(375) Murch, B. P.; Bradley, F. C.; Que, L., Jr. *J. Am. Chem. Soc.* **1986**, *108*, 5027–5028.
(376) Sawyer, D. T.; McDowell, M. S.; Spencer, L.; Tsang, P. K. S. *Inorg. Chem.* **1989**, *28*, 1166–1170.
(377) McCandlish, E.; Miksztal, A. R.; Nappa, M.; Sprenger, A. Q.; Valentine, J. S.; Stong, J. D.; Spiro, T. G. *J. Am. Chem. Soc.* **1980**, *102*, 4268–4271.